University of Pisa

Scuola Superiore Sant'Anna

Joint PhD Program in Crop Science (XXVI Cycle)

PhD School in Agricultural and Veterinary Sciences

SSD AGR/13

Can anthocyanins photoprotect purple genotypes of *Ocimum basilicum* L. against boron toxicity and high light?

Candidate: *Marco Landi*

Supervisor: *Lucia Guidi*

PhD School Director: *Alberto Pardossi*

Academic year 2013-2014

Aotearoa…

…the land of the long, white cloud…

Abstract

In many areas worldwide boron (B) is frequently added as fertilizer, while in other regions the concentration and/or the availability of B in soils or water sources exceed the requirements for crops production. Although the degree of tolerance can significantly differ among different species, and even among cultivars of the same species, once B becomes toxic it leads to visible symptoms of damages on leaf lamina. As a consequence, both the reduction of the photosynthetic leaf area caused by necrosis on and chlorosis as well as the impairment of chloroplast efficiency in leaf areas close to the necrosis strongly reduces the photosynthetic rate.

Anthocyanin-rich plant morphs have been demonstrated many times more tolerant to a wide range of stresses (salinity, drought, heavy metal, etc.) compared to acyanic genotypes belonging to the same species. The reason of the higher tolerance has not always completely understood, albeit in most of the cases it is likely attributable to the photoprotection and/or the antioxidant ability of anthocyanins. Due to these features, anthocyanins can protect the photosynthetic machinery especially when light intensity exceeds the requirements of chloroplasts that are already partially compromised by other stressors. In view of above, in this work we explored the possibility that anthocyanins may exert a benefit for a largely used Mediterranean crop (*Ocimum basilicum* L.) and we utilized a purple (‘Red Rubin’) and a green-leafed (‘Tigullio’) cultivar of sweet basil to evaluate the effects of B toxicity.

Our results demonstrate the negative effects of B on photosynthesis occurred either due to stomatal or mesophyll limitations independently to basil plants leaf pigmentation. Furthermore, anthocyanins effectively represent a benefit for plants subjected to high B (20 mg L^{-1}) as leaves of ‘Red Rubin’ were less damaged than those of ‘Tigullio’. Being anthocyanins localized in the abaxial and adaxial epidermises of basil leaves, in both intact plants and protoplasts we demonstrated that the main advantage of anthocyanin-rich leaves consists in their photoprotective role. Indeed, while the purple cultivar has the possibility to screen a proportion of light otherwise absorbed by chloroplasts, the green cultivar ‘Tigullio’ cannot avoid surplus of excitation energy burden to chloroplasts already compromised by B toxicity. However, when we attempted to simulate the removal of the anthocyanic layer isolating protoplasts from

leaf mesophyll of both ‘Tigullio’ and ‘Red Rubin’, the photosynthetic process was still less impaired and the degree of oxidative stress lower in acyanic protoplasts of ‘Red Rubin’ than in ‘Tigullio’ protoplasts treated with B. Thus, we postulate that in addition to the photoprotective role of anthocyanins in ‘Red Rubin’, other mechanisms, including a higher antioxidant pool, contribute to higher performance of that cultivar when exposed to concomitant conditions of excess B and light. Levels of both ascorbate and glutathione, key antioxidants in plant cells, are indeed 2-fold higher in ‘Red Rubin’ than in ‘Tigullio’. Noteworthy, ‘Red Rubin’ plants grown under high sunlight, exhibited typical morphological and biochemical features of plants grown under shade suggesting that the ‘shade syndrome’ described for anthocyanin-rich species plays a key role in plant adaptations to sunny environments.

In conclusion, due to the sunscreen effect of anthocyanins, and, probably, for the high amount of antioxidants, ‘Red Rubin’ plants appear naturally equipped to survive in an environment, as the Mediterranean area, where light excess may represent a stressor, especially in concomitance to others such as B excess. Nevertheless, other possible functions of anthocyanins in B tolerance can be hypothesised, such as sequestration of boric acid and/or borate in the vacuole of epidermal cells where anthocyanins are localized.

Publications arise from this thesis

LANDI M, PARDOSSI A, REMORINI D, GUIDI L (2013) Antioxidant and photosynthetic response of a purple-leafed and a green-leafed cultivar of sweet basil (*Ocimum basilicum*) to boron excess. Environmental Experimental Botany 85: 64-75.

LANDI M, REMORINI D, PARDOSSI A, GUIDI L (2013) Purple *versus* green-leafed *Ocimum basilicum*: Which differences occur with regard to photosynthesis under boron toxicity? Journal of Plant Nutrition and Soil Science 176: 942-951.

LANDI M, DEGL'INNOCENTI E, PARDOSSI A, GUIDI L (2012) Antioxidant and photosynthetic responses in plants under boron toxicity: a review. American Journal of Agricultural and Biological Sciences 7 (3): 255-270.

LANDI M, REMORINI D, PARDOSSI A, GUIDI L (2013) Boron excess affects photosynthesis and antioxidant apparatus of greenhouse *Cucurbita pepo* and *Cucumis sativus*. Journal of Plant Research 126: 775-786.

Communications in international workshops

LANDI M, GUIDI L, TATTINI M, GOULD KS (2013) 7th IWA – International Workshop on Anthocyanins. Porto (Portugal), 9-11 September. Oral communication: "Can anthocyanins photo-protect sweet basil against boron toxicity?"

1. Introduction

1.1. Boron: chemical identity and distribution

Boron (B) is a metalloid element which exists naturally as 20% ^{10} B and 80% ^{11} B isotope (WHO, 1998). It is an electron-deficient element with a vacant *p*-orbital ($1s^2$ $2s^2$ sp^1), and for that reason B does not form ionic bonds, but stable covalent bonds. Compounds containing B often behave as Lewis acids, readily bonding with electron-rich substances.

Elemental B is found in borax minerals as: tincal ($Na_2B_4O_7 \cdot 10H_2O$), colemanite ($CaB_3O_4(OH)_3$-H_2O), kernite ($Na_2B_4O_7 \cdot 4H_2O$), ulexite ($NaCaB_5O_9 \cdot H_2O$), boric acid [$B(OH)_3$] and borate-derivated (salt or ester of boric acid). Boric acid is the main compound present at neutral pH and, in that condition, it exists as odorless, colorless, translucent crystals or white granules or powder at ambient temperatures (O'Neil et al., 2004). It is a weak acid (pKa 9.2) and it exists primarily (more than 98%) as undissociated $B(OH)_3$ in aqueous solution at physiological pH, as similar as borate salts (Tanaka and Fujiwara, 2008).

The presence of B in the environment derives primarily from the weathering of B-containing minerals (Butterwick et al., 1989), beside to geothermal steams which significantly contribute to natural enrichment of B in soil and water (Pennisi et al., 2006). Global environmentally releases of B through weathering, volcanic, and geothermal processes are estimated at approximately 360,000 metric tons annually (Moore, 1991). However, the most impactful source of high-concentrated B, with an average of 4.5 mg L^{-1} B dissolved as boric acid, is certainly seawater which can mixes and contaminates fresh water in coastal areas following tidal cycle. Moreover, seawater volatilization originates $B(OH)_3$ dissolved in aerosol and originates a gradient of B sedimentation in soil from the cost to inland.

Differently to other elements, environmental release of B directly or indirectly attributable to human activities plays a minor role compared to the amplitude of the environmental B-enrichment deriving from natural sources. Anthropogenic sources listed on the basis of their increasing contribution to B release worldwide are: agriculture, wood burning, power generation from coal and oil, glass manufacture, use

of borates/perborates, borate mining and processing, leaching of treated wood/paper, and sewage disposal of B (HSDB, 2003).

Since the 20's, when it was established the essential role of B in plants of *Vicia faba* (Warington, 1923), B has been considered an essential micronutrient for plant development, and it has been hypothesized that it plays a key role in several metabolic processes (Goldbach et al., 2001; O'Neill et al., 2004). Thus, its availability in irrigation water as well as in soil represents an important factor for crops production, despite concentration and availability of B in soils worldwide are extremely variable (Gupta et al., 1985). In many countries (including Japan, China, USA and Brazil) B concentration in soil is insufficient for agricultural production and B is added as fertilizer (Gupta et al., 1985). On the other hand, other areas are affected by B excess, which impaired crop growth and yield.

B shortage in soil is mainly dependent on the presence of this element as $B(OH)_3$, which is easily leached out by rainwater due to its high solubility (Bolaños et al., 2004). Conversely, B excess preferentially occurs in arid or semiarid countries such as South Australia, Iraq, Egypt, Jordan, Libya, Morocco, Syria, Turkey, Chile and California (You et al., 1995), and Italy as well (Pennisi et al., 2006), where the main reason of B accumulation in topsoil is water evapotranspiration.

1.2. Boron in plant physiology: which roles?

Under physiological conditions, B exists as $B(OH)_3$ or tetrahydroxyl borate anion $B(OH)_4^-$ in plants (Woods, 1996; **Fig. 1.2.1**). However, the 98% of the total B exists in free form as $B(OH)_3$ or even higher (about 99.95%) at lower pH values (such instance 5.5 in apoplast) (for a review refer to Woods, 1996). Boric acid is a weak acid at cytoplasm pH (about 7.0-7.5) and, under physiological conditions, $B(OH)_3$ can easily bind to molecules with mono, di- and poly-hydroxyl groups such as ribose, apiose, sorbitol and other polyalcohols (Raltson and Hunt, 2001). Indeed, the first B-containing compound identified in the plant kingdom, which is stable under physiological conditions, is the pectic polysaccharide rhamnogalacturonan II (RGII), where B cross-links two RGII monomers by a borate bridge providing stability to the cell-wall matrix (O'Neill et al., 1996; Kobayashi et al., 1996; **Fig. 1.2.2**). However, B can also form

complexes with polyalcohols even when those moieties are incorporated into other compounds (i.e. NAD(P)H, ATP, nucleotides; Raltson and Hunt, 2001). Raltson and Hunt (2001) pointed out a gradient of stability of B complexes, in order: apiose > NAD^+ > NADH ≅ 5'ATP > 5'ADP > 5'AMP > adenosine > 3'AMP ≅ 2'AMP ≅ cAMP ≅ adenine. B-NADH, B-NADPH, and B-$NADP^+$ affinity were also demonstrated *in vivo* (Reid et al., 2004).

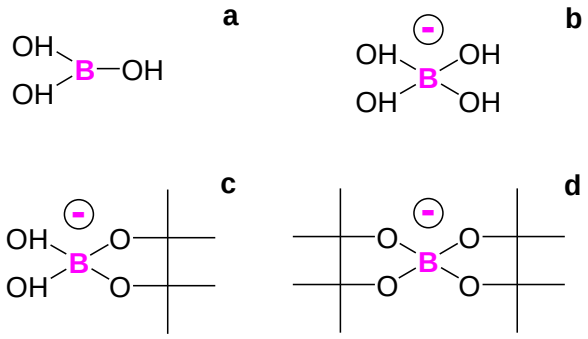

Fig 1.2.1 Chemical structure of boric acid (**a**), borate anion (**b**) and their esters (**c** and **d**).

Furthermore, increasing pH typically stabilized more *cis*-diols than *trans*-diols (Boeseken, 1949). Phenolics and amino acids are other compounds that can originate complexes with B, too (Brown et al., 2002).

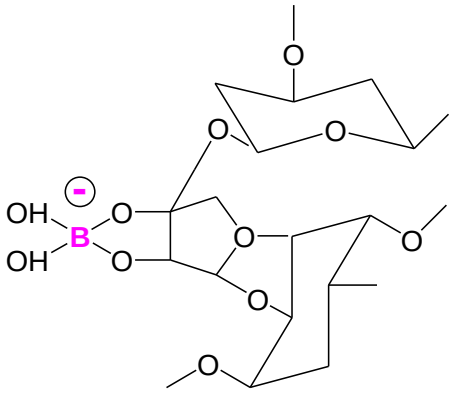

Fig 1.2.2 Site of B attachment in plant cell wall B rhamnogalacturonan II complex.

Many other roles have been proposed for B in plants, such as its influence in reproductive growth and development, stimulation of reproductive tissues, improvement

of seed quality and its influence on the biosynthesis of some metabolic compounds, i.e. antioxidants and phenols (for a complete review see Brown et al., 2002; Goldbach and Wimmer, 2007; Camacho-Cristobal et al., 2008). However, to the best of our knowledge its role as cell wall structure network and the subsequent regulation of cell wall pore size is the only function largely accepted.

1.3. Boron fluxes: from root to shoot

Boron is found principally as undissociated $B(OH)_3$ at common soil pH (5.5-7.5) and it is widely accepted that plants take up B in that form from roots (Camacho-Cristobal et al., 2008). B uptake is considered to involve different mechanisms depending on its availability: (I) passive diffusion across lipid bilayer (II) facilitated transport by major intrinsic protein (MIP) channel and (III) high-affinity B transporters (BOR); the latters in responses to low B supply (Tanaka and Fujiwara, 2008) (**Fig. 1.3.1**).

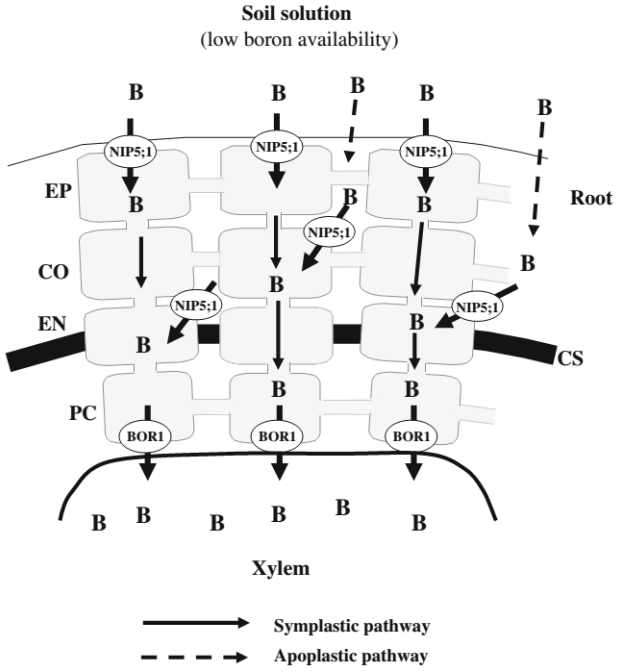

Fig. 1.3.1. Schematic diagram of B movement in plants under low B availability. B: boron; EP: epidermis; CO: cortex; EN: endodermis; CS: Casparian strip; PC: pericycle (source: Tanaka and Fujiwara., 2008. Kindly permission of authors).

Active B uptake occurs under sub-optimal B availability or even in condition of B starvation (Dannel et al., 2000; Stangoulis et al., 2001). However, only OsBOR1, one BOR transporter in rice, has been identified as involved in the efficient uptake from roots under B deficiency (Nakagawa et al., 2007; Tanaka and Fujiwara, 2008).

Conversely, under condition of adequate or excessive B supply the hypothesis that B is principally absorbed passively by roots is the most widely accepted (Brown et al., 2002; Tanaka and Fujiwara, 2008). That process is largely attributable to the high permeability of $B(OH)_3$ to lipid bilayers (Brown and Shelp, 1997; Dordas et al., 2000; Dordas and Brown, 2000).

Once absorbed, B is translocated to leaves *via* non-living cells of the xylem driven by transpiration flux. Thus, xylem translocation is mainly directed to the mature leaves because they represent the sites with the highest transpiration rate. Kohl and Oertli (1961) demonstrated that B uptake followed the passive water flux from roots to leaves and B accumulated especially where leaf veins terminate. Indeed, those tissues showed more evident symptoms of B toxicity such as chlorosis and necrosis. According to this hypothesis, higher B concentrations were found in leaf tissues than in phloem sap (Shelp, 1988). Thus, for long time it has generally been accepted that B is an immobile nutrient in the phloem tissues and therefore it tends to accumulate in highly-transpiring mature leaves.

Conversely, in some plant species, including many important crop genera (e.g., *Pyrus*, *Malus*, *Prunus*, *Allium* and *Brassica*), B has been found to be uniformly distributed within plants or even at a higher concentration in young tissues than in mature leaves (Brown and Hu, 1996; Camacho-Cristobal et al., 2008). These results demonstrated B ability to move along the phloem flux at least in some plant species. Phloem translocation does not follow the transpiration stream and it supplies the major proportion of nutrient requirements for actively growing areas such as young leaves and fruit, organs which do not readily transpire (Brown and Shelp, 1997). *Pyrus*, *Malus*, *Prunus*, *Allium* and *Brassica* commonly produce high amounts of sugar alcohols (i.e. mannitol and sorbitol) which are used for the phloem translocation of photosynthates in place of sucrose (Brown et al., 1999). Sorbitol and mannitol with their *cis*-hydroxyl groups can readily bind to boric acid originating diol-B complexes (Reid et al., 2004) (**Fig. 1.3.2**). That bond is likely to allow B to be transported through phloem where it is present as a stable polyol-B complex with mannitol and sorbitol as ligands (Hu and Brown; 1997).

Of note, plants producing sugar alcohols can better tolerate B deficiency than do plants with a lower ability (Brown et al., 1996). Such instance, transgenic tobacco plants transformed with the sorbitol-synthesizing enzyme produced greater biomass under B starvation as compared to that of wild type plants (Brown et al., 1999).

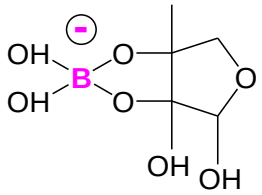

Fig. 1.3.2. Phloem B complex with sorbitol.

It was argued that the transgenic lines had a higher ability to move B through the phloem flow as B-complex sugar alcohol (Brown et al., 1999). Nevertheless, Takano et al. (2002) found that B was transported *via* the phloem sap to young leaves in plants that do not produce sugar alcohols, too. That suggested an alternative mechanism of translocation that involves B channels and transporters. In those species, including *Arabidopsis thaliana* (Takano et al., 2002) and *Brassica napus* (Stangoulis et al., 2001), the translocation was reported under B limitation, but not in conditions of normal or luxury B supply. Indeed, Tanaka and Fujiwara (2008) showed that an active B transport involving channels and transporters (BOR and NIR) play a relevant role in B uptake only under B deficiency. BOR1 was the first B transporter found in *A. thaliana* and it was shown essential under low B supply (Takano et al., 2002). BOR1 is regulated at post-transcriptional level and the protein is degraded under adequate or luxury B supply suggesting a sophisticated regulation of B aimed at maintaining B homeostasis (Noguchi et al., 2003; Takano et al., 2002, 2005). Those results suggest BOR1 is not involved in tolerance to B excess. Nevertheless, a study with a transgenic line of *A. thaliana* has been shown that BOR4, another efflux-type borate transporter, was not degraded at post-transcriptional level differently from BOR1 (Miwa et al., 2007). Accumulation of BOR4-GFP (Green Fluorescence Protein) and B tolerance were positively correlated and the overproduction of BOR4-GFP improved plants growth under high B levels. Takano et al. (2006) reported that also another channel, NIP5, allowed *Arabidopsis* to grown under low B supply. NIP5 belongs to Major Intrinsic Protein (MIPs) including

aquaporin and this channel was supposed a B importer at root level after the evidence that NIP5-deficient plants had lower B concentration in roots and a reduced shoots elongation only under low B supply (Takano et al., 2006). To date, nine NIPs have been identified in *Arabidopsis* (Takano et al., 2006) and other members of that family are probably involved in that sophisticate pathway.

1.4. Boron toxicity in plants

One hand B deficiency represents a serious problem for plant physiology, but on the other hand, excess of B in soil or irrigation water represents a constrain factor for plant growth and development, too.

When plants are subjected to B excess, the first visible symptoms in species with low B mobility are chlorotic and/or necrotic patches (burn) of the older leaves where B tends to accumulate (Nable et al., 1997). In **Fig. 1.4.1** is reported the effect in terms of leaf necrosis in 'Tigullio' sweet basil cultivar subjected to increasing concentration of B in the nutrient solution.

Fig. 1.4.1. Necrosis extent in leaves of 'Tigullio' sweet basil plants grown for 21 d under increasing concentration of B in the nutrient solution (reported as mg L^{-1}).

Conversely, in plants species which produce sugar alcohol, in which B translocation occurs, the symptoms of B toxicity firstly appear in the meristemic regions and fruits while do not occur in mature leaves (Brown and Hu, 1996). Therefore, in

those species main symptoms of toxicity are fruit disorders (gummy nuts, internal necrosis), bark necrosis caused by death of the cambial tissues, and stem die back (Brown and Hu, 1996). Curiously, visible symptoms of B toxicity do not appear in roots and B concentrations in these tissues remain relatively low compared to those found in leaves, even when plants are subjected to high levels of B supply (Nable, 1988).

Excessive B uptake may: (I) impairs cell division and development by binding to ribose, both as the free sugar and as a constituent of RNA; (II) interferes with primary metabolism by binding to ribose in ATP or NAD(P)H; (III) lowers the cytosol pH, thereby affecting protein conformation and biosynthesis (Reid et al., 2004). As a result, key physiological processes such as photosynthesis are strongly perturbed (Cervilla et al., 2007). Indeed, given that the ability to process incident light energy is compromised in plants subjected to B toxicity, they are more prone to generate a surplus of reactive oxygen species (ROS) and consequently they incur in greater oxidative stress level (Cervilla et al., 2007). This phenomenon, in addition to a reduction of photosynthetic area caused by necrosis on leaf lamina, can strongly affect net carbon assimilation rate (Lovatt and Bates, 1984; Reid et al., 2004; Guidi et al., 2011). Reid et al. (2004) stated that inhibition of growth under B toxicity is most likely attributable to retardation of many cellular processes in mature tissues, enhanced by photo-oxidative stress under light condition, rather than to direct effects of B on energy supply or proteins biosynthesis. Conversely, there is no evidence to support the hypothesis that the effect of B toxicity in leaves is attributable to osmotic stress induced by accumulation of borate or boric acid (Reid et al., 2004).

It is evident that some plant species are more tolerant of high concentrations of edaphic B than are others (Reid, 2007). Referring to Keren and Bingham (1985), safe concentrations of B in irrigation water range from 0.3-0.5 mg L^{-1} for sensitive plants (i.e. avocado, apple and bean), 1-2 mg L^{-1} for semi-tolerant plants (oat, maize and potato), 2-4 mg L^{-1} for tolerant plants (carrot, alfalfa and sugar beet) and 8-10 mg L^{-1} for very tolerant species (tomato, *Atriplex* spp.). Plant species can tolerate for a short period even higher dose of B, phenomena that simulate what can naturally occurs after heavy rainfall in B-laden soils.

Tolerant genotypes are usually characterized by the ability to reduce B concentration in shoots due to: (I) reduced uptake of B from both roots and shoots (Nable et al., 1990), and/or (II) the ability to efflux B from roots once in excess (Reid, 2007; Sutton et al., 2007). Less information are available about the first mechanisms, while to support the "efflux-hypothesis" different anion channels have been recognized as responsible for the higher B tolerance, such as BOR4 (*A.thaliana*; Miwa et al., 2007), BOR1 (barley; Sutton et al., 2007), and BOR2 (wheat and barley; Reid, 2007). In some cases it has also been observed that tolerant genotypes have an enhanced antioxidant metabolism (Cervilla et al., 2007), however this genuine adaptation mechanism remains to be elucidated.

To the best of our knowledge, the performances of anthocyanic morphs have never been compared to acyanic genotypes under B toxicity. This aspect would represent the novelty of this experimental work and for that reason the role of anthocyanins represents the main core of this thesis.

1.5. Basil: green and purple genotypes

The genus *Ocimum* (Lamiaceae) collectively called basil, has long been acclaimed for its diversity (Makri and Kintzios, 2007). The genus numbers more than 30 herbs and shrubs species living from the tropical and subtropical regions of Asia to Africa, Central and South America. However, Africa has been recognized as the main centre of diversity (Paton, 1992). *Ocimum* numbers an astonishing source of essential oils and aroma compounds species (Simon et al., 1990), culinary herbs, and attractive, fragrant and ornamental species (Morales and Simon, 1996). Fresh or dried basil is widely used in the Mediterranean cuisine such as in tomato-based products, vegetables, salads, pizza and to flavour meats, soups and marine foods. In addition to the culinary use, those aromatic species are also attributed a folk medicinal value and they are officially accepted in some countries (Zeggwagh et al., 2007). The seeds contain edible oils and a drying oil similar to linseed (Angers et al., 1996), while leaf extracts are used in traditional medicines, and have been shown to contain biologically active constituents with insecticidal, nematicidal, fungistatic, or antimicrobial activity (Simon et al., 1990).

The most important species of genus *Ocimum* are *sanctum* L., *gratissimum* L., *viride* Willd., *basilicum* L., *americanum* L., *canum* Sims., *kilimandscharicum* Guerc and *suave* Willd. However, most commercial basil cultivars available in the market belong to the species *O. basilicum*. Darrah (1974) classified the *O. basilicum* cultivars in seven types: (I) tall slender types, which include the sweet basil group; (II) large-leafed, robust types, including 'Lettuce Leaf' also called 'Italian' basil; (III) dwarf types, which are short and small leafed, such as 'Bush' basil; (IV) compact types, also described, *O. basilicum* var. 'Thyrsiflora', commonly called 'Thai' basil; (V) *purpurascens*, the purple-colored basil types with traditional sweet basil flavour such as 'Red Rubin'; (VI) purple types such as and 'Dark Opal', a possible hybrid between *O. basilicum* and *O. forskolei*, which has lobed-leaves, with a sweet basil plus clove-like aroma; and (VII) *citriodorumtypes*, which includes lemon-flavored basils (Simon et al. 1999). In addition to the traditional genotypes of basil, other *Ocimum* species have been introduced in North American horticultural trade with new culinary and ornamental uses, and as potential sources of new aromatic compounds. However, interspecific hybridization and polyploidy, which commonly occurs in this genus (Harley et al., 1992), have created taxonomic confusion and have made it difficult to determine the genetic relationship between basils genotypes (Grayer et al., 1996). In addition, the taxonomy of basil is further complicated by the existence of numerous botanical varieties, cultivar names, and chemotypes within the same species, which may not differ significantly in morphology (Simon et al., 1990). A system of standardized descriptors, which includes volatile oil, has more recently been proposed by Paton and Putievsky (1996) and this should permit an easier identification of the different forms of *O. basilicum*.

1.6. Anthocyanins in sweet basil

As previously found in other purple-leafed basil genotypes (Phippen and Simon, 1998) in leaves of 'Red Rubin' anthocyanins accumulates exclusively in the epidermises (**Fig. 1.6.1a**) and in xylem parenchyma in the midrib (**Fig. 1.6.1b**). Epidermal anthocyanins are present both in epidermal cells and in trichomes (**Fig. 1.6.1c**). Interestingly, on the adaxis the pigments occur in solution in the cell vacuole, but on the abaxis, anthocyanins

appeared as aggregates known as anthocyanin vacuolar inclusion (AVIs) both in epidermal cells and in trichomes.

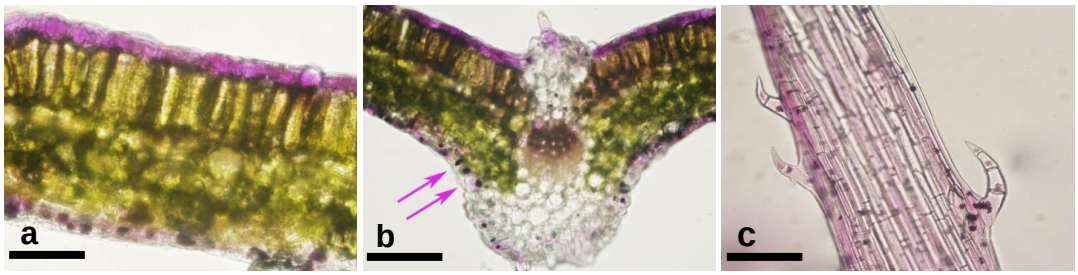

Fig. 1.6.1. Leaf anatomy of *O. basilicum* cultivar 'Red Rubin'. Transverse sections through (a) lamina, showing epidermal anthocyanins, and (b) midrib, showing anthocyanic vacuolar inclusions (arrows). (c) Epidermal peel showing anthocyanins in trichomes. Bars: a, b, = 150 µm; c = 30 µm.

Table 1.6.1. Comparison of purple basil to other natural anthocyanin fruit and leaf sources. Modified from Phippen and Simon (1998).

Source	Plant organ	Anthocyanins (µg g^{-1} FW ± SD)
Grape (*V. labrusca* 'Concord')	Fruit skin	2.5 ± 0.3
Perilla (*P. frutescens* 'Crispa')	Leaf	1.8 ± 0.1
Plum (*P. domestica* L. 'Stanley')	Fruit skin	1.6 ± 0.2
Purple sage (*S. officinalis* 'Purpurea')	Leaf	0.8 ± 0.1
Red cabbage (*B. oleracea* 'Cardinal')	Leaf	0.8 ± 0.1
Red raspberry (*R. idaeus* 'Heritage')	Leaf	0.1 ± 0.1
Purple basil (*O. basilicum* 'Red Rubin')	**Leaf**	**1.8 ± 0.3**

Purple basil can be considered a good source of anthocyanins (**Table 1.6.1**) compared to other natural sources. However, the amount of anthocyanins in different cultivars of pigmented basil can significantly differ, ranging from 0.7 to 1.9 µg g^{-1} FW (**Table 1.6.2**). As similarly reported by Phippen and Simon (1998) in *O. basilicum* cultivar 'Purple Ruffles', we found that the main anthocyanins in 'Red Rubin' are cyanidin derivates, especially cyanidine-based moieties coniugated with *ρ*-coumaryl and malonyl acid (see **Table 3.4.4** and **Table S3.4.3**)

Table 1.6.2 Total extractable anthocyanins yields among commercial purple basil cultivars. Modified from Phippen and Simon (1998).

Cultivar	Seed source	Anthocyanins (μg g^{-1} FW ± SD)
'Dark Opal'	Richters	1.6 ± 0.2
	Rupp Seeds	1.9 ± 0.1
'Holy Sacred Red'	Rupp Seeds	0.8 ± 0.1
'Opal'	Companion Plants	1.3 ± 0.1
'Osmin Purple'	Johnny's	1.8 ± 0.1
'Purple Bush'	Richters	0.7 ± 0.1
'Purple Ruffles'	Ball Seed	1.9 ± 0.1
	Johnny's	1.6 ± 0.1
'Rubin'	Richters	1.7 ± 0.1
'Red Rubin'	Johnny's	1.7 ± 0.1
'Red Rubin Purple Leaf'	Shepard's Garden Seeds	1.8 ± 0.1

1.7. Anthocyanins in plants: the intriguing debate on photoprotection *vs* antioxidant role

The physiological roles of anthocyanin in plants have intrigued scientists for well over a century. To date, despite a lot of knowledge has been gained on matter, the presence of anthocyanins in almost all organ cells and the wide distribution of these pigments in the *Plantae* kingdom remain far from obvious. Indeed, despite it is undeniable the selective pressure has driven evolution to anthocyanins in such disparate vegetative organs, the selective factors that led to the production of these pigments remain partially a mystery. In addition, a unified explanation for anthocyanins in plants is impossible given that for each species the presence of anthocyanins cannot be described isolating those pigments neither from the metabolic framework nor from the ecological niche of the species. Thus, any two species might receive different benefit from anthocyanins in such different ways and degrees despite identical histological localization and chemical composition of anthocyanins within tissue.

Despite the predication of above, what anthocyanin-rich plant have in common in many cases is the up-regulation of the biosynthesis of anthocyanins as a cross response

to different environmental constrains such as high light, UV-B waveband, drought, high temperatures, ozone, mineral unbalance, bacterial and fungal infections, wounding, herbivores, herbicides and many other pollutants (i.e. heavy metals, etc.) (Chalker-Scott, 1999). Starting from those evidences, during the last decades many researches have been addressed to the evaluation of a direct or indirect role for anthocyanins under different stress conditions. In view of the chemical structure of anthocyanins and their histological localization different protective functions have been hypothesized even though, concerning plant protection against abiotic stress, photoprotection (from high light and UV-B) and ROS scavenging ability are the most widely postulated as stress reliever (Gould et al., 2009).

Photoprotection of photosynthetic apparatus

When light exceeds the requirements of photosystems, the accumulation of excitation energy within photosynthetic apparatus can lead to impairment of chloroplast structures. Many evidences indicate that foliar anthocyanins can protect photosynthetic cells from the adverse effects of excess light (reviewed in Steyn et al., 2002; Close and Beadle, 2003; Gould et al., 2009). Indeed, when chloroplasts receive more light quanta than they can use in photosynthesis, the quantum efficiency of photosystem II (PSII) rapidly declines. Protracted exposures to strong light, particularly in combination with another stressor such as B excess, can lead to the production of ROS that potentially damage thylakoid membranes and proteins (Nishio, 2000).

Anthocyanins, by intercepting a proportion of the photons that might otherwise cause damage, have the potential to reduce the incidence, and/or mitigate the severity, of photo-oxidative load (Feild et al., 2001). The effect is particular relevant when anthocyanin are epidermally located; in those species, the presence of anthocyanins is not far from having a constitutive layer of sunblock over the leaves. As similar as some molecules contained in many sunscreens (oxybenzone, ethylhexyl methoxycinnamate), anthocyanins are, indeed, able to absorb a particular sunlight waveband reducing light burden on photosystems. In particular, anthocyanic leaves absorb more green and yellow wavebands than do green leaves (Gitelson et al., 2001). The light-attenuation effect has been reported many times either reduce the degree of photoinhibition or

promptly recover photosynthetic apparatus from light stress in red as compared to green leaves (Steyn et al., 2002).

The benefit of photoprotection exerted by anthocyanins has been demonstrated in senescing leaves of deciduous tree species (Feild et al., 2001), in mature winter red leaves of evergreen species (Hughes et al., 2005) and even in young developing leaves (Hughes et al., 2007). Different types of leaves have in common the necessity to protect the photosynthetic machinery from light that can over exceed the requirements when leaves are particularly vulnerable. Another confirmation of the light attenuation effect of anthocyanin is the 'shade syndrome' described for red-leafed species (Manetas et al., 2003). When genotypes of the same plant species with different leaf color are compared, red-leafed plants often have higher chl *a:b* ratio, as typically found in shade-adapted leaves (Gould et al., 2009). Other morph-anatomical traits typical of shade plants (e.g., reduced axillary branches, expanded leaves with a reduced thickness) have been reported for red and purple-leafed plants, too (see **Fig. 6.1**).

Despite chemical and optical properties of anthocyanin moieties are constant, it is surprising that the degree by which anthocyanins contribute to photoprotection of leaves is extremely variable in different species. Karageorgou and Manetas (2006) suggested that the photoprotection is probably more important for ticker leaves that have whose mesophyll with a large amount of chlorophyll, and for which the abatement of green waveband represents a greater benefit. Conversely, thinner leaves use almost exclusively red and blue wavebands for photosynthesis; thus the photoprotection of anthocyanins would be lesser relevant. The "leaf-thickness hypothesis" however is not universally applicable as leaves of different deciduous tree species took advantage of red pigmentation independently of their thickness (Hughes et al., 2007). In addition, the contribution of anthocyanins in visible light abatement is likely to play a more relevant role when plants are simultaneously subjected to different stressor (Pietrini et al., 2002).

Anthocyanins represent only one of the mechanisms to avoid or dissipate excess of light energy. Other physiological processes, such as heat dissipation or transfer of electrons to alternative sinks, might further contribute to contrast deleterious effect of undissipated excitation energy (Niyogi, 2000). Xanthophyll cycle is a key mechanism through which leaves dissipate excess excitation energy *via* heat (Demmig-Adams and

Adams, 2006). Many authors have reported that red leaves have a reduced pool of xanthophylls and suggested that anthocyanins may constitute an alternative photoprotective strategy (Kytridis et al., 2008; Hughes et al., 2012), although sometimes this barrier is not enough to contrast the excess of light in plants with reduced xanthophyll cycle components (Zeliou et al., 2009).

While the abatement of visible light waveband represents a prerogative for almost all the coloured anthocyanins, mostly related to their concentration within tissues, the presence of anthocyanins with a determinate molecular structure inside the pool can also conferee photoprotection against particular wavebands, such as UV (Takahashi et al., 1991). Due to the UV-absorbing ability of phenolic acids, anthocyanins combined with those moieties (i.e. acylated anthocyanins), can protect the photosynthetic apparatus against UV radiation (Burger and Edwards, 1996). Anthocyanins in leaves are not commonly found as acylated and other compounds (i.e. flavonoids) resulted more effective in the photoabatement of UV, thus UV filtering is unlikely to represent universally the primary role for anthocyanins in plants (Gould et al., 2009). However, due to the richness of acylated pigments in purple basil leaves, the involvement of anthocyanins as UV shield cannot be excluded.

Antioxidant ability to scavenge ROS

Environmental stressors can lead to free radical production within tissues; mitochondria and chloroplast are considered as the main sites for ROS production in plants (Foyer et al., 1994). Being ROS generated within chloroplast due to undissipated excitation energy (Mittler et al, 2004), once the organelles ability to process light is compromised ROS production can increase even 3-fold (Polle, 2001). The deleterious effect of ROS consists in the capacity to rapidly oxidize biological molecules, in particular the lipid bilayer of membranes as well as proteins and nucleotides (Alscher et al., 1997). Anthocyanins exhibit either the ability to reduce light absorbed by photosystems or to scavenge directly molecules with unpaired electrons; however, the relative contribute of those pigments in each mechanism of protection is still under debate (Steyn et al., 2002; Manetas, 2006; Gould et al., 2009). Similarly to other flavonoids, anthocyanins have greater antioxidant ability than that of antioxidants with low molecular weight, such as

tocopherol and ascorbate (Rice-Evans et al., 1997). However, despite a strong body of results for antioxidant ability *in vitro* (for a review see Gould et al., 2009) only few researches demonstrated the antioxidant prerogative directly *in plantae* (Gould et al., 2002a; Agati et al., 2007).

The paradigm of their antioxidant ability derives from the localization within plant tissues. Anthocyanins are synthetized in the endoplasmic reticulum and then transported into vacuoles (Gould et al., 2009). The cytosolic anthocyanins would be better located to scavenge chloroplast and mitochondria ROS than would vacuolar anthocyanins. For a long time anthocyanins were thought to diffuse passively from the endoplasmic reticulum to vacuole, thus having the transient possibility to scavenge cytosolic ROS (Kytridis and Manetas, 2006). More recently other authors hypothesized that anthocyanins by-pass the cytosol moving from the site of biosynthesis to vacuole into vescicles. In that way they cannot have the possibility to act directly as antioxidant in the cytosol (Poustka et al., 2007). In addition, in some species (such as in purple pigmented basil), anthocyanins are mainly located in the vacuole of epidermis cells, that is far from the main source of ROS production (i.e. mesophyll cell chloroplasts). A direct role as antioxidants is therefore less probable in those species (Kytridis and Manetas, 2006).

2. Aim

In many Mediterranean countries, characterized by poor rainfall, excess of edaphic B can occur naturally and it has been shown to affect significantly the photosynthetic process in different crop species. For that reason, our work was addressed to the evaluation of the effect of B toxicity on the photosynthetic machinery of some cultivars of sweet basil (*Ocimum basilicum* L.).

Given anthocyanin-enriched morphs have been generally demonstrated to have a greater degree of tolerance than that of green genotypes to different environmental stressor, we tested the hypothesis that anthocyanins might represent a benefit also against B excess and we screened basil cultivars with green or purple leaves. The less sensitivity to high B exhibited by the purple-leafed cultivars compared to green ones drove our investigation deeper on the role of anthocyanins in that tolerance.

In view of the epidermal localization of anthocyanins in sweet basil, we tested their involvement as photoprotective pigments. The constitutive photoabatement of determinate wavebands (yellow and green), indeed, has been shown to reduce the pressure of excitation energy, aspect that results a great benefit especially when other stresses (such as B toxicity) impaired the photosynthetic apparatus, and photons exceed the requirements for photosystems.

Once the photoprotective role of anthocyanins as B stress reliever was revealed, in the last experiment we gave up the treatment with B. That to explore on deep the full potentiality of 'Red Rubin' compared to the green 'Tigullio' plants grown under high light during a typical hot Mediterranean summer. The latter experiment was focused mainly on the evaluation of differential biochemical and/or morphological responses exhibited by the green and purple-leafed cultivar under full sun or partially-shaded conditions.

3. Antioxidant and photosynthetic response of a purple and a green-leafed cultivar of sweet basil (*Ocimum basilicum*) to boron excess

Introduction

Excess of boron (B) may naturally occur in soil or as a result of over-fertilization and/or irrigation with water rich in B. Moreover, B toxicity is an important factor that reduces crop productions in many regions of the world (Nable et al., 1997). Conversely, in other areas natural B levels are insufficient for crop productions since it is present in soil as boric acid, which is easily leached out (Tanaka and Fujiwara, 2008). Therefore, B is frequently added as fertilizer in agricultural systems (Gupta et al., 1985).

B is unique as a micronutrient: it has restricted mobility in many plant species while it is freely mobile in others (Brown and Shelp, 1997). B mobility within plant parts determines the visible symptoms of B excess: in plants with low B mobility, the typical symptoms are chlorotic and/or necrotic patches (burn) of the older leaves where B tends to accumulate (Nable et al., 1997). Differently, in plants with high B mobility (e.g. *Prunus* spp., *Malus* spp. and *Pyrus* spp.) the symptoms of B toxicity firstly appear in meristematic regions and in fruits, but not in mature leaves (Brown and Hu, 1996). Moreover, B toxicity can affect crop productions through the reduction of leaf expansion, photosynthetic efficiency and fruit set (Nable et al., 1997).

Since photosystem II (PSII) is thought to play a key role in response of photosynthesis to environmental stress (Biswal and Biswal, 1999), the analysis of chlorophyll fluorescence and the evaluation of CO_2 assimilation under conditions of B excess might reflect the PSII behavior. Although there are many reports concerning leaf symptoms induced by B excess, there is a lack of knowledge relating to the behavior of photosynthetic and antioxidant systems and the role played by antioxidants in plant responses to B excess. In *S. lycopersicum*, Guidi et al. (2011) observed that B toxicity induced a decrease in the maximum quantum yield of PSII (F_v/F_m) and in the actual PSII quantum yield (Φ_{PSII}) particularly in leaf margins. Furthermore, a reduction in CO_2 assimilation and in the F_v/F_m ratio was described in citrus leaves both under B-excess and B deficiency (Han et al., 2009). The decline of CO_2 assimilation caused by B excess can potentially lead to the production of oxygen reactive species (ROS). In fact, the reduction of ATP and NADPH utilized in photoassimilation induces an excess of

excitation energy that can origin $^1O_2$ and others oxygen radicals damaging photosynthetic apparatus and membranes.

It has long been known that plants respond to the oxidative damage generated by a large number of biotic and abiotic stress (Mittler, 2002) by increasing antioxidant systems composed by antioxidant molecules, such as reduced glutathione (GSH) and ascorbate (AsA), and antioxidant enzymes, such as ascorbate peroxidase (APX), catalase (CAT) and superoxide dismutase (SOD). Cervilla et al. (2007) and Melgar et al., (2009) shown B excess stimulated antioxidant enzymes and in particular the activity of the ascorbate cycle related enzymes. Conversely, in citrus leaves B deficiency stronger enhanced antioxidant defences than B toxicity; in fact AsA and GSH contents were reduced in comparison to control leaves of plants submitted to B excess (Han et al., 2009). Furthermore, many evidences confirm that other molecules, such as phenols, anthocyanins and flavonoids, can raise antioxidant ability in many species, in particular in plants belonging to the *Lamiaceae* family such as basil, rosemary, sage, oregano and thyme (Zheng and Wang, 2001; Javanmardi et al., 2002; Shan et al., 2005; Surveswaran et al., 2007; Lee and Scagel, 2009). Typically, polyphenolic compounds are produced by plants for different reasons: defense against microorganisms, insects, or herbivores (Herms and Mattson, 1992; Crozier et al., 2006, Mullen et al., 2007), nutrient availability (Herms and Mattson, 1992) and exposure to UV radiation (Rozema et al., 1997). Moreover, anthocyanins, which are responsible for the primary red and blue pigments in plants, have been recognized as contributing to plant growth and development (Holton and Cornish, 1995) and they have also shown a significant antioxidant ability (Tsuda et al., 1996). Winthrop and James (1998) reported that purple-leafed cultivars of sweet basil could be a rich source of anthocyanins and, on the view explained above, a source of antioxidant power. The antioxidant ability of phenols and anthocyanins is mainly attributable to their redox properties, which allows them the ability to act as reducing agents, hydrogen donators and singlet oxygen quenchers. In addition to the previous consideration, they have a metal chelation potential (Rice-Evans et al., 1997). It has also been suggested that the buildup of anthocyanins under direct salt stress is mainly referable to the photoprotection of chlorophylls by these compounds (Gould et al., 2000). Moreover, anthocyanins are hypothesized to be involved in osmotic

regulation (Choinski and Johnson, 1993; Chalker-Scott 2002) and many studies have confirmed that plant tissues containing high levels of anthocyanins are usually rather resistant to drought and salt (Chalker-Scott, 1999). For example, a purple-leafed pepper tolerated salt stress better than a green-leafed cultivar (Bahler et al., 1991) and it is interesting to underline that the high drought and salt tolerant resurrection plant (*Craterostigma plantagineum*) contains the greatest amount of anthocyanins during dehydration as compared to the hydrated stage (Sherwin and Farrant, 1998). Eraslan et al. (2008) found an anthocyanins increment in *Spinacia oleraceae* exposed to B excess and also under other salt stress conditions, i.e. NaCl.

Limited information is available about antioxidant responses to B toxicity; therefore, a study was carried out to establish modifications and contribution of antioxidants in plant protection against B excess. To this aim two sweet basil cultivars were compared: the purple-leafed 'Red Rubin' that exhibited scarce symptoms of B toxicity, and the green-leafed 'Tigullio', which shown extended symptoms of leaf damage.

Materials and Methods

Plant materials and growing conditions

The experiments were conducted in a glasshouse in Pisa from May to July 2011 utilizing rockwool plug trays (Grodan® Pro Plug) for both germination and hydroponic cultivation. After germination, the trays were placed in "floating raft systems" with 8 L of stagnant nutrient solution, which was continuously aerated. The nutrient solution contained the following concentration of macronutrient and trace elements: NO_3^- 14 mM, NH_4^+ 0,5 mM, P 1.2 mM, K^+ 10 mM, Ca^{2+} 4 mM, Mg^{2+} 0.75 mM, Na^+ 10-01 mM, SO_4^{2-} 1.97 mM, Fe^{2+} 56 µM, BO_3^- 23.1 µM, Cu^{2+} 1 µM, Zn^{2+} 5 µM, Mn^{2+} 10 µM, Mo^{3+} 1 µM. Electrical conductance (EC) was 3.04 dS m^{-1}; pH values adjusted to 5.5-6 with diluted sulphuric acid. One month after sowing, plants were submitted to two different concentrations of B (2 and 20 mg L^{-1}) adding boric acid to the nutrient solution mentioned above. Control plants were subjected to 0.2 mg L^{-1} of B that represents a safe concentration for a lot of plant species.

Climatic parameters were continuously monitored by means of a weather station located inside the glasshouse. The minimum and ventilation air temperature were 16°C and 27°C respectively; maximum temperature reached up to 30-32°C in sunny hours. Daily global radiation and mean air temperature averaged respectively 12.3 MJ m^{-2} and 24.8°C. Sweet basil leaves were randomly collected for physiological and biochemical analysis after 20 d of treatments.

Boron determination

Each sample was dried at 50° C for 48 h, and 0.5 g of dry weight (DW) was digested with nitric and perchloric acid at 230°C for 1 h. The B concentration was colorimetrically determined (420 nm) using azometine-H method (Wolf, 1974).

Photosynthetic parameters, chlorophyll a fluorescence, chlorophylls and carotenoids content

Gas exchange measurements were performed for net CO_2 assimilation rate (A, mol CO_2 m^{-2} s^{-1}), stomatal conductance (g_s, mol H_2O m^{-2} s^{-1}), transpiration (E, mol H_2O m^{-2} s^{-1}) and intercellular CO_2 concentration (Ci, µmol CO_2 mol air^{-1}) at 10.00–13.00 am (5 replicates) in fully expanded leaves. All measurements were carried out in the greenhouse at saturating light (800 µmol m^{-2} s^{-1} over the PAR waveband) using a portable infrared gas analyzer Li-Cor 6400 (Li-Cor Inc., Lincoln, NE, USA) operating at 35±0.5 Pa ambient CO_2.

The imaging technique was performed utilizing an IMAGING-PAM Chlorophyll Fluorometer (Walz, Effeltrich, Germany). Details of chlorophyll fluorescence imaging capture are reported by Guidi et al. (2007). The current fluorescence yield (F_t) was continuously measured and the F_o images were recorded in a quasi-dark state. The maximum fluorescence yield F_m was determined with a saturating pulse of 8000 µmol m^2 s^1 PPFD for 1–2 s. The images of F_o and F_m were subtracted and divided [(F_m-F_o)/F_m] to draw the maximum quantum efficiency of PSII photochemistry F_v/F_m image. The current fluorescence yield (F_t) and the maximum light adapted fluorescence (F'_m) were determined in the presence of an actinic illumination of 400 µmol m^2 s^1, then Φ_{PSII} was computed as the quotient (F'_m-F'_t)/F'_m (Genty et al., 1989). The coefficients of

photochemical and non-photochemical quenching (q_P and q_{NP}) were calculated according to Schreiber et al. (1986). Correct F_o determinations require the application of far red light, which could disturb the fluorescence imaging. Therefore, F'_o was computed using the approximation of Oxborough (2004): $F_o = F_o/(F_v/F_m + F_o/F_m)$. Images of the fluorescence parameters were displayed by means of a false color code ranging from 0.00 (black) to 1.00 (purple). Single leaves were utilized for analysis.

Chlorophylls and carotenoids were determined following the method described by Jingxian and Kirkham (1996) with some modifications. Leaf samples, 0.3 g fresh weight (FW), were ground in 8 mL of 80% acetone. The homogenate was centrifuged at 7000 rpm for 10 min. The supernatant was collected and the pellet was suspended in 1 mL of 80% acetone. Sample was again centrifuged as mentioned above; eluitions and centrifugations were repeated until the pellet was completely discolored. The supernatant absorbances at 663, 648 and 470 nm were measured. Chl *a* and *b* content and total carotenoids (xanthophylls and *β*-carotene) were calculated according to Lichtenthaler (1987).

Phenols and anthocyanins

Leaf samples were dried for 48 hours at 50°C in an oven. The dried material (within 10-15 mg) was mixed with 1 mL of 80% aqueous methanol and shaken overnight at room temperature. The mix was centrifuged at 12000 rpm for 20 min and the extract was stored at -80°C until analysis. Phenols were evaluated according to the method reported by Dewanto et al. (2002) based on Folin-Ciocalteau reagent. Values were expressed as mg gallic acid g^{-1} dry weight (DW).

For anthocyanins quantification, 10-15 mg of dried samples were mixed with 1 mL of acidified methanol (15% HCL v/v) and shaken overnight at room temperature. Total anthocyanins were evaluated with a slightly modified version of Abdel-Aal and Huel's (1999) method. Anthocyanin-containing basil extract (150 µL) was added to 1 mL of acidified methanol (15% HCL v/v) and its absorbance was read at 535 nm against a blank. Calibration curve was realized with cyanidin-3-glucoside in acidified methanol (15% HCL v/v). Total anthocyanins concentration was expressed as mg anthocyanins equivalent (AE) g^{-1} DW.

Antioxidant molecules: ascorbate and glutathione

Total ascorbate (AsA_T), dehydroascorbate (DHA) and reduced ascorbate (AsA) were determined as described by Degl'Innocenti et al. (2005), based on the method of Kampfenkel et al. (1995). Ascorbate (AsA_T, DHA and AsA) content was expressed as mg 100 g^{-1} FW.

Total glutathione (Glu_T), oxidized glutathione (GSSG) and reduced glutathione (GSH) were determined as described by Ryang et al. (2009) with a few modifications. Raw material (2 g) was grounded in 5 mL of HCl 0.1 M to prepare the supernatant; calibration curve was realized with glutathione disulphide (GSSG) from 4.5 μM to 90 μM and the absorbances were read at 412 nm against a blank. Glutathione content (Glu_T, GSSG and GSH) was expressed as nmol g^{-1} FW.

Antioxidant enzymes: APX, SOD, CAT

Antioxidant enzyme activities were measured in fresh leaf material, which was extracted as described by Di Cagno et al. (2001). APX (EC 1.11.1.11) activity was measured as described by Nakano and Asada (1981), comparing the absorbance at 290 nm, resulting from ascorbate oxidation. SOD (EC 1.15.1.1) activity was measured at 560 nm, based on the inhibition of nitroblue tetrazolium (NBT) reduction by SOD. One unit of SOD was defined as the enzymatic amount needed to reduce by 50% the NBT reduction state (Beyer and Fridovich, 1987). CAT (EC 1.11.1.6) activity was measured at 270 nm (Cakmak and Marschner, 1992) determining the rate of conversion of H_2O_2 to O_2.

DPPH scavenging ability

The antioxidant activity of each basil sample was determined using a modified version of the 2,2-diphenyl-1-picrylhydrazyl radical (DPPH) scavenging assay as described by Kim et al. (2005). The % of DPPH free radical scavenging activity was calculated according to the following equation:

$$\% \text{ DPPH free radical scavenging} = [\ 1 - (\text{ABS sample}/\text{ABS control})\ ] \times 100$$

The antioxidant activity was determined comparing the % of DPPH free radical scavenging of each basil sample to a calibration curve prepared with trolox, a well-known antioxidant standard. Antioxidant activities were expressed as the trolox equivalent antioxidant capacity (TEAC, mmol of trolox equivalents g^{-1} DW).

Lipid peroxidation

Oxidative damage was estimated in terms of lipid peroxidation measuring the MDA accumulation (Hodges *et al.*, 1999), which takes into account the possible influence of interfering compounds in the assay (e.g. anthocyanins) for the 2-thiobarbituric acid (TBA)-reactive substances. MDA level were expressed as nmol g^{-1} FW.

Statistics

The experiment was repeated twice with similar results; a representative run is reported herein. Reported data represent at least the mean of five replications (n=5). The data were compared by two-way analysis of variance (ANOVA) with B treatment and genotype as variability factors. Differences among treatment means were evaluated by Fisher's least-significant difference test (LSD) for P=0.05. Percentage values were angularly transformed before ANOVA test. For comparison between two means, paired-*t* Student's test was applied.

Results

Plant growth and B accumulation

The most important result obtained was the difference in the response to high B concentrations recorded for the two cultivars. The harshest B concentration in nutrient solution induced a decrease in FW of total plants particularly in 'Tigullio', where the reduction was about by 60% in comparison to the controls (**Table 3.1**). A similar decrement was recorded for total DW in 'Tigullio' whereas in 'Red Rubin' plants DW significantly increased with B concentration in the nutrient solution (**Table 3.1**). However, the DW/FW ratio declined in both cultivars at 20 mg L^{-1} B; the different pattern observed in 'Red Rubin' and 'Tigullio' was confirmed by the picture recorded for FW and DW (**Table 3.1**).

Table 3.1. Total plant biomass (Fresh weight, FW; dry weight, DW; DW/FW % variation) of two cultivars of *O. basilicum* (T; 'Tigullio' and RR; 'Red Rubin') after 20 days of treatment with different concentrations of B (expressed as mg L^{-1}).

	TREATMENTS	FW (g)	DW (g)	DW/FW (%)
Total Plant Biomass	T 0.2 mg/L	10.16 ± 0.03 [b]	0.61 ± 0.01 [c]	6.00 ± 0.02 [f]
	T 2 mg/L	10.97 ± 0.09 [a]	0.71 ± 0.01 [a]	6.55 ± 0.03 [e]
	T 20 mg/L	3.82 ± 0.05 [e]	0.29 ± 0.01 [f]	7.59 ± 0.04 [b]
	RR 0.2 mg/L	8.47 ± 0.06 [c]	0.57 ± 0.01 [e]	6.75 ± 0.01 [d]
	RR 2 mg/L	8.57 ± 0.04 [c]	0.59 ± 0.01 [d]	6.92 ± 0.02 [c]
	RR 20 mg/L	7.88 ± 0.04 [d]	0.63 ± 0.01 [b]	8.00 ± 0.02 [a]
	B	*** $LSD_{0.05}$ 0.13	*** $LSD_{0.05}$ 0.010	*** $LSD_{0.05}$ 0.05
	Cultivar	ns	*** $LSD_{0.05}$ 0.08	*** $LSD_{0.05}$ 0.04
	B x cultivar	*** $LSD_{0.05}$ 0.18	*** $LSD_{0.05}$ 0.014	*** $LSD_{0.05}$ 0.07

All data are reported as mean of 5 replicates ± SE. Means with different letters are at least significantly different (P=0.05) according to Fisher's least-significant difference test (LSD). ns (not significant, P>0.05); *P<0.05; **P<0.01; ***P<0.001.

The occurrence of leaf symptoms induced by B toxicity was evaluated by using IMAGEJ Software that allows assessing the percentage of necrotic area and in **Fig. 3.1** the obtained results are reported. 'Tigullio' necrotic areas mean was significantly wider than in 'Red Rubin' leaves: 40% ± 4.4 against 14 % ± 1.6, respectively.

Leaf B content increased following B severity in the nutrient solution (**Fig. 3.2**). However, B content was larger in 'Tigullio' leaves as compared to 'Red Rubin', in fact at 20 mg L^{-1} B 'Tigullio' leaves contained about 1200 mg kg^{-1} DW of B against 600 mg kg^{-1} DW recorded in 'Red Rubin' (**Fig. 3.2**).

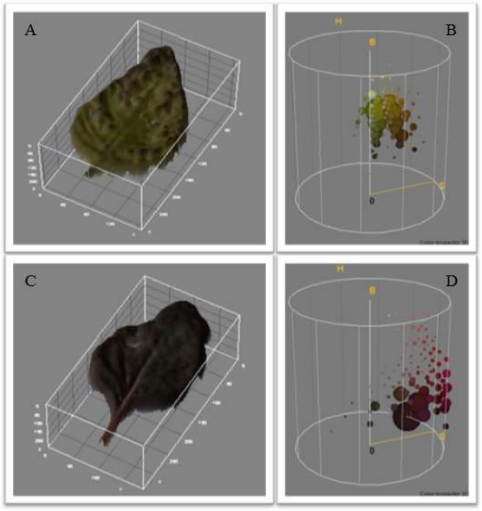

Fig. 3.1. Typical output of IMAGEJ Software with HSB Histogram analysis output of 'Tigullio' (A) and 'Red Rubin' (C) leaf with necrotic areas from plants grown at 20 mg L^{-1} of boron. (B) and (D) respectively represent the color analysis of A and C leaf with Color Inspector 3D Tool of IMAGEJ.

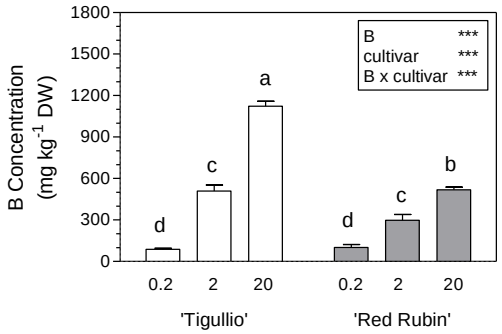

Fig. 3.2. B concentration in leaves of two cultivars of *O. basilicum* ('Tigullio' white bars and 'Red Rubin' dark bars) hydroponically grown for 20 d with different B concentrations in the nutrient solution (expressed as mg L^{-1}). Means (n=5±SE) keyed with different letters were at least significantly different (P=0.05) according to Fisher's least-significant difference test (LSD). Legend: ns (not significant, P>0.05); *: P<0.05; **: P<0.01; ***: P<0.001.

Gas exchange, chlorophyll a fluorescence and pigments content

CO_2 assimilation rate at light saturation level significantly decreased at the higher B concentration in both cultivars and this reduction was attributable to stomatal closure (**Fig. 3.3**). However, in 'Tigullio' Ci did not significantly change indicating, in addition, the occurrence of mesophyllic limitations that were not noticed in 'Red Rubin' where Ci significantly decreased.

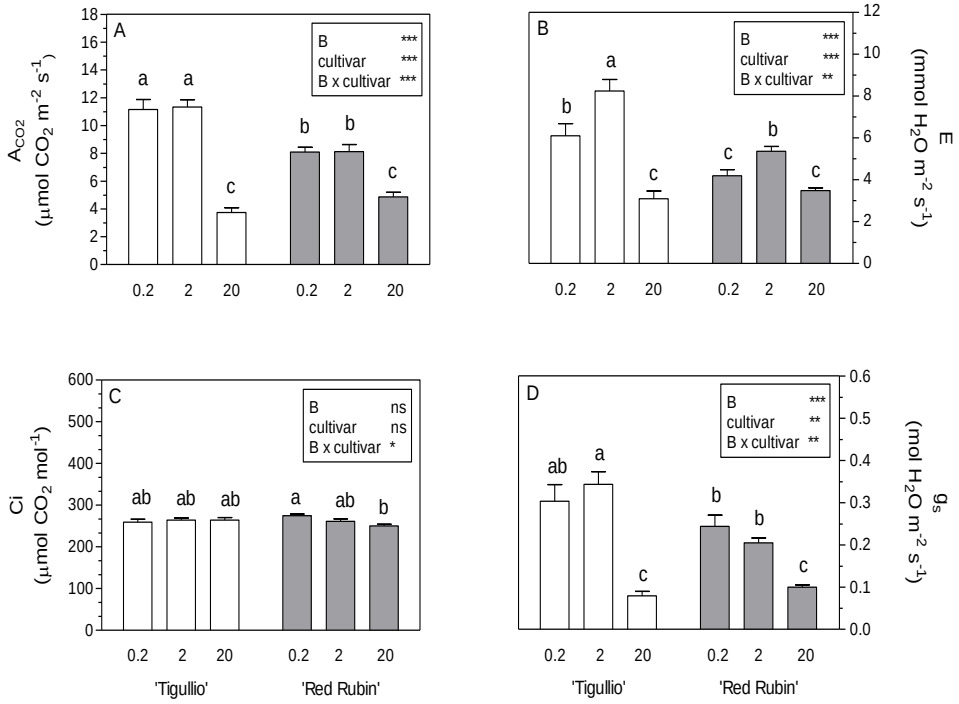

Fig. 3.3. CO_2 assimilation rate (A), transpiration (B), intercellular CO_2 concentration (C) and stomatal conductance (D) in leaves of two cultivars of *O. basilicum* ('Tigullio' white bars and 'Red Rubin' dark bars) hydroponically grown for 20 d with different B concentrations in the nutrient solution (expressed as mg L^{-1}). Means (*n*=5±SE) keyed with different letters were at least significantly different (P=0.05) according to Fisher's least-significant difference test (LSD).). Legend: ns (not significant, P>0.05); *: P<0.05; **: P<0.01; ***: P<0.001.

In 'Tigullio' leaves from plants grown at the harshest B concentration the ratio F_v/F_m, which indicates the maximal photochemical efficiency of PSII, shown large heterogeneity on leaf lamina; in many areas it was closed to 0 (**Fig. 3.4**). However, in non-symptomatic regions F_v/F_m shown typical values found in healthy leaves (Bjorkman and Demmig, 1994) (**Fig. 3.4** and **Table 3.2**). A similar pattern was observed in 'Tigullio' concerning the actual photochemical efficiency Φ_{PSII} although in the presence of 2 mg L^{-1} of B in the nutrient solution this parameter also changed (**Fig. 3.4** and **Table 3.2**). The decrease in Φ_{PSII} was attributable to a decline in q_P (**Fig. 3.4**).

Even in 'Red Rubin' grown at 20 mg L^{-1} of B, the F_v/F_m ratio significantly increased in leaf margins, where necrotic areas were evidenced (**Fig. 3.4** and **Table 3.2**). Differently to 'Tigullio', in 'Red Rubin' the actual PSII photochemical efficiency, q_P

and q_{NP} significantly increased and the heterogeneity on leaf lamina was evidenced only at the margins of leaves and only in the most severe B condition (**Fig. 3.4**).

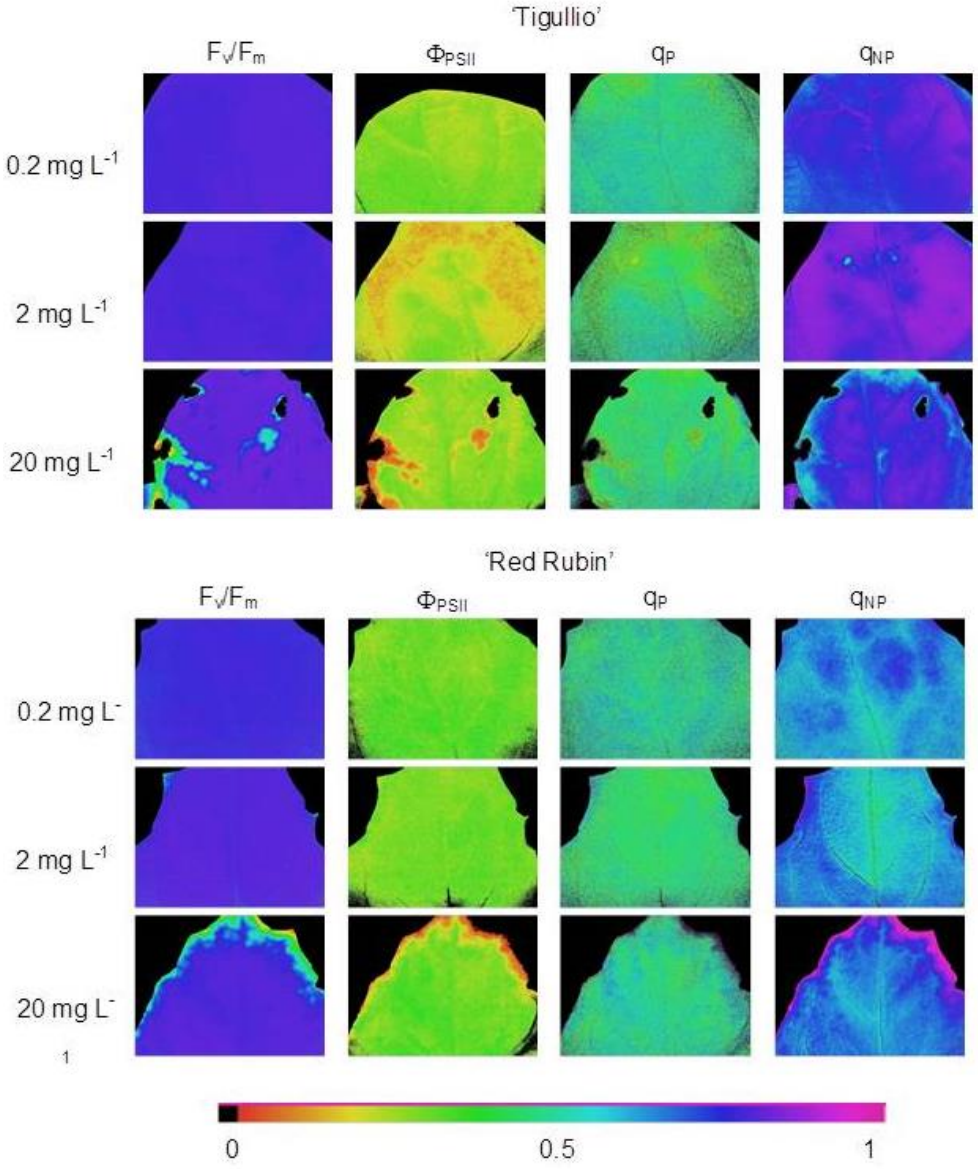

Fig. 3.4. Representative fluorescence images of maximum of PSII (F_v/F_m) efficiency, the proportion of absorbed light, which is utilized for photosynthetic electron transport (Φ_{PSII}), the photochemical quenching coefficient (q_P) and non-photochemical quenching coefficient (q_{NP}) in leaves of two cultivars of *O. basilicum* ('Tigullio' and 'Red Rubin') hydroponically grown for 20 d with different B concentrations in the nutrient solution (expressed as mg L^{-1}). All images are normalized to the false colors bar provided. The pixel value display is based on a false-color scale ranging from black (0-0.04) via red, yellow, green, blue to purple (ending at 1).

Table 3.2. Chlorophyll fluorescence parameter (F_v/F_m ratio and Φ_{PSII}) in leaves of two varieties of *O. basilicum* ('Tigullio' and 'Red Rubin') after 20 days of treatment with different concentrations of B (expressed as mg L^{-1}). Not present (np) represent samples without necrotic area on leaves.

	TREATMENTS	HEALTHY AREA	NECROTIC AREA
F_v/F_m	T 0.2 mg/L	0.796 ± 0.004 ^{c}	np
	T 2 mg/L	0.796 ± 0.002 ^{c}	np
	T 20 mg/L	0.811 ± 0.006 ^{a}	0.055 ± 0.013 B
	RR 0.2 mg/L	0.781 ± 0.001 ^{d}	np
	RR 2 mg/L	0.780 ± 0.002 ^{d}	np
	RR 20 mg/L	0.801 ± 0.001 ^{b}	0.27 ± 0.025 A
	B	*** $LSD_{0.05}$ 0.002	** $LSD_{0.05}$ 0.077
	Cultivar	*** $LSD_{0.05}$ 0.001	
	B x cultivar	* $LSD_{0.05}$ 0.003	
Φ_{PSII}	T 0.2 mg/L	0.282 ± 0.009 ^{d}	np
	T 2 mg/L	0.218 ± 0.015 ^{e}	np
	T 20 mg/L	0.279 ± 0.005 ^{d}	0.038 ± 0.002 A
	RR 0.2 mg/L	0.307 ± 0.011 ^{c}	np
	RR 2 mg/L	0.318 ± 0.005 ^{b}	np
	RR 20 mg/L	0.325 ± 0.007 ^{a}	0.083 ± 0.002 A
	B	*** $LSD_{0.05}$ 0.002	ns
	Cultivar	*** $LSD_{0.05}$ 0.002	
	B x cultivar	*** $LSD_{0.05}$ 0.003	

Each value represents the mean of 5 replicates ± SE. Means with different letters are at least significantly different (P=0.05) according to Fisher's least-significant difference test (LSD). ns (not significant, P>0.05); *: P<0.05; **: P<0.01; ***: P<0.001. Means with different capital letters for necrotic area values are at least significantly different (P<0.05) according to T-student test.

In both genotypes Φ_{PSII} decreased increasing light intensity and no differences were found between controls and leaves of plants grown with 2 mg L^{-1} of B (**Fig. 3.5**). This pattern was dramatically altered in necrotic portions of the leaf lamina. Similar trend was observed for 'Red Rubin' even though Φ_{PSII} values were higher when compared to 'Tigullio' (**Fig. 3.5**).

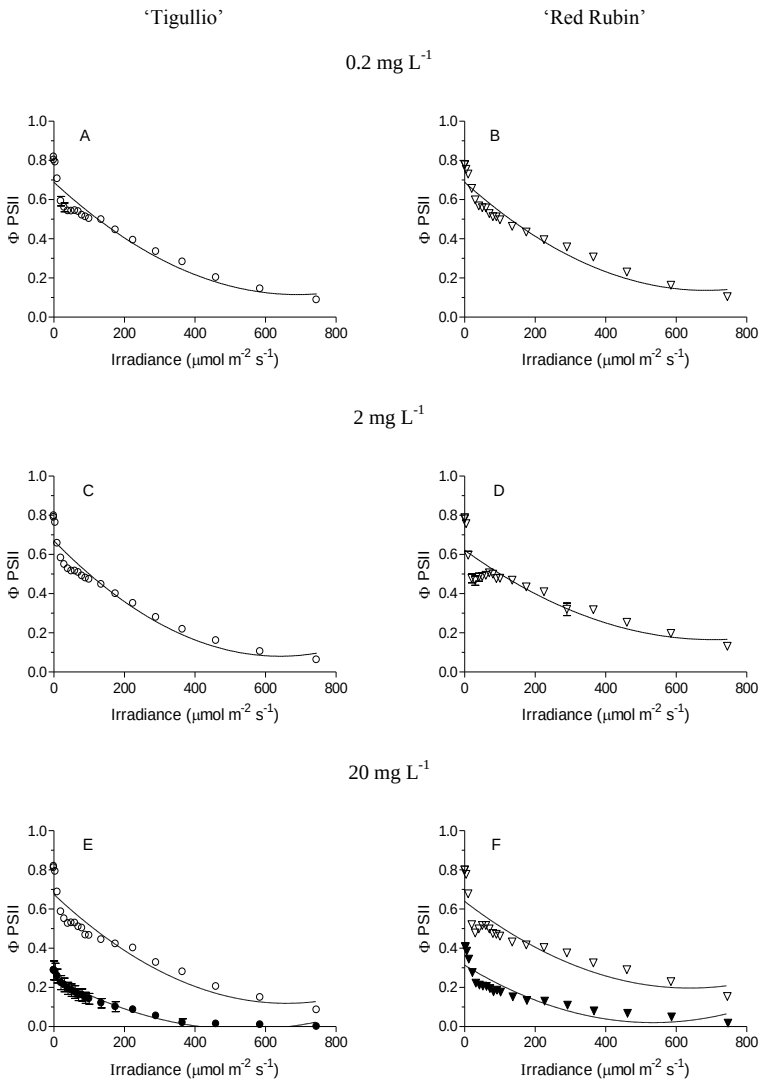

Fig. 3.5. Light response curves of photochemical PSII efficiency (Φ_{PSII}) of healthy leaf areas in two cultivars of *O. basilicum* ('Tigullio' open circles, 'Red Rubin' open triangles) hydroponically grown for 20 d with different B concentrations: 0.2, 2, 20 represent mg L^{-1} of B in nutrient solution. Full circles and full triangles represent respectively 'Tigullio' necrotic areas and 'Red Rubin' necrotic areas. Measurements were performed at 25±0.5 °C. Each data set represents the mean of 5 replicates ± SE.

Although chlorophylls total content did not show significant differences for the 'B *x* cultivar' interaction of factors (**Fig. 3.6A**), B significantly induced a decline in chlorophylls content at 20 mg L^{-1}. After the stress induced by B excess, in 'Tigullio' leaves higher chlorophylls total content than 'Red Rubin' leaves was recorded.

Carotenoids were incremented in ‘Tigullio’ leaves by the most severe B treatment while in ‘Red Rubin’ the highest carotenoids content was recorded for control leaves and it was significantly decreased for 2 and 20 mg L^{-1} of B in the growing medium (**Fig. 3.6B**).

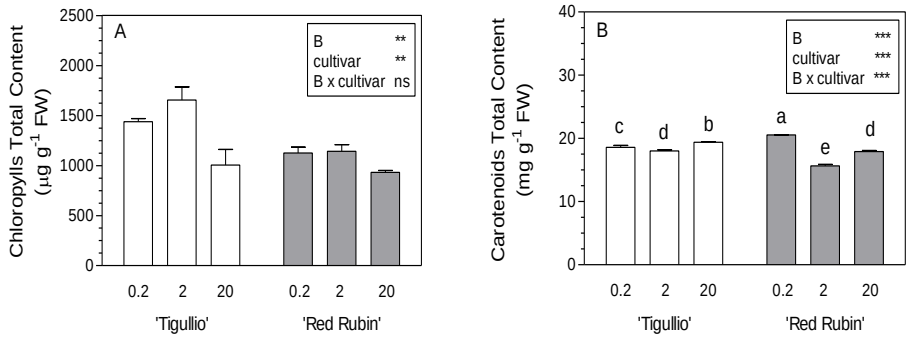

Fig. 3.6. Chlorophylls (A) and carotenoids total content (B) in leaves of two cultivars of *O. basilicum* (‘Tigullio’ white bars and ‘Red Rubin’ dark bars) hydroponically grown for 20 d with different B concentrations in the nutrient solution (expressed as mg L^{-1}). Means (n=5±SE) keyed with different letters were at least significantly different (P=0.05) according to Fisher’s least-significant difference test (LSD). Legend: ns (not significant, P>0.05); *: P<0.05; **: P<0.01; ***: P<0.001. For chlorophyll content the two factors interaction was not significant and keyed letters for different means are not reported.

Total phenols, anthocyanins

Boron treatments enhanced the total phenolic content in both cultivars (**Fig. 3.7A**) and the highest concentration was recorded at 20 mg L^{-1} of B (6±0.20 and 6±0.01 mg GA g^{-1} DW respectively in ‘Tigullio’ and ‘Red Rubin’ leaves). On the other hand, B influenced anthocyanins content only in ‘Red Rubin’ leaves (**Fig. 3.7B**), where their content was increased for both treatments in comparison to the control leaves. Conversely, no differences among treatments were observed in ‘Tigullio’.

Antioxidant molecules: ascorbate and glutathione

The two cultivars demonstrated a different behavior under B excess concerning the extent of the two main antioxidant molecules: ascorbate and gluthatione (**Table 3.3** and **3.4**). In ‘Tigullio’ plants AsA_T in leaves resulted significantly incremented (+54% and +81% respectively for 2 and 20 mg L^{-1} of B treatment than control plants), while a fall

in its concentration was recorded in 'Red Rubin' leaves at 20 mg L^{-1} B compared to control (-37%).

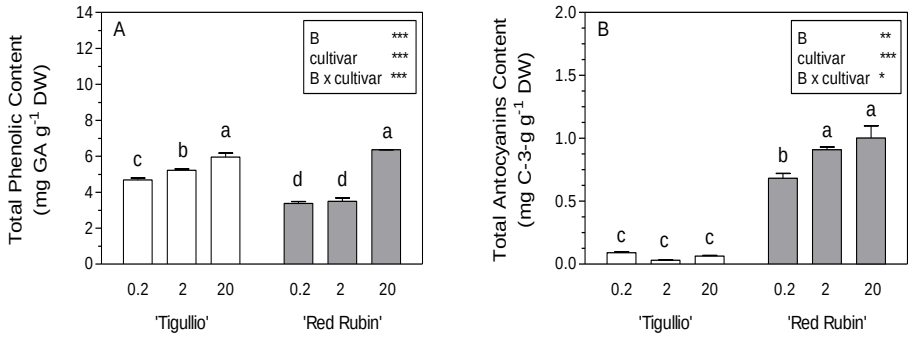

Fig. 3.7. Total phenolic (A) and total anthocyanins content (B) in leaves of two cultivars of *O. basilicum* ('Tigullio' white bars and 'Red Rubin' dark bars) hydroponically grown for 20 d with different B concentrations in the nutrient solution (expressed as mg L^{-1}). Means (n=5±SE) keyed with different letters were at least significantly different (P=0.05) according to Fisher's least-significant difference test (LSD).). Legend: ns (not significant, P>0.05); *: P<0.05; **: P<0.01; ***: P<0.001.

However, one has to consider that AsA_T content was significantly higher in 'Red Rubin' control plants in comparison to 'Tigullio' controls. Thus, in 'Red Rubin' the constitutive ascorbate amount could strongly contribute to avoid oxidative load. Moreover, we recorded a decrease in the ratio AsA/AsA_T for the two cultivars under investigation and it suggested that both 'Tigullio' and 'Red Rubin' reacted to the oxidative stress generated by B toxicity utilizing ascorbate as antioxidant.

A similar trend to that recorded for AsA_T was also found for Glu_T (**Table 3.4**); in fact, under control condition 'Red Rubin' leaves shown a significantly stronger Glu_T content than 'Tigullio' leaves (110±1.10 against 4±0.01 nmol g^{-1} FW).

Moreover, in the purple cultivar Glu_T content decremented concurrently with the most severe B concentration whereas in 'Tigullio' plants a significant buildup was recorded at 2 and 20 mg L^{-1} compared to control. Furthermore, in 'Tigullio' leaves at 20 mg L^{-1} of B the ratio Glu/Glu_T decreased in comparison to control, whereas the opposite phenomenon was observed in 'Red Rubin' leaves.

Table 3.3. AsA, DHA, AsA_T concentrations and AsA/AsA_T ratio in leaves of two cultivars of *O. basilicum* (T; 'Tigullio' and RR; 'Red Rubin') after 20 days of treatment with different concentrations of B (expressed as mg L^{-1}).

TREATMENTS	Asa (mg 100 g^{-1} FW)	DHA (mg 100 g^{-1} FW)	Asa_T (mg 100 g^{-1} FW)	AsA/AsA_T (%)
T 0.2 mg/L	3.80 ± 0.26 ^{e}	4.48 ± 0.71 ^{c}	8.28 ± 0.53 ^{d}	45.93 ± 0.35 ^{c}
T 2 mg/L	3.38 ± 0.43 ^{e}	9.36 ± 0.39 ^{b}	12.74 ± 0.71 ^{c}	23.63 ± 0.89 ^{e}
T 20 mg/L	5.96 ± 0.50 ^{d}	9.04 ± 0.79 ^{b}	15.00 ± 0.68 ^{c}	39.58 ± 1.60 ^{d}
RR 0.2 mg/L	19.05 ± 0.09 ^{a}	16.77 ± 1.24 ^{a}	34.92 ± 0.94 ^{a}	54.64 ± 1.22 ^{a}
RR 2 mg/L	17.48 ± 0.57 ^{b}	16.41 ± 1.60 ^{a}	33.88 ± 1.40 ^{a}	51.61 ± 0.78 ^{ab}
RR 20 mg/L	11.08 ± 0.57 ^{c}	10.91 ± 0.74 ^{b}	21.99 ± 1.19 ^{b}	50.38 ± 0.66 ^{b}
B	*** $LSD_{0.05}$ 0.96	* $LSD_{0.05}$ 2.17	** $LSD_{0.05}$ 2.09	*** $LSD_{0.05}$ 2.18
Cultivar	*** $LSD_{0.05}$ 0.78	*** $LSD_{0.05}$ 1.77	*** $LSD_{0.05}$ 1.71	*** $LSD_{0.05}$ 1.78
B x cultivar	*** $LSD_{0.05}$ 1.35	*** $LSD_{0.05}$ 3.06	*** $LSD_{0.05}$ 2.95	*** $LSD_{0.05}$ 3.08

All data are reported as mean of 5 replicates ± SE. Means with different letters are at least significantly different (P=0.05) according to Fisher's least-significant difference test (LSD). ns (not significant, P>0.05); *P<0.05; **P<0.01; ***P<0.001.

Table 3.4. GSH, GSSG, Glu_T concentrations and GSH/Glu_T ratio in leaves of two cultivars of O. basilicum (T; Tigullio and RR; Red Rubin) after 20 days of treatment with different concentrations of B (expressed as mg L^{-1}).

TREATMENTS	GSH (nmol g^{-1} FW)	GSSG (nmol g^{-1} FW)	Glu_T (nmol g^{-1} FW)	GSH/Glu_T (%)
T 0.2 mg/L	3.38 ± 0.01	1.00 ± 0.01 ^{e}	4.38 ± 0.01 ^{d}	77.11 ± 0.05 ^{b}
T 2 mg/L	42.27 ± 2.93	4.39 ± 0.01 ^{e}	46.65 ± 2.93 ^{c}	90.53 ± 0.60 ^{a}
T 20 mg/L	23.67 ± 0.01	20.17 ± 1.13 ^{d}	44.97 ± 1.95 ^{c}	52.85 ± 2.30 ^{d}
RR 0.2 mg/L	32.69 ± 1.13	77.65 ± 2.25 ^{a}	110.35 ± 1.13 ^{a}	26.62 ± 0.92 ^{f}
RR 2 mg/L	65.38 ± 4.91	41.58 ± 1.95 ^{c}	106.96 ± 2.98 ^{a}	60.96 ± 2.88 ^{c}
RR 20 mg/L	47.34 ± 5.17	50.60 ± 2.98 ^{b}	97.95 ± 2.98 ^{b}	42.10 ± 3.93 ^{e}
B	*** $LSD_{0.05}$ 7.24	*** $LSD_{0.05}$ 3.89	*** $LSD_{0.05}$ 5.21	*** $LSD_{0.05}$ 2.30
Cultivar	*** $LSD_{0.05}$ 5.91	*** $LSD_{0.05}$ 3.17	*** $LSD_{0.05}$ 4.25	*** $LSD_{0.05}$ 1.87
B x cultivar	ns	*** $LSD_{0.05}$ 5.74	*** $LSD_{0.05}$ 7.38	*** $LSD_{0.05}$ 6.92

All data are reported as mean of 5 replicates ± SE. Means with different letters are at least significantly different (P=0.05) according to Fisher's least-significant difference test (LSD). For GSH parameter the interaction of the two factors was not significant and keyed letters for different means are not reported. ns (not significant, P>0.05); *P<0.05; **P<0.01; ***P<0.001.

Lipid peroxidation

Both 'Tigullio' and 'Red Rubin' plants subjected to the harshest B concentration shown the largest MDA values in leaf tissues (**Fig. 3.8**). However, in 'Tigullio' MDA levels were significantly higher than those recorded in 'Red Rubin' while no differences were found at 0.2 mg L^{-1} B (**Fig. 3.8**).

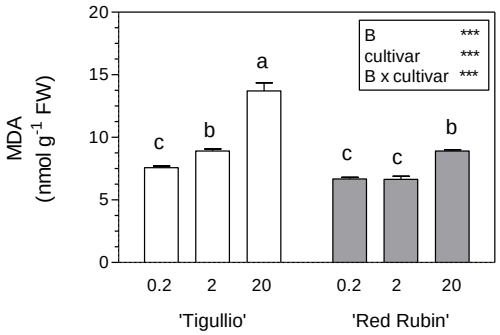

Fig. 3.8. Lipid peroxidation evaluated by MDA concentrations in leaves of two cultivars of *O. basilicum* ('Tigullio' white bars and 'Red Rubin' dark bars) hydroponically grown for 20 d with different B concentrations in the nutrient solution (expressed as mg L^{-1}). Means (*n*=5±SE) keyed with different letters were at least significantly different (P=0.05) according to Fisher's least-significant difference test (LSD). Legend: ns (not significant, P>0.05); *: P<0.05; **: P<0.01; ***: P<0.001.

DPPH scavenging ability

'Red Rubin' leaves from plants grown at 20 mg L^{-1} of B shown the strongest non-enzymatic antioxidant activity (**Fig. 3.9**) (150±0.10 mmol TE 100 g^{-1} FW).

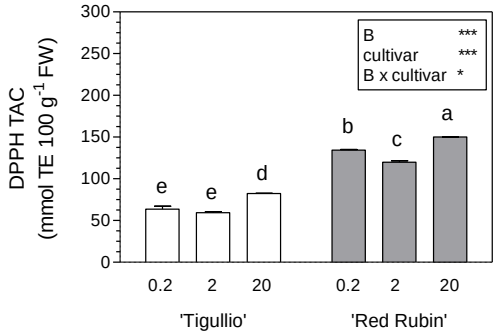

Fig. 3.9. Antioxidant ability determined by DPPH in leaves of two cultivars of *O. basilicum* ('Tigullio' white bars and 'Red Rubin' dark bars) hydroponically grown for 20 d with different B concentrations in the nutrient solution (expressed as mg L^{-1}). Means (*n*=5±SE) keyed with different letters were at least significantly different (P=0.05) according to Fisher's least-significant difference test (LSD).). Legend: ns (not significant, P>0.05); *: P<0.05; **: P<0.01; ***: P<0.001.

Notable, control plants of this cultivar already shown higher values of antioxidant ability (134±0.80 mmol TE 100 g^{-1} FW) than 'Tigullio' leaves from plants grown under each B concentration. However, the highest B concentration in the medium increased DPPH scavenging ability also in 'Tigullio' leaves from 64±3.50 mmol TE 100 g^{-1} FW (control) to 82±0.40 mmol TE 100 g^{-1} FW (20 mg L^{-1} B).

Antioxidant enzymes: SOD, APX, CAT

The activity of SOD, APX and CAT significantly increased for both cultivars at the most severe B treatment (**Fig. 3.10**). SOD larger increased in 'Tigullio' (+51% at 20 mg L^{-1} of B with respect to the control) than in 'Red Rubin' (+30%). On the other hand, APX and CAT activities were higher in 'Red Rubin' than in 'Tigullio' suggesting that all these three enzymes were involved in antioxidant responses albeit with a different contribution to ROS scavenging.

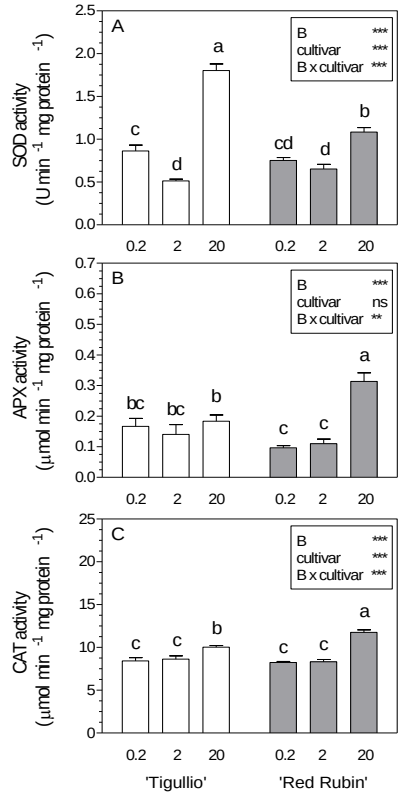

Fig 3.10. Activity of SOD (A) APX (B) CAT (C) in leaves of two cultivars of *O. basilicum* ('Tigullio' white bars and 'Red Rubin' dark bars) hydroponically grown for 20 d with different B concentrations in the nutrient solution (expressed as mg L^{-1}). Means (n=5±SE) keyed with different letters were at least significantly different (P=0.05) according to Fisher's least-significant difference test (LSD).). Legend: ns (not significant, P>0.05); *: P<0.05; **: P<0.01; ***: P<0.001.

Discussion

The first visible result obtained in this experiment was the different sensitivity to B excess shown by the two basil cultivars evaluated. In fact, marginal portion of leaves exhibited evident and marked symptoms of damage in 'Tigullio' whereas these were scarce in 'Red Rubin'. Our findings also demonstrated that high B concentration in the growth medium promoted B uptake in leaves and, consequently, a reduction in biomass for both cultivars was recorded. This outcome is in agreement with earlier researches in tomato (Gunes et al., 1999, Alpaslan and Gunes, 2001; Ben-Gal and Shani, 2002; Cervilla et al., 2007), pepper (Yermiyahu et al., 2008), cucumber (Alpaslan and Gunes, 2001) and sunflower (Ruiz et al., 2003). However, 'Red Rubin' shown lesser biomass reduction and lesser B accumulation in leaves than 'Tigullio'.

CO_2 photoassimilation significantly declined in both cultivars following B stress but in 'Tigullio' the reduction was related to mesophyllic and stomatal limitations while in 'Red Rubin' only stomatal closure was recorded. Stomatal and non-stomatal limitations attributable to B excess were already shown in 'Navelina' orange plants (Papadakis et al., 2004a) while in kiwifruit B toxicity induced a reduction in CO_2 photoassimilation without changes in stomatal conductance (Sotiropoulos et al., 2002).

Results obtained from gas exchange were in agreement with those found in chlorophyll fluorescence analysis. In fact, the q_P recorded in healthy tissue of the leaves was significantly higher in B stressed leaves of 'Red Rubin' as compared to 'Tigullio'. In both red and green leaves, chronic photoinhibition did take place according to variable to maximum chlorophyll fluorescence ratio (F_v/F_m). In 'Tigullio' the recorded reduction in CO_2 assimilation was related to stomatal closure as well as to a reduced q_P, which induced a fall of Φ_{PSII}. On the other hand, in the green-leafed cultivar the mechanisms aimed to dissipate the excess of excitation energy were not enhanced and q_{NP} decreased following B stress. The picture of 'Red Rubin' leaves was completely different; q_{NP} and Φ_{PSII} values significantly rose in response to B excess according to previous findings in *Fagopyrum dibotrys*, where red leaves shown a higher q_{NP} as compared to green leaves (Lan et al., 2011). In conclusion, red leaves demonstrated a better photoprotection ability than green leaves even thought this trait influenced the reduction of CO_2 assimilation rate and consequently the reduced plant growth rate as

demonstrated by differences in biomass production between the two cultivars under optimal B supply.

In general, B induced a decrease in chlorophylls content in both cultivars ($LSD_{0.05}$=155.82) in accordance with recent reports (Papadakis et al., 2004a, 2004b; Eraslan et al., 2007a, 2008; Han et al., 2009; Wang et al., 2011). This decline was probably influenced by damages that occur in the chloroplast structure, in particular in the thylakoid membrane due to lipid peroxidation propagated by ROS triggered by B toxicity. Moreover, a concomitant abatement in carotenoids content took place under B toxicity in 'Red Rubin' leaves, as already described by Wang et al. (2011) and Singh et al. (2012). The decrease of carotenoids could be related to the observed buildup in anthocyanins, which can actively contribute to photoprotect the photosynthetic apparatus and also to act as antioxidant molecules.

Sweet basil plants subjected to the harshest B treatment exhibited the highest MDA levels as already reported for other species (e.g. grape, Gunes et al., 2006 and Soylemezoglu et al., 2009; tomato, Cervilla et al., 2007; and; chickpea, Ardic et al., 2009). However, it is interesting to underline that lower MDA levels in leaves were recorded for 'Red Rubin' cultivar grown at 20 mg L^{-1} of B compared to 'Tigullio' plants submitted to the same severity of treatment. Moreover, in 'Red Rubin' MDA products did not yield significant differences between control plants and plants grown at 2 mg L^{-1} while the opposite result was found in 'Tigullio'. This suggested that purple-leafed basil can contrast oxidative damage that already affected 'Tigullio' at 2 mg L^{-1} B. The best protection of 'Red Rubin' against oxidative damage could be positively related to an enhanced antioxidant system, especially due to AsA, GSH and anthocyanins. In fact, 'Red Rubin' leaves shown the highest non-enzymatic antioxidant activity. Moreover, in both sweet basil cultivars, 20 mg L^{-1} B increased leaf antioxidant ability, albeit it was considerably higher in purple leaves than in green leaves also under control conditions. Similar results were recorded in other species, for instance in tomato (Cervilla et al., 2007), apple (Sotiropolus et al., 2006) and spinach (Gunes et al, 2007; Eraslan et al., 2008). Thus, it is suggested that B excess can enhance non-enzymatic antioxidant response in plants.

In this work B (20 mg L^{-1}) promoted a reduction in AsA_T content in 'Red Rubin' leaves while a rise was recorded for 'Tigullio' leaves in response to B excess. However, the ratio AsA/AsA_T declined in both 'Tigullio' and 'Red Rubin' suggesting that both genotypes utilized ascorbate as antioxidant, as it was previously hypothesized in tomato (Cervilla et al., 2007). Furthermore, it is remarkable that species and/or cultivars (like 'Red Rubin') with strong APX activity and then large AsA consumption, usually show a decrease in AsA_T compared to genotypes in which APX plays a minor role in ROS scavenging such as in 'Tigullio' (Eraslan et al., 2007a; Han et al., 2009).

To confirm greater ability of 'Red Rubin' to contrast oxidative load than 'Tigullio', the ratio GSH/Glu_T increased in the purple cultivar while in 'Tigullio' B toxicity negatively influenced this ratio. A different behavior between cultivars concerning B excess effects in Glu_T was also recorded by Cervilla et al. (2007).

Phenols did not significantly change in leaves of 'Red Rubin' at 0.2 and 2 mg L^{-1} indicating that for this cultivar 2 mg L^{-1} did not represent a dramatic stress while in 'Tigullio' phenols incremented following the severity of treatments. This indicates that phenols in these two cultivars did not act as antioxidant but as complex agent mitigating the negative effects of free B within the cells. In fact, B forms complexes (>90% of the foliar content), mainly with pectins and phenols in the cell wall and plasma membrane, respectively, resulting in higher stability of these structures. When B supply is adequate more than 60% of this element is in free form in leaves tissues (Brown and Hu, 1996). In conditions of B excess phenols may play a role in B compartmentalization.

As reported above, anthocyanins play an important role in photosynthetic apparatus photoprotection to oxidative stress (Bahler et al., 1991; Steyn et al., 2002; Eryılmaz, 2006). We found a rise in anthocyanins content only in 'Red Rubin' plants submitted to 2 and 20 mg L^{-1} of B in the medium while no differences among 'Tigullio' control and treated plants were recorded. Thus, 'Red Rubin' contains a wide pool size of antioxidants that can provide strong antioxidant ability against ROS triggered by B.

Furthermore, B stress induced a different pattern of antioxidant enzymes for the two basil cultivars evaluated. Our results evidenced a buildup in SOD activity in plants submitted to the most severe B treatment and it was notable that green-leafed cultivar shown the highest values of SOD activity. According to our results, a general

stimulation of SOD was also reported by many studies on B toxicity (Gunes et al., 2006; Molassiotis et al., 2006; Cervilla et al., 2007; Ardic et al., 2008; Kaya et al., 2009; Han et al. 2009). Catalase and APX were significantly increased in both cultivars grown with B excess in agreement with earlier results in pear (Wang et al., 2011). In 'Tigullio' it seems SOD and CAT were the principal enzymes involved in response to B stress, whereas in 'Red Rubin' APX was also affected by B toxicity.

In conclusion, the obtained results demonstrated that B toxicity promoted oxidative stress and oxidative damage in sweet basil leaves triggering the production of ROS. This negatively influenced the photosynthetic process and stomatal conductance. Moreover, high B concentration in the growing medium enhanced the antioxidant enzyme activities in both cultivars. Furthermore, for 'Tigullio' plants, stimulation in the synthesis of antioxidant molecules such as AsA and GSH was observed while 'Red Rubin' plants, with a constitutive higher antioxidants level compared to 'Tigullio', did not manifest the same buildup in the synthesis of these compounds. Furthermore, in 'Red Rubin' leaves the relevant anthocyanins level could significantly contribute to B tolerance. However, further works will be necessary to clarify the mechanisms by which anthocyanins could make their contribution to reduce B-induced damage in leaves and in order to establish if they act as antioxidant molecules and/or as photoprotective compounds.

4. Purple *versus* green-leafed *Ocimum basilicum*: which differences occur with regard to photosynthesis under boron toxicity?

Introduction

Boron (B) is a unique micronutrient because it is freely mobile in many plant species while it has restricted mobility in others (Brown and Shelp, 1997). In species characterized by low B mobility, such as tomato (Guidi et al., 2011) and sweet basil (Landi et al., 2013a,b), the typical symptoms of B toxicity are leaf chlorosis and necrosis (leaf burn) on leaves where B tends to accumulate (Nable et al., 1997). In species where B is highly mobile (e.g. *Malus* spp., *Prunus* spp. and *Pyrus* spp.) the symptoms of B toxicity principally appear in meristematic regions and fruits (Brown and Hu, 1996). Boron toxicity limits crop production in many regions of the world, especially in arid and semi-arid areas (Nable et al., 1997). Excess of this micronutrient may naturally occur in soils or as a result of over-fertilization and/or irrigation with B-enriched water. An approach to increase crop production under conditions of B toxicity is the selection and breeding of crop genotypes with higher B tolerance (Nable et al., 1997). Several studies showed a large intra-specific variation in response to B toxicity, for instance in wheat, barley (*Nable*, 1988) and *Brassica rapa* (Kaur et al., 2006). To our knowledge, no experiments were carried out to screen genotypes of sweet basil (*Ocimum basilicum* L.) for B tolerance. Sweet basil is a commercially relevant crop that is cultivated worldwide due to its large use as flavoring agent for food (Makri and Kintzios, 2007) and as a source of active principles (Kiferle et al., 2011). Genotypes (cultivars, ecotypes) belonging to this species, show an elevated number of morphologic differences in terms of plant biomass, leaf dimension, pigmentation and canopy conformation (Makri and Kintzios, 2007).

Recent studies have reported the occurrence of leaf burn and oxidative stress induced by B toxicity in edible species (Eraslan et al., 2007a,b; Cervilla et al., 2007; Yermiyahu et al., 2008, Ardic et al., 2009), while relatively little attention has been paid to the effect of B excess on photosynthesis. Therefore, the present study was undertaken to investigate the effects of B toxicity on photosynthesis in 10 sweet basil cultivars differing in their leaf pigmentation.

In ‘Dark Opal’ and ‘Red Rubin’ sweet basil cultivars, the purple color of leaves is attributable to constitutively elevated levels of anthocyanins (0.6-1.0 mg g^{-1} DW), compared to the almost negligible concentrations (less than 0.05 mg g^{-1} DW) found in green-leafed cultivars (Landi et al., 2013a; Phippen and Simon, 2000). Polyphenols, including flavonoids and anthocyanins, can increase the antioxidant ability of plant species by quenching the reactive oxygen species (ROS) originated under stress conditions (Camacho-Cristóbal et al., 2002; Steyn et al., 2002; Kytridis and Manetas, 2006). Anthocyanins can also provide the photoprotection of chlorophylls in plants subjected to several stresses such as drought, salinity or elevated irradiance (Steyn et al., 2002; Gould et al., 2010). However, little information is available on the role of anthocyanins in the response of plants to B toxicity.

In the present work, the effect of B toxicity on photosynthesis was investigated by measuring both leaf gas exchange and chlorophyll *a* fluorescence in 10 sweet basil cultivars which differed in leaf pigmentation. The aim was to investigate the involvement of anthocyanins in the response of the photosynthetic apparatus to B toxicity.

Materials and methods

Plant material and growing conditions

The experiments were conducted in a glasshouse located in Pisa (Italy) equipped for hydroponic cultivation (floating raft system), from May to July 2011. Seeds of all the sweet basil cultivars were purchased from Franchi Sementi (Bergamo, Italy) and germinated in rockwool tray plugs.

Ten cultivars were screened: two with purple leaves (‘Dark Opal’, DO; ‘Red Rubin’, RR) and eight with green leaves (‘Foglia di Lattuga’, FL; ‘Gigante’, GI; ‘Greco a Palla’, GP; ‘Limone’, LM; ‘Liquirizia’, LQ; ‘San Valentino’, SV; ‘Sweet Thai’, ST; ‘Tigullio’, TI).

Two weeks after sowing, at the second leaf stage, the plants were transferred into six separate hydroponic systems, each consisting of a polystyrene tray floating in a 10-L plastic tank with stagnant nutrient solution. A hundred plants was positioned in each tray

(10 plants for each cultivar) in order to have 30 plants of each genotype for both B treatments. Crop density was approximately 350 plants m^{-2} (on a ground area basis).

The nutrient solution was continuously aerated in order to maintain oxygen content higher than 6.0 g m^{-3}. The nutrient solution contained the following concentration of macronutrients and trace elements: NO_3^- 14.0 mM, NH_4^+ 0,5 mM, PO_4^{2-}.2 mM, K^+ 10.0 mM, Ca^{2+} 4.0 mM, Mg^{2+} 1.0 mM, Na^+ 10.1 mM, SO_4^{2-} 2.0 mM, Fe^{2+} 56.0 µM, H_3BO_3 23.1 µM, Cu^{2+} 1.0 µM, Zn^{2+} 5 µM, Mn^{2+} 10.0 µM, Mo^{3+} 1.0 µM. Electrical conductance (EC) was 3.1 dS m^{-1}; pH values were adjusted to 5.5-6.0 with diluted sulfuric acid. The B concentration was differentiated one month after sowing, when plants were transferred into newly-prepared nutrient solution containing 18 µM (0.2 mg L^{-1}, considered as control) or 1800 µM (20.0 mg L^{-1}) of B that was added as boric acid. Plant water uptake was compensated by refilling each tank with complete nutrient solution that was checked for pH and EC almost daily. In addition, nutrient solutions were completely replaced every three days. Frequent discharge of the nutrient solution minimized the variations of pH, EC and ion composition in all the hydroponic cultures (*data not shown*).

Climatic parameters were continuously monitored by a weather station placed inside the glasshouse. The minimum and ventilation air temperature were 16 and 27°C, respectively; maximum temperature reached up to 30-32°C in sunny hours. Daily global radiation and mean air temperature averaged 11.0 MJ m^{-2} (photosynthetic active radiation, PAR of approximately 600 µmol $m^{-2}s^{-1}$) and 24.6°C, respectively.

Sample preparation

After 20 days of cultivation with the respective B supply, sweet basil leaves were randomly sampled for physiological and biochemical determinations. Physiological determinations (gas exchanges and chlorophyll fluorescence analyses) and assessment of visible symptoms were carried out *in vivo*, whereas lipid peroxidation was determined using fresh leaf tissue, and boron content was analyzed using dried leaf tissue.

Boron toxicity symptoms

The occurrence of leaf symptoms (necrosis) induced by B toxicity was evaluated by using the open source software IMAGEJ ver. 1.47 (National Institute of Mental Health, USA) and expressed as percentage of the necrotic area over total leaf area.

Boron determination

Leaf samples were rapidly washed with tap water, rinsed in deionized water, dried at 80°C and digested with a mixture of nitric and perchloric acid at 230°C for 1 h. Boron was determined by the Azomethine-H method (Wolf, 1974) and was expressed as mg kg^{-1} DW.

Lipid peroxidation

In order to assess the oxidative damage in leaf tissues, lipid peroxidation was determined by measuring the accumulation of malondialdehyde (MDA) by-products as described by Hodges et al. (1999**)** by using 0.1 to 0.2 g of fresh leaves. MDA by-products concentration was expressed as nmol g^{-1} FW.

Leaf gas exchange and chlorophyll a fluorescence

Net CO_2 assimilation rate (Pn, µmol CO_2 $m^{-2}s^{-1}$), stomatal conductance (g_s, mol H_2O $m^{-2}s^{-1}$), transpiration (E, mmol H_2O $m^{-2}s^{-1}$) and intercellular CO_2 concentration (Ci, µmol CO_2 mol air^{-1}) was measured in fully expanded leaves between 10am and 1pm (5 replicates). All measurements were carried out inside the glasshouse at saturating PAR (800 µmol m^{-2} s^{-1}) using a portable infrared gas analyzer (Li-Cor 6400, Li-Cor Inc., Lincoln, NE, USA) that operated at ambient CO_2 concentration (380 ± 5 µmol CO_2 mol air^{-1}).

Chlorophyll *a* fluorescence imaging was performed using an IMAGING-PAM Chlorophyll Fluorometer (Walz, Effeltrich, Germany) as reported by Guidi et al. (2007). In leaves with symptoms of B toxicity, fluorescence parameters were estimated near (but not inside) the necrotic areas (*n*=5). In asymptomatic leaves, measurements were taken in the regions of the leaf lamina corresponding to those evaluated for the unhealthy leaves. Chlorophyll *a* fluorescence parameters were measured at 400 µmol m^{-}

$^{2}s^{-1}$ PAR. The fraction of open PSII centers (q_L) and the quantum yield of regulated (Φ_{NPQ}) or non-regulated (Φ_{NO}) photochemical energy loss in PSII were determined as reported by Kramer et al. (2004). The light curve response of the apparent electron transport rate (ETR) was determined in leaves that had been adapted to each irradiance level for 5 min.

Statistics

The experiment was carried out following a completely randomized design. Data were submitted to two-way analysis of variance (ANOVA) with B level and cultivar as sources of variation. Mean values were separated by the Fisher's least-significant difference test (LSD). Percentage values were subjected to angular transformation before ANOVA. The relationships between the accumulation of MDA, the incidence of leaf necrosis and the B content were analyzed by linear regression. The response of ETR to PAR level was modeled by fitting second-order polynomial curves to the measurements. The coordinates of the vertex of the parabola, the maximal ETR and the saturating PAR level were determined from the vertex of the parabola interpolated by the regression equation. Statistical analysis was performed by using CoStat™ software package (CoHort™ Software, 1994; Berkley, California, USA).

Results

Leaf boron, MDA and necrosis

When the plants were supplied with 0.2 mg L^{-1} B, the content of both B and MDA by-products did not differ in the sweet basil cultivars under investigation (**Fig. 4.1a,b**) and no leaf necrosis was observed in any plant. On average, the concentration of B and MDA in leaf tissues was 102.3 ± 14.2 mg kg^{-1} DW and 7.0 ± 0.7 nmol g^{-1} FW, respectively. In contrast, supplying plants with B-enriched (20.0 mg L^{-1} B) nutrient solution resulted in large accumulation of this element in leaf tissues, to a greater extent in the green cultivars than in the purple ones (**Fig. 4.1a**).

A similar pattern was observed with regard to MDA (**Fig. 4.1b**), which was accumulated to a larger extent in the green cultivars (e.g. +98% compared to the control in TI) than in the purple ones in response to B excess. In the latter, only a moderate but

significant build-up of MDA concentration (+21%, on average) was found under B excess. The accumulation of MDA was significantly correlated to leaf B content (linear correlation, R^2=0.906; **Fig. 4.2a**).

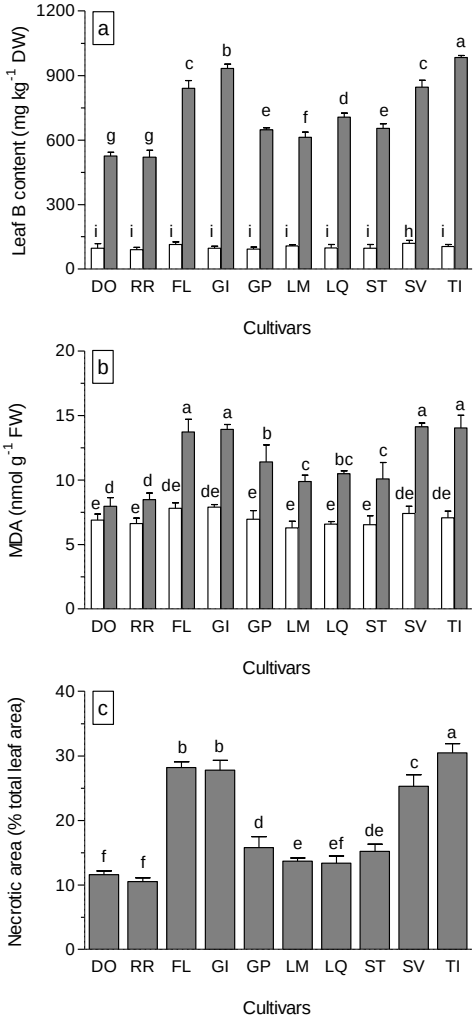

Fig. 4.1. Leaf concentration of boron (a), malondialdehyde (MDA) by-products (b) and severity of leaf necrosis (c) in different cultivars of sweet basil (*Ocimum basilicum*) hydroponically grown for 20 days with different B concentrations in the nutrient solution: 0.2 (empty bar) or 20.0 (filled bar) mg B L^{-1}. The cultivars had either purple ('Dark Opal', DO; 'Red Rubin', RR) or green leaves ('Foglia di Lattuga', FL; 'Gigante', GI; 'Greco a Palla', GP; 'Limone', LM; 'Liquirizia', LQ; 'Sweet Thai', ST; 'San Valentino', SV; 'Tigullio', TI). No leaf necrosis was observed in the plants grown at 0.2 mg B L^{-1}. Data were subjected to ANOVA with B level and/or cultivar as source of variability. Mean values (± SD; *n*=5) followed by different letters were significantly different (P = 0.05) according to Fisher's least-significant difference test (LSD).

The symptoms of B toxicity (leaf burn) were more severe in the green cultivars, particularly in FL, GI, SV and TI. In these cultivars, more than 25% of the whole leaf lamina was necrotic, while in the purple-leafed plants this percentage averaged 11%. The magnitude of leaf necrosis was significantly correlated to the content of B (linear correlation, R^2=0.921; **Fig. 4.2b**) and MDA (linear correlation, R^2=0.909; **Fig. 4.2c**).

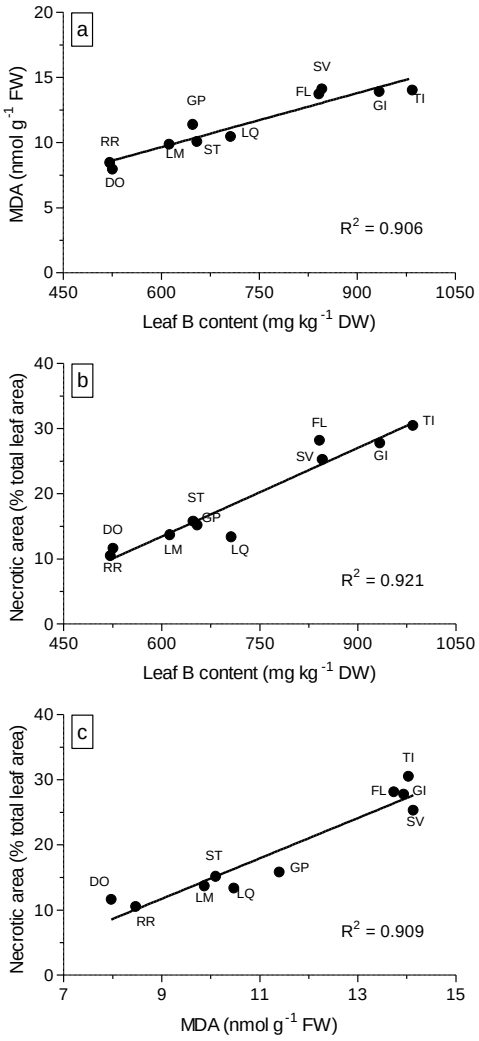

Fig. 4.2. Relationship between leaf concentration of boron and malondialdehyde (MDA) (a), boron and severity of leaf necrosis (b) and MDA concentration and leaf necrosis (c) in different cultivars of sweet basil (*Ocimum basilicum*) hydroponically grown for 20 days with 20.0 mg B L^{-1}. The cultivars had either purple ('Dark Opal', DO; 'Red Rubin', RR) or green leaves ('Foglia di Lattuga', FL; 'Gigante', GI; 'Greco a Palla', GP; 'Limone', LM; 'Liquirizia', LQ; 'Sweet Thai', ST; 'San Valentino', SV; 'Tigullio', TI). Data were subjected to linear regression analysis. Filled circles represent mean values (± SD; *n*=5).

Gas exchanges

When plants were supplied with optimal B concentration (0.2 mg L^{-1}), there were no remarkable differences among the tested cultivars in terms of leaf gas exchange, with some exceptions (**Fig. 4.3**). For instance, the light-saturated CO_2 assimilation rate was significantly lower in the green cultivars GP and SV (**Fig. 4.3a**), and GP, LQ and ST exhibited lower transpiration rates than other cultivars (**Fig. 4.3b**).

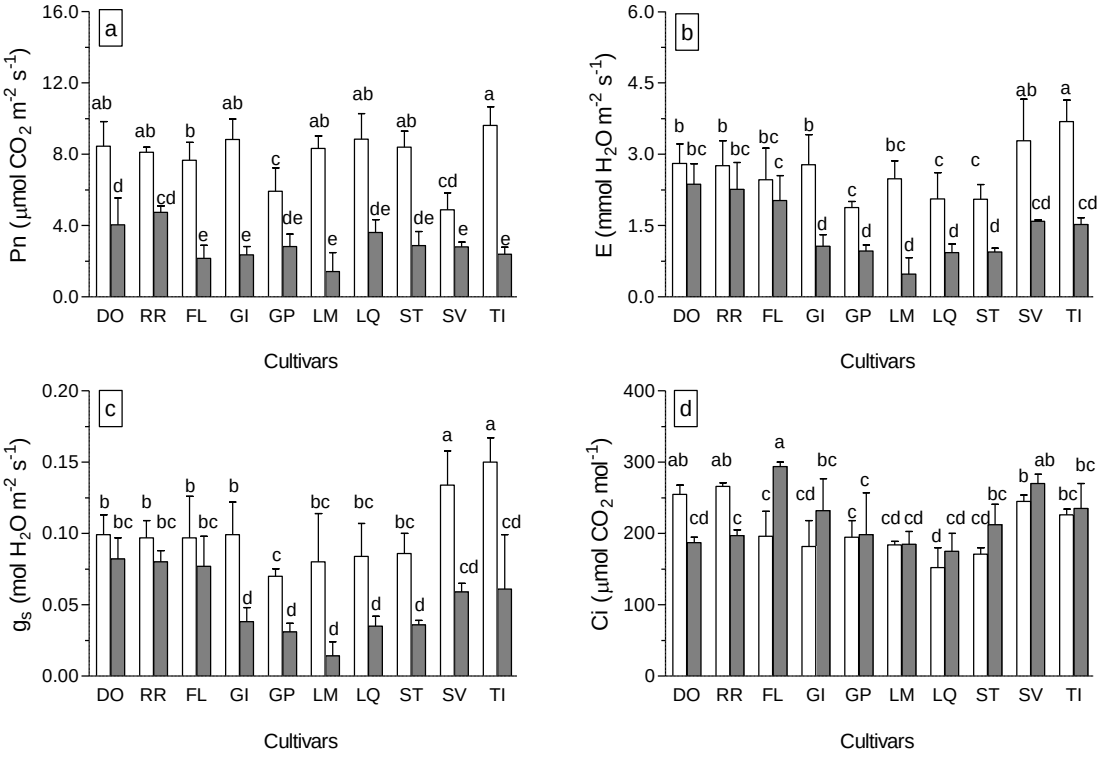

Fig. 4.3. Net CO_2 assimilation rate (Pn; a), transpiration rate (E; b), stomatal conductance (g_s; c) and intercellular CO_2 concentration (Ci; d) in leaves of different cultivars of sweet basil (*Ocimum basilicum*) hydroponically grown for 20 days with different B concentrations in the nutrient solution: 0.2 (empty bar) or 20.0 (filled bar) mg B L^{-1}. The cultivar had either purple ('Dark Opal', DO; 'Red Rubin', RR) or green leaves ('Foglia di Lattuga', FL; 'Gigante', GI; 'Greco a Palla', GP; 'Limone', LM; 'Liquirizia', LQ; 'Sweet Thai', ST; 'San Valentino', SV; 'Tigullio', TI). Data were subjected to ANOVA with B level and/or cultivar as source of variation. Mean values (± SD; *n*=5) followed by different letters were significantly different (P = 0.05) according to Fisher's least-significant difference test (LSD).

Boron excess reduced net CO_2 assimilation (Pn) and transpiration rate (E) at light saturation level in all cultivars, especially in the green ones (**Fig. 4.3a** and **4.3b**). Compared to the control plants, reductions in Pn and E averaged 65% and 54%,

respectively, in the green genotypes, compared to 47% and 17% in the purple cultivars. The reduction in Pn and E induced by B excess was associated with a decline of stomatal conductance to water vapor (g_s), which was less pronounced in the purple (-17%) compared to the green-leafed cultivars (-56%) (**Fig. 4.3c**). Green cultivars exhibited higher or unchanged values of intercellular CO_2 concentration (Ci) in response to B excess while this parameter significantly decreased in DO and RR (**Fig. 4.3d**).

Chlorophyll a fluorescence

When plants were grown at 0.2 mg L^{-1} B, the F_v/F_m ratio, which is used to evaluate the potential photochemical efficiency of PSII, did not significantly differ among all cultivars under investigation (**Fig. 4.4**). Purple plants exhibited lower actual photochemical PSII efficiency (Φ_{PSII}) values than the most of the green ones. However, it was not possible to draw a clear picture of the differences among the cultivars concerning the photochemical (q_P) and not-photochemical quenching of PSII (q_N). Boron excess reduced the F_v/F_m ratio in all cultivars and the values of Φ_{PSII} in the green-leafed cultivars (**Fig. 4.4**). However, the latter were not significantly affected by excess B in the purple leaves. The minimum fluorescence level F_0 increased following B treatment in all cultivars, whereas the maximum fluorescence yield F_m increased significantly in purple, but generally decreased in green cultivars (**Table 4.1**). The only exceptions were cultivar LM, in which no change in F_m was observed, and cultivar SV, in which F_m increased significantly (**Table 4.1**). In general, q_N was significantly higher in the plants grown under high B as compared to the controls. Boron toxicity did not consistently affect q_P in all cultivars, but significantly increased q_P values of RR, FL, GI and TI (**Fig. 4.4**). In many green cultivars the chlorophyll *a* fluorescence parameters (F_v/F_m, Φ_{PSII}, q_P and q_N) were 0 or close to 0 (black areas) even in asymptomatic areas of the leaf lamina, suggesting the occurrence of a severe damage to the PSII photosystem.

Compared to the purple cultivars, some green-leafed cultivars exhibited higher values of ETR which, however, saturated at lower light intensities (**Fig. 4.5**). Boron excess induced a strong decline of the electron transport rate (ETR) values at a light intensity higher than 80 µmol $m^{-2}s^{-1}$ in the green-leafed cultivars (-56% compared to the

controls), while a less severe decrease was observed in DO and RR (–22% on average; **Fig. 4.5**).

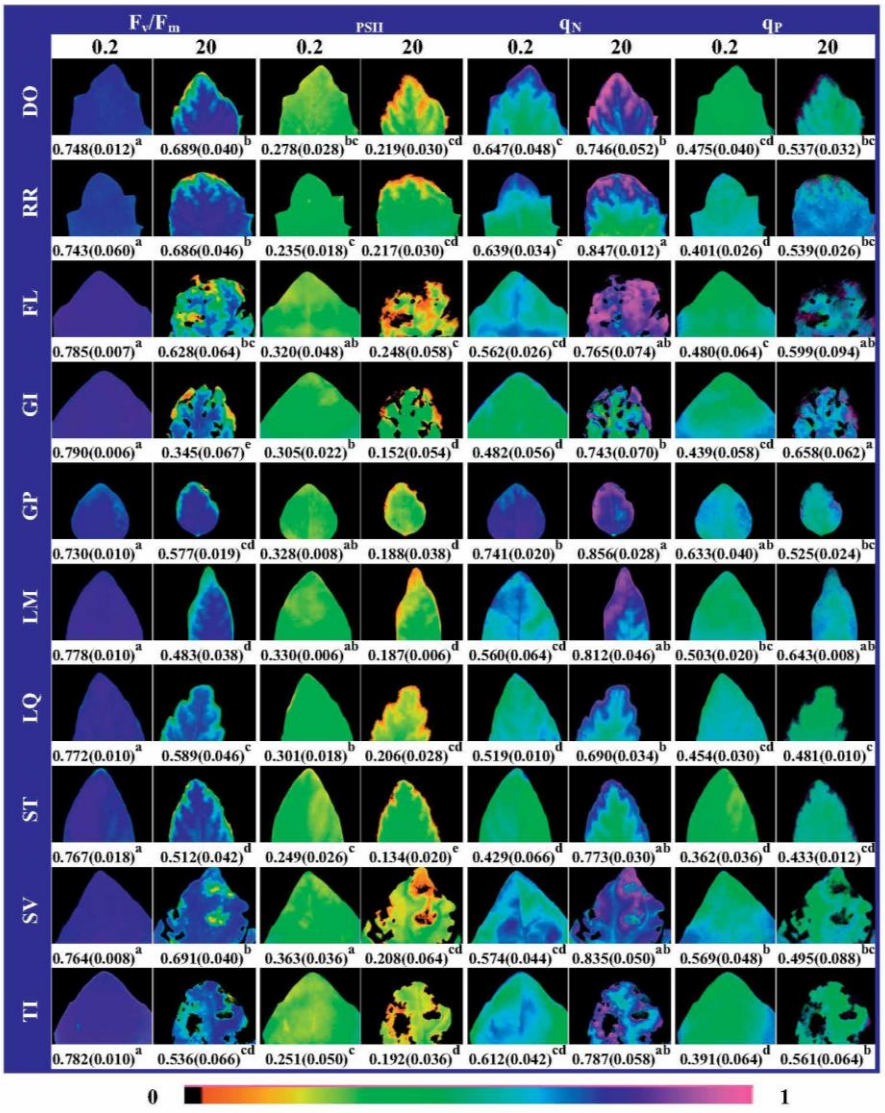

Fig. 4.4. Representative fluorescence images of the maximum efficiency of PSII (F_v/F_m), the proportion of absorbed light, which is utilized for photosynthetic electron transport (Φ_{PSII}), the photochemical quenching coefficient (q_P) and non-photochemical quenching coefficient (q_N) in leaves of different cultivars of sweet basil (*Ocimum basilicum*) hydroponically grown for 20 days with 0.2 or 20.0 mg B L^{-1}. The cultivars had either purple ('Dark Opal', DO; 'Red Rubin', RR) or green leaves ('Foglia di Lattuga', FL; 'Gigante', GI; 'Greco a Palla', GP; 'Limone', LM; 'Liquirizia', LQ; 'Sweet Thai', ST; 'San Valentino', SV; 'Tigullio', TI). Data were subjected to ANOVA with B level and/or cultivar as source of variation. Mean values (± SD; *n*=5) followed by different letters were significantly different (P = 0.05) according to Fisher's least-significant difference test (LSD).

Boron decreased the light saturation level for ETR by about 17% in the green cultivars, while this level was decreased only by about 7% in the purple ones (**Fig. 4.5**).

Table 4.1. Minimum (F_0) and maximum (F_m) fluorescence yield in leaves of different cultivars of sweet basil (*Ocimum basilicum*) grown hydroponically for 20 days with 0.2 or 20 mg B L^{-1} in the nutrient solution. The cultivars had either purple ('Dark Opal', DO; 'Red Rubin', RR) or green leaves ('Foglia di Lattuga', FL; 'Gigante', GI; 'Greco a Palla', GP; 'Limone', LM; 'Liquirizia', LQ; 'Sweet Thai', ST; 'San Valentino', SV; 'Tigullio', TI). Data were subjected to ANOVA with B level and/or cultivar as source of variation. Mean values (± SD; *n*=5) followed by different letters were significantly different (P = 0.05) according to Fisher's least-significant difference test (LSD).

CULTIVAR	TREATMENT (mg L^{-1} B)	F_0	F_m
DO	0.2	112 (10.1)^{h}	446 (21.3)^{ef}
	20	158 (18.2)^{e}	510 (12.3)^{cd}
RR	0.2	120 (10.2)^{gh}	469 (31.6)^{de}
	20	162 (18.0)^{e}	518 (30.5)^{c}
FL	0.2	94 (12.3)^{i}	525 (15.2)^{c}
	20	110 (29.6)^{h}	298 (20.3)^{gh}
GI	0.2	138 (11.0)^{f}	659 (37.8)^{ab}
	20	178 (10.5)^{d}	268 (25.4)^{h}
GP	0.2	182 (11.3)^{d}	674 (30.2)^{a}
	20	221 (12.3)^{b}	521 (3.62)^{c}
LM	0.2	117 (12.0)^{h}	525 (36.0)^{c}
	20	271 (12.7)^{a}	523 (28.5)^{c}
LQ	0.2	118 (10.6)^{gh}	516 (10.3)^{cd}
	20	125 (9.2)^{fgh}	318 (68.2)^{g}
ST	0.2	125 (8.9)^{fgh}	540 (60.5)^{c}
	20	160 (10.6)^{e}	328 (23.7)^{g}
SV	0.2	123 (11.5)^{fgh}	524 (18.9)^{c}
	20	205 (10.7)^{c}	669 (12.7)^{a}
TI	0.2	133 (12.3)^{fg}	612 (60.3)^{b}
	20	189 (11.6)^{d}	403 (24.9)^{f}

No relevant differences among all the sweet basil cultivars were found for the quantum yield of regulated photochemical energy loss Φ_{NPQ} and the photochemical quenching coefficient (q_L), while the quantum yield of non-regulated energy loss (Φ_{NO}) values were different between the cultivars (**Table 4.2**). High B increased both Φ_{NPQ}

and q_L in all genotypes albeit this increase was not significant in some cultivars (**Table 4.2**). In contrast, Φ_{NO} slightly decreased (in DO, RR, ST and SV) or remained unchanged (**Table 4.2**).

Table 4.2. Quantum yield of regulated (Φ_{NPQ}) and non-regulated (Φ_{NO}) non-phochemical energy loss and the fraction of open PSII centers (q_L) in the leaves of different cultivars of sweet basil (*Ocimum basilicum*) grown hydroponically for 20 days with 0.2 or 20 mg B L^{-1} in the nutrient solution. The cultivars had either purple ('Dark Opal', DO; 'Red Rubin', RR) or green leaves ('Foglia di Lattuga', FL; 'Gigante', GI; 'Greco a Palla', GP; 'Limone', LM; 'Liquirizia', LQ; 'Sweet Thai', ST; 'San Valentino', SV; 'Tigullio', TI). Data were subjected to ANOVA with B level and/or cultivar as source of variation. Mean values (± SD; *n*=5) followed by different letters were significantly different (P = 0.05) according to Fisher's least-significant difference test (LSD).

CULTIVAR	TREATMENT (mg L^{-1} B)	Φ_{NPQ}	Φ_{NO}	q_L
DO	0.2	0.375(0.048)^{c}	0.346(0.020)^{c}	0.271(0.028)^{cd}
	20	0.539(0.018)^{a}	0.242(0.012)^{d}	0.407(0.032)^{bc}
RR	0.2	0.390(0.032)^{cb}	0.375(0.018)^{bc}	0.217(0.018)^{d}
	20	0.539(0.018)^{a}	0.242(0.012)^{d}	0.412(0.022)^{bc}
FL	0.2	0.314(0.036)^{cd}	0.366(0.018)^{c}	0.241(0.044)^{cd}
	20	0.435(0.079)^{b}	0.317(0.020)^{cd}	0.692(0.095)^{a}
GI	0.2	0.274(0.026)^{d}	0.421(0.048)^{b}	0.194(0.032)^{d}
	20	0.349(0.072)^{cd}	0.498(0.052)^{a}	0.591(0.081)^{ab}
GP	0.2	0.403(0.020)^{cb}	0.269(0.030)^{d}	0.454(0.050)^{bc}
	20	0.535(0.054)^{a}	0.277(0.032)^{d}	0.503(0.071)^{b}
LM	0.2	0.304(0.042)^{cd}	0.365(0.036)^{c}	0.259(0.028)^{cd}
	20	0.455(0.058)^{b}	0.359(0.058)^{c}	0.560(0.016)^{ab}
LQ	0.2	0.291(0.012)^{d}	0.407(0.010)^{bc}	0.219(0.026)^{d}
	20	0.385(0.040)^{cb}	0.408(0.068)^{bc}	0.353(0.030)^{cd}
ST	0.2	0.255(0.038)^{d}	0.496(0.060)^{a}	0.152(0.004)^{d}
	20	0.513(0.018)^{ab}	0.353(0.002)^{c}	0.361(0.002)^{c}
SV	0.2	0.296(0.042)^{d}	0.342(0.008)^{c}	0.328(0.038)^{cd}
	20	0.541(0.074)^{a}	0.252(0.012)^{d}	0.361(0.064)^{c}
TI	0.2	0.376(0.054)^{c}	0.373(0.006)^{bc}	0.188(0.038)^{d}
	20	0.450(0.052)^{b}	0.360(0.064)^{c}	0.460(0.056)^{bc}

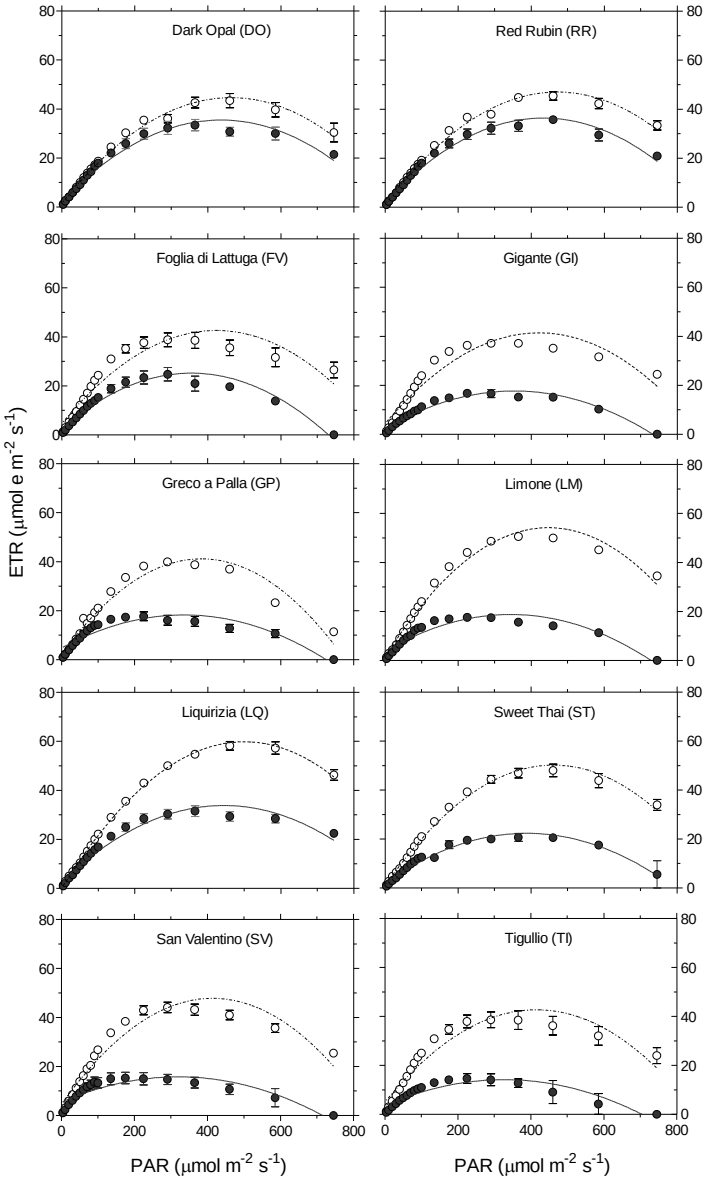

Fig 4.5. Light response curves of photochemical electron transport rate (ETR) efficiency in the leaves of different cultivars of sweet basil (*Ocimum basilicum*) hydroponically grown for 20 days with 0.2 (empty circles) or 20.0 (filled circles) mg B L^{-1}. The cultivars had either purple ('Dark Opal', DO; 'Red Rubin', RR) or green leaves ('Foglia di Lattuga', FL; 'Gigante', GI; 'Greco a Palla', GP; 'Limone', LM; 'Liquirizia', LQ; 'Sweet Thai', ST; 'San Valentino', SV; 'Tigullio', TI). Lines represent polynomial second-order curves fitted to mean values (± SD; *n*=5).

Discussion

The first relevant result achieved in this experiment was the lower sensitivity to B toxicity exhibited by the two purple cultivars, DO and RR, which exhibited a lower B accumulation as well as less visible symptoms of damage compared to the green

cultivars. This is in agreement with our previous results (Landi et al., 2013a) and confirms that B uptake and accumulation were certainly the main determinants of the induction of leaf damages. This was also confirmed by the positive and highly significant correlation (r^2=0.921) between leaf B concentration and the percentage of necrotic area (**Fig 4.2**), which was similar to that found in a recent report in tomato (Guidi et al., 2011).

In agreement with other authors (Molassiotis et al, 2006; Cervilla et al., 2007; Landi et al., 2013a), we also observed a positive and significant correlation between the accumulation of B in leaves and MDA by-products (r^2=0.906) (**Fig. 4.2**).

The chloroplast represents a primary target for the oxidative load triggered by many environmental stresses (Foyer and Noctor, 2005). Some results have demonstrated that B toxicity induces alterations in photosynthesis as well (Soylemezoglu et al., 2009; Han et al., 2009; Ruuhola et al., 2011; Landi et al., 2013a,c). In our experiment the photoassimilation of CO_2 was reduced by B toxicity in both the green and the purple cultivars of sweet basil (**Fig. 4.3**). In accord with previous findings in citrus (Han et al., 2009), orange and mandarin (Papadakis et al., 2004 a,b), this reduction was related to stomatal and non-stomatal alterations in the green-leafed cultivars, where g_s was reduced and Ci rose or remained unchanged under B excess. In contrast, the reduction of Pn appeared mainly related to stomatal limitations in DO and RR, since Ci significantly decreased under B toxicity and g_s was slightly reduced (**Fig. 4.3**).

The F_v/F_m ratio is a good indicator of photoinhibitory conditions of PSII and generally a decrease of this value was reported under high B stress (Han et al., 2009; Papadakis et al., 2004a,b). The potential photochemical efficiency of asymptomatic leaf portions was significantly reduced in all the sweet basil cultivars even though the decline of F_v/F_m was more pronounced in the green as compared with the purple ones (**Fig. 4.4**). However, the mechanism responsible for the decrease of F_v/F_m was different among all the cultivars. In DO and RR, this reduction was attributable to higher values of both F_0 and F_m, with a larger increase of the former parameter (**Table 4.1**), indicating a reversible accumulation of the reduced form of Q_A, the primary electron acceptor of PSII (Buhkov et al., 1990). On the contrary, a decline in F_m along with an increase in F_0 was observed in the green cultivars. The build-up of F_0 indicates an inactivation of PSII,

which can rapidly recover from moderate stress (Bohlar-Nordenkampf et al., 1989), while the decline in F_m likely denotes an irreversible damage to the PSII reaction centers and/or antennas (Klughammer and Schreiber, 2008; Maxwell and Johnson, 2000). In addition, other reasons can determined changes in F_0 and F_m especially when the variation of these parameters is on the same direction (both increase or decrease) as we found in the purple cultivars (e.g. a strong reduction of chlorophyll concentrations).

Similarly to F_v/F_m, Φ_{PSII} and ETR strongly decreased (**Fig. 4.4** and **4.5**) in B-stressed green plants. These reductions appear related to the ROS-induced damage at the electron transport level. In the purple cultivars DO and RR, ETR decreased to a lower extent and Φ_{PSII} remained unchanged. The lowering of Φ_{PSII} values in the green cultivars was generally associated with a strong build-up of q_N indicating dissipation of the surplus of excitation energy by non-photochemical mechanisms. However, albeit compromised chloroplast conditions were evident in all green cultivars supplied with high B, stressed plants maintained the ability to dissipate excess energy through non photochemical mechanisms as suggested by a general enhancement of Φ_{NPQ} (**Table 4.2**). In several green cultivars (FL, GI and TI), B toxicity additionally increased q_P (**Fig. 4.4**), while the CO_2 photoassimilation declined. This indicates that in these plants, the excess energy was also dissipated through other processes, such as the Mehler reaction, photorespiration and/or the pseudo-cyclic electron transport (Takahashi and Badger, 2011).

Higher B tolerance shown by the purple cultivars was mainly attributable to a lower accumulation of B in leaves as compared to the green cultivars. This is particularly evident from the comparison between the purple cultivars with the cultivars GI, FL, SV and TI, In the present experiment, transpiration rates were significantly higher in B-treated DO and RR plants compared to the green cultivars with the lowest B accumulation (GP, LM, LQ, and ST). We therefore hypothesize that B was passively translocated within plants following the transpiration flux, but at the same time we cannott exclude other mechanisms, such as exclusion or extrusion, may contribute to the restricted leaf B accumulation found especially in the purple cultivars.

Anthocyanins in leaves have long been known as “stress attenuators” against many environmental stresses such as drought, salinity and low temperature (Chalker-

Scott, 1999). It seems possible that these pigments might also be involved in the mitigation of B stress. The comparison between low B accumulator cultivars (i.e., purple cultivars and GP, LM, LQ and ST green leaf cultivars) and high B accumulators (the remaining green cultivars) indicates that anthocyanins may alleviate the oxidative stress induced by the combination of B toxicity and light. Indeed, although the GP, LM, LQ and ST plants exhibited reduced B accumulation under high B supply, the decline in photochemical efficiency and gas exchange was comparable to that of the high B accumulator green cultivars. The protective effect of anthocyanins appears reasonable considering the oxidative load as the sum of B toxicity and light. Both of these stressors commonly result in an increase of oxidative load in photosynthesizing cells. Here, the light saturation levels for ETR were more severely decreased by B stress in all the green cultivars (without differences related to different B concentration in leaves), indicating a great ability of DO and RR to tolerate high irradiance even when they were subjected to B toxicity. This hypothesis is further supported by a previous experiment, where DO and RR plants grown under lower irradiances (autumn 2011) than those used in the present experiment, exhibited a decline of leaf pigmentation and, in parallel, an increased extent of leaf damage when grown under high B supply (*data not shown*).

The contribution of anthocyanins to the reduction of the photo-oxidative stress found for the purple-leafed cultivars is likely the result of a sunscreen effect (Gould et al., 2010; Steyn et al., 2002) and/or a ROS quenching ability (Gould et al., 2002a; Neill and Gould, 2003; Kytridis and Manetas, 2006). Despite of an overall defensive advantage of purple/red plants belonging to various species under several stress conditions (Chalker-Scott, 1999, Close and Beadle, 2003), the predominant protective mechanism of anthocyanins (antioxidant or sunscreen) might be related to the localization of these compounds. It has been argued that, in order to scavenge oxy-radicals, anthocyanins should be located near the source of ROS production (e.g. chloroplasts) (Steyn et al., 2002).

In purple basil, anthocyanins are localized in the epidermal cell layer of leaf, steam and floral tissue (Phippen and Simon, 2000). Even though they are therefore not optimally located in relation to the chloroplast source of ROS, they may still contribute to the ROS scavenging when free oxygen radicals move out this organelle (Kytridis and

Manetas, 2006). Alternatively, they may also contribute to scavenge ROS originated in the epidermal layers, e.g. in mitochondria or directly in the cell wall. On the other hand, the localization of anthocyanins seems to support the sunscreen hypothesis also suggested by Merzlyak et al. (2008) and Manetas et al. (2003), which might partially explain the lower damage and oxidative stress found in DO and RR subjected to B toxic conditions. A sunscreen effect of anthocyanins is also supported by the observation that the light saturation point for ETR was slightly higher in DO and RR as compared to the green cultivars at both optimal and excessive B concentrations. Even though leaf anthocyanins absorb maximally in the green waveband (520-540 nm), where the probability of photon capture is reduced (Manetas, 2006), these compounds can still contribute to the reduction of the excitation pressure to PSII.

Conclusions

In summary, our data confirm a wide intra-specific variation in the tolerance of sweet basil to B toxicity. The differential response of the cultivars was associated with different abilities to restrict B accumulation in leaf tissues. In addition, the purple cultivars were able to counteract the negative effects caused by B-induced oxidative load by reducing the excitation energy burden to chloroplast and/or because anthocyanins can acting as ROS scavenger in the epidermis cells (i.e. for mitochondrial, guard cell chloroplast or cell wall ROS-produced abetment). This is deduced from the behavior of several green cultivars (GP, LM, LQ and ST), in which leaf B levels were similar to those found in the purple ones, but which exhibited a reduction in photochemical efficiency and CO_2 photoassimilation similar to the other green cultivars (GI, FL, SV and TI) with much higher leaf B concentrations. Work is in progress to investigate why B accumulates to a lesser extent in the leaves of the purple cultivars and to clarify the role of anthocyanins in the mitigation of B toxicity.

5. Photoprotection by foliar anthocyanins mitigates effects of boron toxicity in sweet basil (*Ocimum basilicum*)

Introduction

Boron (B) is a microelement for which the window between essential and toxic concentrations is extremely narrows (Nable et al., 1997). B accumulation is particularly prominent in soils from arid and semi-arid environments, and in areas prone to geothermal activity; edaphic concentrations of B in soil solution between 5 and 100 mg L^{-1} are toxic for many species (Ryan et al., 1998). In the soil solution, B is found primarily as boric acid $B(OH)_3$, which can either diffuse passively into root hair cells or else is taken up through channels (Dannel et al., 2000). The primary function of B is considered to be its contribution to the rhamnogalacturonan II complex in plant cell wall (Matoh, 2000).

Excessive uptake of B may: (I) impair cell division and development by binding to ribose, both as the free sugar and as a constituent of RNA; (II) interfere with primary metabolism by binding with ribose as a part of ATP, NADH or NADPH and nucleotides; and (III) lower the pH of the cytosol, thereby affecting protein conformation and biosynthesis (Reid et al., 2004). As a result, key physiological processes such as photosynthesis are strongly perturbed (Cervilla et al., 2007; Landi et al., 2013c). Thus, because the capacity to process incident light energy is compromised, plants growing on B-rich soil are more likely to produce a surplus of reactive oxygen species (ROS) and consequently incur oxidative stress (Cervilla et al., 2007; Landi et al., 2013a). This, in addition to a reduction in photosynthetic area caused by necrosis of leaf margins, can greatly reduce net carbon assimilation rate (Lovatt and Bates, 1984; Reid et al., 2004; Guidi et al., 2011).

It is evident that some plant species are more tolerant of high concentrations of edaphic B than are others (Reid, 2007). This differential sensitivity to B can extend to differences between cultivars of the same species. For example, Landi et al (2013,b) reported that two purple-leafed cultivars of sweet basil (*Ocimum basilicum*) were less sensitive than eight green-leafed cultivars to an excess of B. When supplied with B at 20 mg L^{-1} (approximately 1.8 mM B), the purple cultivars showed less necrosis, less

oxidative damage and a smaller decline in photosynthesis. Nothing is known of the mechanism by which apparent tolerance to B is achieved in these purple cultivars. However, the presence of concentrated anthocyanins in the leaf epidermis and veins of their leaves is the most obvious difference between the two cultivars (Makri and Kintzios, 2007). Given the putative protective functions of foliar anthocyanins in response to other stressors such as drought, wounding, pathogens, herbivores, extreme temperatures and ionic unbalance (reviewed by Gould et al., 2009), it is at least possible that these, or related flavonoids, are involved in the tolerance to excess B.

There are at least three possible mechanisms through which anthocyanins might mitigate the effects of B toxicity. First, anthocyanins might chelate to supernumerary B ions and sequester them in the cell vacuole. The ability of anthocyanins to chelate to heavy metals has been reported for tungsten (Hale et al., 2002), aluminium (Elhabiri et al., 1997), copper (Somaatmadja et al., 2006), gallium (Elhabiri et al., 1997, Buchweitz et al., 2012), iron (Buchweitz et al., 2012), and molybdenum (Hale et al., 2001). However, there is as yet no experimental evidence for B-anthocyanin chelates in *planta*. Second, anthocyanins may function indirectly by reducing the oxidative load on chloroplasts for which the ability to process light energy has been compromised through B toxicity. Anthocyanins are extremely potent antioxidants, capable of scavenging most species of reactive oxygen in *vitro* (Gould et al., 2002a; Gould 2004), and may well contribute to the antioxidant pool in purple-leafed basil (Landi et al., 2013a). However, because the anthocyanins reside exclusively in the abaxial and adaxial epidermises of basil leaves (Makri and Kintzios, 2007), the pigments are not optimally located to scavenge chloroplast-derived ROS in this species. Third, by absorbing a proportion of the incident light energy, anthocyanins may diminish the generation of ROS by B-affected chloroplasts within leaf mesophyll. A possible protective effect of photoabatement by anthocyanins has been postulated many times (Neill and Gould, 2003; Kytridis et al., 2008; Hughes et al., 2012; Hatier et al., 2013), but has never been evaluated in relation to B tolerance.

Here, we test the hypothesis that light-screening by epidermal anthocyanins diminishes the severity of photo-oxidative stress in subjacent mesophyll cells of sweet basil compromised by B toxicity. We report the responses of purple-leafed (‘Red

Rubin') and green-leafed ('Tigullio') basil cultivars to a combination of B and high light treatments, as measured by changes in chlorophyll fluorescence parameters, hydrogen peroxide production, and lipid peroxidation. Finally, we disentangle possible effects of anthocyanins as antioxidants from those as light filters by comparing the responses of green (acyanic) protoplasts isolated from the two cultivars.

Materials and methods

Plant material

Seeds of sweet basil (*O. basilicum* L.) cultivar 'Tigullio' and cultivar 'Red Rubin' were purchased from Franchi Sementi (Milan, Italy). Plants were grown from seed in a sandy soil-peat mixture (60:40, v:v) using 1.25 L pots, and watered with tapwater (which contained less than 18 µM B) for 14 d after sowing. They were then irrigated daily with B-enriched tapwater (1.8 mM B, added as boric acid) at pH 6.0 for 20 d. Control plants were watered only with tapwater, adjusted with sulfuric acid to the same pH. All plants were grown under natural light in an unheated glasshouse in Wellington, New Zealand (41°17′00″S 174°46′00″E) between March and July 2013. The minimum and maximum air temperature averaged 13° C and 24° C, respectively. Irradiance averaged 650 µmol m^{-2} s^{-1} with peaks around 1000 µmol m^{-2} s^{-1} at midday.

Leaf anatomy

Transverse hand sections were taken through fresh leaf leaves, examined in an Olympus AX70 photomicroscope (Olympus Optical Co., Hamburg, Germany) and photographed using an Olympus DP70 digital camera.

Light treatments

Five B-treated and five control plants were randomly selected, and the third or fourth youngest fully expanded leaf on each was irradiated on the adaxial surface with 1000 µmol m^{-2} s^{-1} white light for 4 h at 23° C. The light source was a bank of 12 x 1 W LEDs (Shaoxing Prolux Lighting Co., Zheijiang, China), which produced white light with a colour temperature of 6500 K. To simulate the effect of epidermal anthocyanins in the green plants, one leaf on each of five 'Tigullio' B-treated plants was covered with a

purple polycarbonate film (Supergel Rosco no. 35 “light pink”, Sydenham, UK) before being irradiated. The film attenuated approximately 30% of the incident light, primarily in the green and yellow portions of the visible spectrum. This approximated the absorbance spectrum of anthocyanins from the ‘Red Rubin’ epidermis; transmittance and chromaticity coordinates of the film are available at: http://www.rosco.com/filters/supergel.cfm. An additional set of B-treated ‘Red Rubin’ plants (*n*=5) was randomly chosen, from which one leaf per plant was irradiated with 1300 µmol m^{-2} s^{-1} white light for 4 h at 23° C. The additional 30% of light approximated the additional quantum flux that would have reached leaf mesophyll had not the leaves been equipped with anthocyanins.

Protoplast isolation

Acyanic (green) protoplasts were isolated from the leaf mesophyll of both ‘Tigullio’ and ‘Red Rubin’ control plants using the method by Bi et al. (2009) with some modifications. The abaxial cuticle was manually removed, and the exposed surface floated on a solution of 1% cellulase from *Tricoderma viride* (1 U mg^{-1}, Sigma-Aldrich, Auckland, NZ) and 0.25% pectinase from *Aspergillus niger* (1.7 U mg^{-1}, Sigma-Aldrich, Auckland, NZ) in an isolation medium comprising 8% mannitol, 10 mM $CaCl_2$, 20 mM KCl, 20 mM 2-(N-morpholino)ethanesulfonic acid (MES) buffer at pH 5.7. They were gently agitated overnight under darkness at 23°C. The partially digested leaves were removed, and the remaining suspension centrifuged at 40 *g* for 3 min. The pellet was suspended in Cell Protoplast Washing solution (CPW) containing 0.45 M sucrose (pH 5.8), and protoplast viability was assessed using Evans blue dye. Protoplasts were diluted using the same isolation medium without enzymes to obtain a suspension of about 2.5 x 10^6 protoplasts mL^{-1}. The suspensions were gently agitated under 20 µmol m^{-2} s^{-1} white light at 23°C until required.

Purple protoplasts from ‘Red Rubin’ epidermis were isolated by incubating leaves without a cuticle in the enzymatic solution for 2 h as described by D’Onofrio et al. (1999). The protoplasts were counted with a hemocytometer and then re-suspended in CPW with sufficient 0.4 M sucrose in 0.1 M sorbitol to obtain 2.5 x 10^6 prot mL^{-1}.

Protoplast treatments

Acyanic protoplasts were treated with 4 µM $B(OH)_3$ in 20 mM MES buffer (pH 5.7) for 30, 90 or 180 min at 23°C. Control protoplasts were supplied with 20 mM MES buffer adjusted to pH 5.7 with HCl. Both B-treated and control protoplasts were irradiated with either 35 or 100 µmol m^{-2} s^{-1} white light for which the spectral characteristics were similar to that used to induce photoinhibition. Protoplasts were maintained gently agitated during treatments.

Further acyanic protoplasts were exposed to 100 µmol m^{-2} s^{-1} of white light that had been filtered by (I) the same purple polycarbonate filter used in the leaf photoinhibition experiments, or (II) a glass tube holding a 1:1 mix of green and purple protoplasts. In the mix, the purple protoplasts had settled above the green ones due to their lower density, and thereby simulated the effects on optical paths of a transverse section through the 'Red Rubin' leaves.

Chlorophyll fluorescence analysis

Modulated chlorophyll (Chl) *a* fluorescence analysis was conducted at 23°C for 40-min dark-adapted leaves using a PAM-2000 chlorophyll fluorometer (Walz, Effeltrich, Germany) connected to a Walz 2030-B leaf clip. Ratios of variable to maximum fluorescence (F_v/F_m) were measured, and then leaves were subjected to a light ramp comprising 12 steps from 0 to 1850 µmol m^{-2} s^{-1} using the light source supplied by the fluorometer. For protoplasts, Chl *a* fluorescence was analysed using a Walz Water-PAM fluorometer (Walz, Effeltrich, Germany), and F_v/F_m values were recorded after 20-min dark adaptation. Light response curves for the protoplasts were performed using a light ramp of 9 steps from 0 to 345 µmol m^{-2} s^{-1} using the light source supplied by the Water-PAM. Light response curves for quantum yield of photosystem II (Φ_{PSII}) were calculated using the equations of Genty et al. (1989); photochemical (q_P) and non-photochemical quenching (NPQ) were calculated as described by Schreiber et al. (1986); and the apparent electron transport rate (ETR) was estimated according to Krall and Edwards (1992). For details of instrument settings and measured parameters see Guidi et al. (2010).

Chlorophyll determination

Chl levels in protoplasts and leaves were determined using a method modified after Jingxian and Kirkham (1996). Aliquots containing approximately 3.1 x 10^6 viable protoplasts collected after 180 min of treatments were centrifuged at 7000 *g* for 5 min, and then the pellet re-suspended in 1 mL 80% aqueous acetone. The suspension was centrifuged and eluted repeatedly until the pellet was completely decoloured. For leaves, 0.3 g (DW) was homogenized in 80% aqueous acetone, and then the same procedure adopted. Concentrations of Chl *a* and *b* were calculated according to Lichtenthaler (1987).

Boron determination

The third and fourth youngest fully-expanded leaves were randomly collected from plants after 20 d of B treatment. Each sample was dried at 50° C for 48 h, and 0.5 g (DW) digested with HNO_3 and $HClO_4$ at 230° C for 2 h. B concentration was determined colorimetrically using the azometine-H method (Wolf, 1974) from absorbance measurements at 420 nm taken using an Ultrospec 2100 Pro spectrophotometer (GE Healthcare Ltd, England).

Malondialdehyde determination

Oxidative damage was estimated as malondialdehyde (MDA) accumulation by the thiobarbituric acid (TBA) reaction as reported in Guidi et al., 2011. Protoplasts were homogenized in 0.1% trichloroacetic acid (TCA) and mixed with an equal volume of TBA (20% of TCA and 0.5% w/v TBA). The solution was heated at 90° C for 25 min, and then cooled and centrifuged at 3000 *g* for 15 min. This method overcomes possible interference by anthocyanins in the TBA assay. Absorbances at 600, 532 and 400 nm were measured, and MDA levels calculated using the MDA extinction coefficient 155 mM^{-1} cm^{-1}. MDA concentrations were expressed per unit soluble protein, which was determined spectrophotometrically at 595 nm as described by Bradford (1976), with bovine serum albumin as a standard.

Anthocyanin quantification

Anthocyanins were extracted in acidified methanol (1.5% HCl v/v) overnight at room temperature, and their absorbance taken at 535 nm using a Ultrospec 2100 Pro spectrophotometer (GE Healthcare Ltd, England). Absorbance values were converted to cyanidin-3-*O*-glucoside equivalents using a calibration curve obtained for an authentic sample in the same solvent.

H_2O_2 production

To detect H_2O_2 production, protoplasts were incubated in 5 µM of 2',7'-dichlorofluorescein diacetate (DCFH-DA) dissolved in 15% aqueous ethanol for 30 min at 23° C under darkness. The protoplast solutions were gently agitated throughout the incubation (180 min). Green fluorescence, indicative of the oxidation by H_2O_2 of DCFH-DA to 2',7'-dichlorofluorescin (DCF), was observed in a Leica TCS4D confocal laser scanning microscope (Leica Microsystems, Wetzlar, Germany). A Krypton-Argon laser (488 nm) was used for excitation, and emission above 515 nm was collected. At least 30 protoplasts per treatment were examined. Autofluorescence of chlorophyll was recorded at 648 nm.

To observe H_2O_2 production in foliage, the third or fourth youngest fully-expanded leaves were harvested, rinsed twice in double distilled water and then incubated for 30 min at 23° C under darkness in loading buffer (50 mM Tris-KCl, pH 7.0) with 120 µM of DCFH-DA. After incubation, leaves were rinsed for 2 min in the loading buffer solution, mounted in fresh buffer on a microscope slide, examined for green fluorescence in an Olympus AX70 compound microscope (Olympus Optical Co., Hamburg, Germany), and photographed using an Olympus DP70 digital camera.

Statistics

Reported data are the means ± SD of at least five replicates. DCFH-DA fluorescence images of infiltrated leaves are representative of at least 10 replicates *per* treatment, and those of protoplasts of at least 30 replicates. Means were compared by two-way ANOVA. Differences among treatment means were evaluated by Fisher's least-significant difference test (LSD) for P=0.05. Percentage values were arcsine

transformed prior to analysis. All statistical analyses were performed using CoStat software package (CoHort^{TM} Software, 1994; Berkeley, CA, USA).

Results

Histological location of anthocyanins

Anthocyanins in 'Red Rubin' leaves were found exclusively in the epidermis (see **Fig. 7.1a**) and in xylem parenchyma in the midrib (**Fig. 7.1b**). Epidermal anthocyanins were present both in epidermal cells and in trichomes (**Fig. 7.1c**). Interestingly, on the adaxial epidermid the pigments occurred in solution in the cell vacuole, but on the abaxial epidermid, anthocyanins appeared as aggregates known as anthocyanin vacuolar inclusion (AVIs) both in epidermal cells and in trichomes. Anthocyanin pigmentation was not evident in any tissue in 'Tigullio' leaves.

Responses of plants to B and high light

Relative to the controls, foliar concentrations of B increased seven-fold in 'Red Rubin' and ten-fold in 'Tigullio' when plants were grown with B-enriched water (**Table 5.1**).

Table 5.1. Boron (B) content (µg mg^{-1} DW) total chlorophyll (Chl *a*+*b*) (µmol g^{-1} DW), Chl *a*/*b* ratio and anthocyanin concentration (mg g^{-1} DW) in leaves of *Ocimum basilicum* cultivars 'Red Rubin' and 'Tigullio' grown with negligible (control) or excess (1.8 mM) B. Means ± SD, *n*=5. Letters indicate significant differences within cultivars at P=0.05.

Treatment	B content	Chl *a*+*b*	Chl *a*/*b*	Anthocyanin
'Red Rubin'				
Control	48 (4.3)^{c}	9.8 (0.94)^{a}	1.2 (0.08)^{b}	2.2 (0.14)^{b}
B	344 (26.3)^{b}	7.9 (0.45)^{b}	1.3 (0.07)^{b}	2.9 (0.38)^{a}
'Tigullio'				
Control	55 (8.41)^{c}	9.2 (0.81)^{a}	1.7 (0.01)^{a}	*n.d*
B	560 (33.8)^{a}	7.4 (0.55)^{b}	1.8 (0.03)^{a}	*n.d*

Both cultivars showed a reduction in total chlorophyll content after B treatment, though the ratio of Chl *a*/*b* remained unchanged. The Chl *a*/*b* ratio was, however, lower in 'Red Rubin' leaves. Anthocyanin levels increased by about 30% in B-treated 'Red Rubin' leaves (**Table 5.1**).

Maximum quantum yields of photosystem II (PSII), as estimated by F_v/F_m values in dark-acclimated leaves, declined only slightly in response to B treatment in both the cultivars (**Table 5.2**).

Table 5.2. Maximal photochemical efficiency of PSII (F_v/F_m) in leaves of *Ocimum basilicum* cultivars. 'Red Rubin' and 'Tigullio' after 20 d with 1.8 mM boron (B) and/or a 4 h x1000 µmol $m^{-2}s^{-1}$ light treatment (B+L and L, respectively). Some 'Tigullio' plants were shielded by an anthocyanic filter (B+L+PF); others 'Red Rubin' were exposed to a stronger light (1300 µmol $m^{-2}s^{-1}$ for 4 h; B+L+L). Means ± SD, *n*=5. Letters indicate significant differences at P=0.05.

Treatment	F_v/F_m	Treatment	F_v/F_m
'Red Rubin'		'Tigullio'	
Control	0.82 (0.01)^{ab}	Control	0.83 (0.01)^{a}
B	0.81 (0.02)^{abc}	B	0.81 (0.03)^{abc}
L	0.79 (0.04)^{cd}	L	0.77 (0.04)^{d}
B+L	0.79 (0.02)^{cd}	B+L	0.77 (0.03)^{d}
B+L+L	0.79 (0.02)^{cd}	B+L+PF	0.80 (0.02)^{bc}

When those B-treated plants were exposed to high light (1000 µmol m^{-2} s^{-1}) for 4 h and then returned to darkness for 40 min, F_v/F_m values declined further, significantly more so in the green-leafed 'Tigullio' than in the purple 'Red Rubin'. However, when a polycarbonate filter, for which the optical properties approximated those of 'Red Rubin' anthocyanins, was inserted between the 'Tigullio' leaf and light source, differences in the decline of F_v/F_m values between the two cultivars were abolished. In contrast, when B-treated 'Red Rubin' was given 30% additional light to compensate for the light-attenuating properties of the purple pigments, the plants did not show any further decline in F_v/F_m value (**Table 5.2**).

Light-responses curves for PSII quantum yield (Φ_{PSII}) and non-photochemical quenching (NPQ) did not significantly vary (P>0.05) between control and B-treated 'Red Rubin' plants (**Fig. 5.1a,b**).

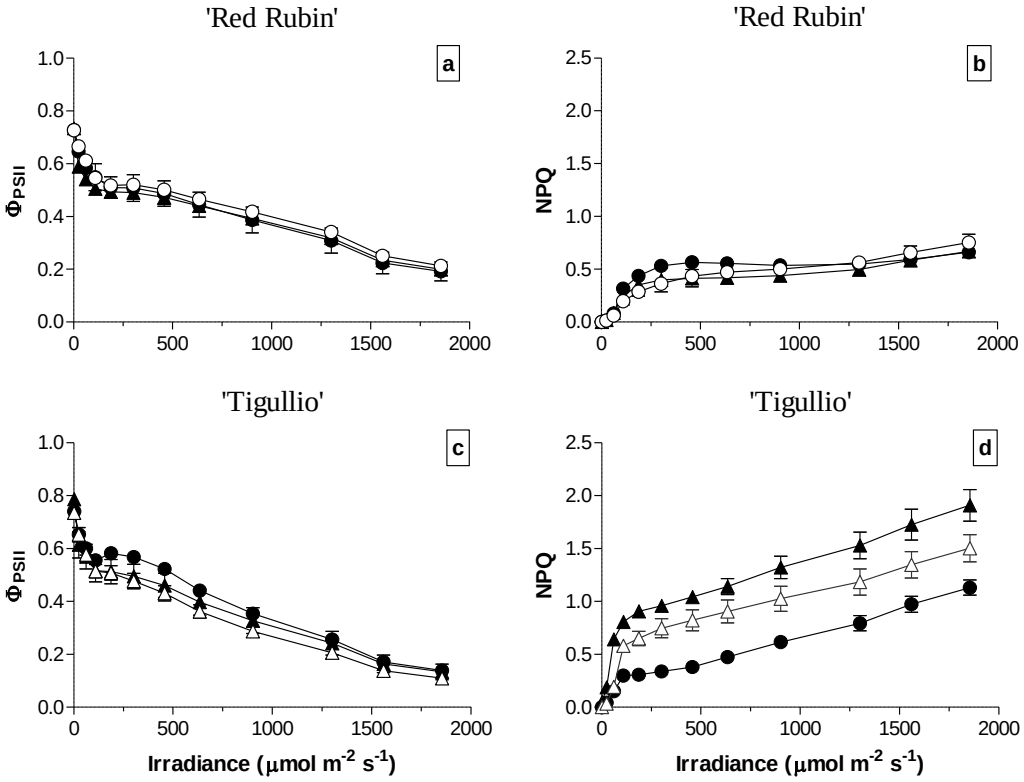

Fig. 5.1. PSII photochemical efficiency (Φ_{PSII}; a,c) and non-photochemical quenching (NPQ; b,d) in control (●) and B-treated plants of *Ocimum basilicum* cultivars 'Red Rubin' and 'Tigullio'. B-treated plants were subjected to 4h white light at 1000 μmol m^{-2} s^{-1} (▲) or 1300 μmol m^{-2} s^{-1} (○) . Some B-grown 'Tigullio' plants were shielded by a purple polycarbonate film (Δ). Means ± SD, *n*=5.

For 'Tigullio', too, Φ_{PSII} profiles did not change appreciably across treatments (**Fig. 5.1c**), although the light-saturated values of Φ_{PSII} were significantly lower in 'Tigullio' than in 'Red Rubin' (P<0.05). In contrast, NPQ patterns were far greater in 'Tigullio' than in 'Red Rubin', especially at irradiances above 950 μmol m^{-2} s^{-1} (**Fig. 5.1d**). The imposition of a purple polycarbonate filter between the light source and the B-treated 'Tigullio' leaf lamina reduced the effect of high light on NPQ values (**Fig. 5.1d**). Nevertheless, NPQ remained greater than in the 'Tigullio' controls.

Epifluorescence signals from leaves infiltrated with DCFH-DA indicated that 'Red Rubin' generated less H_2O_2 following high light and/or B treatments than did 'Tigullio' (**Fig. 5.2a-j**).

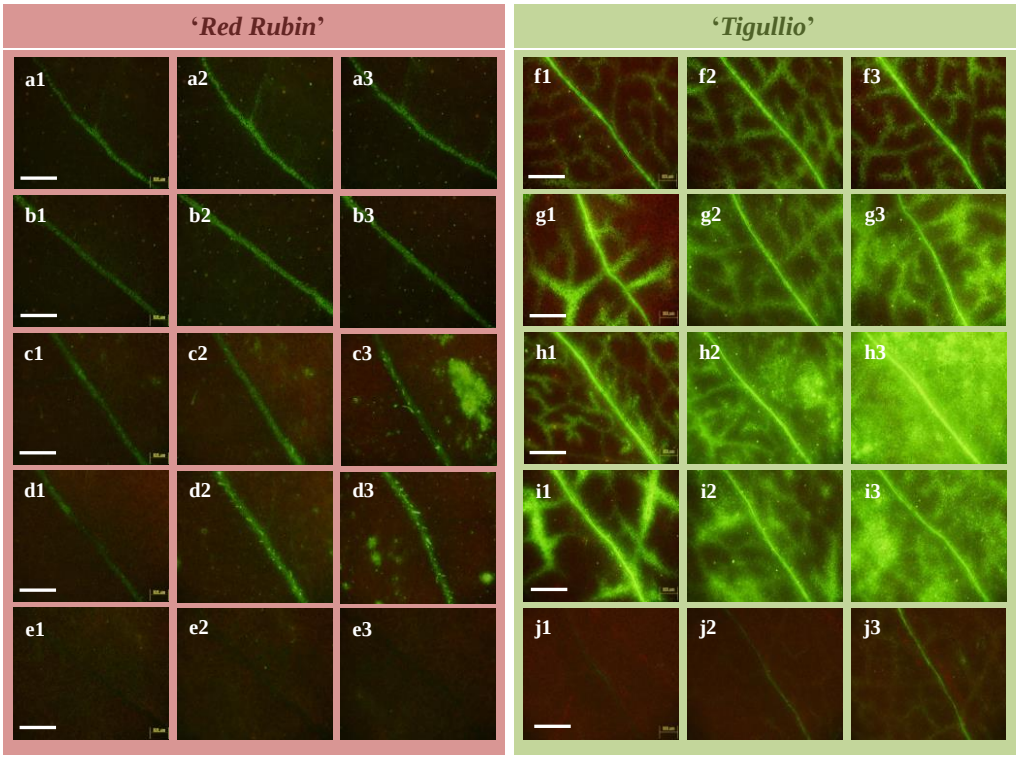

Fig. 5.2. Epifluorescence micrographs of DCFH-infiltrated leaves of *Ocimum basilicum* cultivars 'Red Rubin' (a-e) and 'Tigullio' (f-j). Plants were treated with boron (B) and white light at 400 µmol m^{-2} s^{-1} (a,f); 1000 µmol m^{-2} s^{-1} white light (b,g); B and 1000 µmol m^{-2} s^{-1}(c,h); B and 1300 µmol m^{-2} s^{-1} white light (d); B and 1000 µmol $m^{-2}s^{-1}$ shielded by a purple filter (i); or 400 µmol $m^{-2}s^{-1}$(e,j). Columns 1, 2, 3 represent 30, 60 and 180 min of treatments, respectively. Images are representative of at least 10 replicates. Bars = 150 µm.

In 'Red Rubin' leaves, fluorescence was predominantly located around the midrib and major veins; neither the distribution nor the intensity of fluorescence varied greatly across treatments (**Fig. 5.2a-d**). In contrast, for 'Tigullio' H_2O_2 was evident both in the veins and the lamina tissue (**Fig. 5.2f-i**); fluorescence was most intense when a high light treatment was applied to B-treated plants (**Fig. 5.2h**). When the polycarbonate red filter was interposed between leaves of 'Tigullio' and the light source, a slight reduction in H_2O_2-induced fluorescence was observed after 180 min in comparison to B-

treated plants exposed to full light (**Fig. 5.2i,h**). Control plants exhibited zero or extremely low levels of fluorescence (**Fig. 5.2e,j**).

Responses of protoplasts to B and high light

Protoplasts isolated from both cultivars appeared more sensitive to light stress than were intact leaves; irradiances as low as 100 µmol m^{-2} s^{-1} were sufficient to diminish the maximal quantum yield appreciably (**Fig. 5.3**).

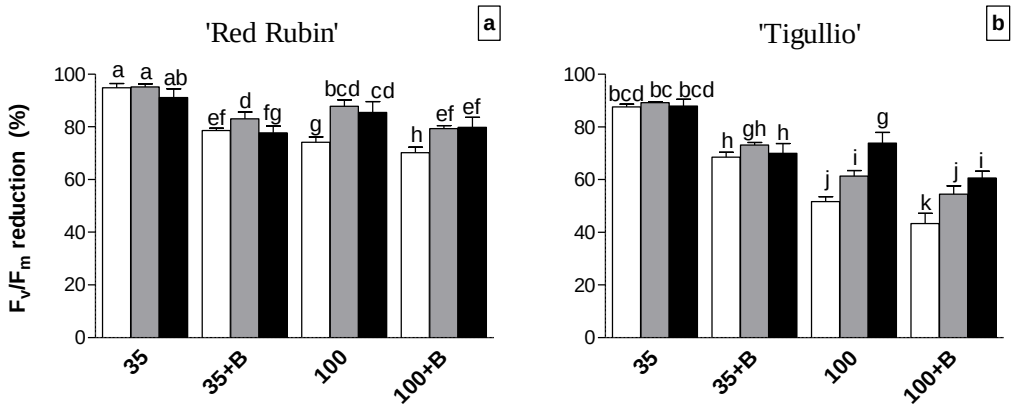

Fig. 5.3. Maximum photochemical efficiency of PSII (F_v/F_m) in leaf mesophyll protoplasts of *Ocimum basilicum* cultivars 'Red Rubin' (a) and 'Tigullio' (b). White bars: green protoplasts. Grey bars: green protoplasts beneath a layer of anthocyanic protoplasts from 'Red Rubin' epidermis. Black bars: green protoplasts shielded by a purple polycarbonate filter. Protoplasts were treated with: 35 µmol m^{-2} s^{-1} (35); boron (B) and 35 µmol m^{-2} s^{-1} (35+B); 100 µmol $m^{-2}s^{-1}$ (100); or B and 100 µmol $m^{-2}s^{-1}$ (100+B). Means $\pm$ SD, *n*=5. Letters indicate significant differences at P=0.05.

The reduction in F_v/F_m was less pronounced for 'Red Rubin' (29%) than for 'Tigullio' (52%). The addition of B to protoplast suspensions augmented the decline of F_v/F_m in both cultivars (**Fig. 5.3**; **Table 5.3**). When a layer of purple protoplasts isolated from 'Red Rubin' epidermis was positioned over acyanic mesophyll protoplasts and the mix irradiated from above, F_v/F_m declined less, irrespective of B-treatment or cultivar (**Fig. 5.3**). For 'Red Rubin', the light-filtering effects of a protoplast layer were similar to those of a purple polycarbonate filter, while for 'Tigullio', the polycarbonate filter had the greater ameliorative effect (**Fig 5.3**).

Φ_{PSII} and q_P both declined when acyanic protoplasts from 'Red Rubin' and 'Tigullio' were treated with strong light and/or B (**Table 5.3**). A purple filter placed between light source and protoplasts partially mitigated these effects of light on 'Red Rubin' protoplasts, but had little impact on 'Tigullio' (**Table 5.3**).

Table 5.3 Maximal and actual PSII efficiency (F_v/F_m and Φ_{PSII}), photochemical quenching (q_P) and non-photochemical quenching (NPQ) in green protoplasts of *Ocimum basilicum* cultivars 'Red Rubin' and 'Tigullio'. Protoplasts were treated with white light at 35 or 100 µmol m^{-2} s^{-1} and/or 4 µM boron (B). Some protoplasts were shielded by a purple polycarbonate filter (PF). Means ± SD, *n*=5. Letters indicate significant differences at P=0.05.

Treatment	F_v/F_m	Φ_{PSII}	q_P	NPQ
'Red Rubin'				
35	0.59 (0.01)^{b}	0.27 (0.03)^{b}	0.23 (0.01)^{a}	0.16 (0.02)^{b}
35+B	0.47 (0.06)^{cd}	0.21 (0.03)^{c}	0.18 (0.02)^{bc}	0.14 (0.03)^{bc}
100	0.49 (0.04)^{c}	0.22 (0.02)^{c}	0.16 (0.03)^{cd}	0.20 (0.01)^{a}
100+B	0.44 (0.04)^{d}	0.16 (0.02)^{d}	0.15 (0.01)^{d}	0.22 (0.02)^{a}
100+B+PF	0.50 (0.01)^{c}	0.21 (0.01)^{c}	0.19 (0.01)^{b}	0.15 (0.03)^{bc}
'Tigullio'				
35	0.66 (0.05)^{a}	0.33 (0.05)^{a}	0.24 (0.01)^{a}	0.03 (0.01)^{f}
35+B	0.42 (0.01)^{de}	0.11 (0.02)^{e}	0.18 (0.03)^{bc}	0.14 (0.01)^{bc}
100	0.36 (0.04)^{e}	0.21 (0.02)^{c}	0.20 (0.02)^{b}	0.13 (0.01)^{cd}
100+B	0.27 (0.01)^{g}	0.13 (0.02)^{de}	0.20 (0.03)^{b}	0.08 (0.01)^{e}
100+B+ PF	0.40 (0.04)^{ef}	0.13 (0.02)^{de}	0.19 (0.04)^{b}	0.11 (0.01)^{d}

NPQ values were greater in acyanic protoplasts from 'Red Rubin' than from 'Tigullio' across most of the treatments, though high light caused a greater proportionate increase in NPQ in 'Tigullio' (**Table 5.3**). The purple filter effectively lowered NPQ in protoplasts of both cultivars. NPQ values were consistently lower for protoplasts than for intact leaves. Maximum PSII electron transport rates were about 32% higher for 'Tigullio' than for 'Red Rubin' control protoplasts at saturated light (**Fig 5.4a,b**). All treatments resulted in a decline in ETR; the different treatments affected ETR to a similar degree in 'Red Rubin', but in 'Tigullio' ETR appeared most affected by B (with or without high light).

Total chlorophyll content did not differ (P>0.05) between protoplasts of both cultivars, but decreased significantly following light and B treatments (**Table 5.4**). Chl *a*/*b* ratios were lower for 'Red Rubin' than for 'Tigullio' protoplasts. Of note, Chl *a*/*b* values for 'Tigullio' protoplasts, when shielded by a purple filter, declined to a ratio comparable to that for 'Red Rubin' control protoplasts (**Table 5.4**).

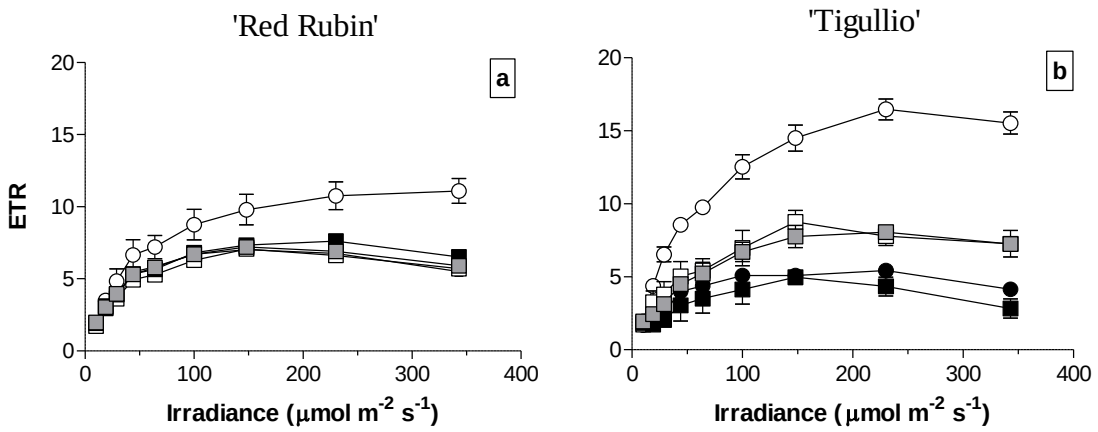

Fig. 5.4. Electron transport rate (ETR) in green protoplasts of *Ocimum basilicum* cultivars 'Red Rubin' (a) and 'Tigullio' (b). Protoplasts were treated with: 35 µmol m^{-2} s^{-1} white light (○); boron (B) and 35 µmol m^{-2} s^{-1} (●); 100 µmol $m^{-2}s^{-1}$ (□); or B and 100 µmol $m^{-2}s^{-1}$ with (◘) or without (■) a purple filter. Means ± SD, *n*=5.

Oxidative stress in protoplasts

MDA accumulated in green protoplasts within 180 min of both B and high light treatments. The combination of the two stressors elicited more MDA than did either stressor alone, or the effect was greater for 'Tigullio' than for 'Red Rubin' (P<0.05; **Fig. 5.5**).

The polycarbonate purple filter placed between the protoplasts and light source effectively reduced the extent of lipid peroxidation. Those results were corroborated by observations of H_2O_2 production, seen as epifluorescence from protoplasts infiltrated with DCFH-DA (**Fig. 5.6**). For both cultivars, the strongest fluorescence was observed under the combination of high light and B (**Fig. 5.6**) H_2O_2 production was consistently higher in 'Red Rubin' than in 'Tigullio' acyanic protoplasts, irrespective of treatment (**Fig. 5.6**).

Table 5.4. Total chlorophyll content (Chl *a+b*; µg mL^{-1}) and Chl *a:b* ratio in green protoplasts of *Ocimum basilicum* cultivars 'Red Rubin' and 'Tigullio'. Protoplasts were treated with white light at 35 or 100 µmol m^{-2} s^{-1} and/or 4 µM boron (B). Some protoplasts were shielded by a purple polycarbonate filter (PF). Means ± SD, *n*=5. Means without letters are not significant different at P=0.05.

TREATMENT	Chl *a+b*	Chl *a:b*
'Red Rubin'		
35	82.34 (1.86)	1.63 (0.04)
35+B	75.63 (3.15)	1.71 (0.12)
100	69.88 (1.69)	1.98 (0.11)
100+B	62.96 (2.88)	2.04 (0.07)
100+B+ PF	68.73 (1.78)	1.65 (0.05)
'Tigullio'		
35	86.73 (1.66)	2.25 (0.12)
35+B	83.12 (0.86)	2.29 (0.13)
100	72.93 (1.83)	2.19 (0.16)
100+B	65.96 (2.50)	2.27 (0.09)
100+B+ PF	73.91 (2.81)	1.73 (0.08)

Chloroplast numbers and dimensions within protoplasts were similar between the two cultivars, and no appreciable changes in chloroplast conformation and distribution were found across all the treatment as revealed by chlorophyll autofluorescence (**Fig. 5.6**).

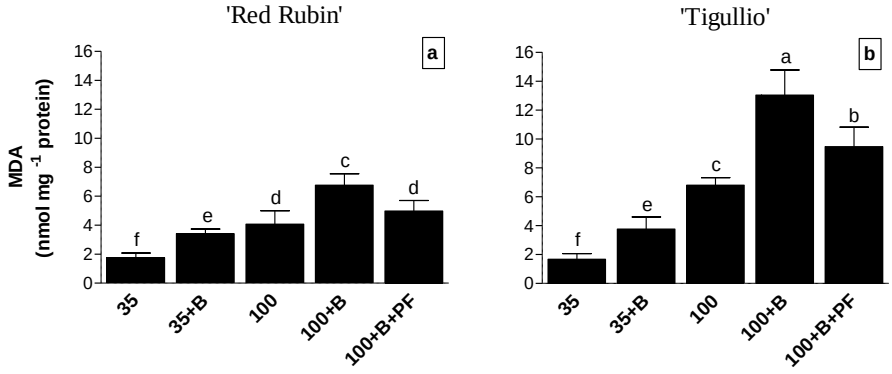

Fig. 5.5. MDA content in green protoplasts of *Ocimum basilicum* cultivars 'Red Rubin' (a) and 'Tigullio' (b). Protoplasts were treated with: 35 µmol m^{-2} s^{-1} white light (35); boron (B) and 35 µmol m^{-2} s^{-1} (35+B); 100 µmol $m^{-2}s^{-1}$ (100); B and 100 µmol $m^{-2}s^{-1}$ (100+B); or B and 100 µmol $m^{-2}s^{-1}$ with a purple filter (100+B+PF) for 180 min. Means ± SD, *n*=5. Letters indicate significant differences at P=0.05.

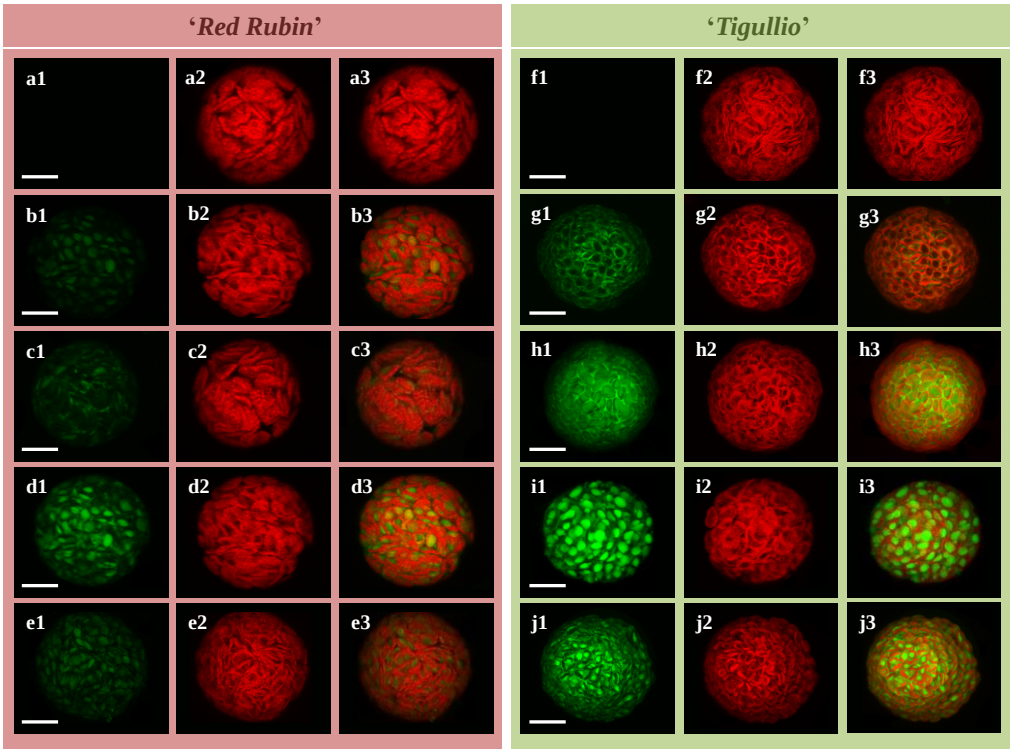

Fig. 5.6. Confocal laser scanning micrographs of protoplasts of *Ocimum basilicum* cultivars 'Red Rubin' (a-e) and 'Tigullio' (f-j) infused with DCFH. Protoplasts were treated with: 35 µmol m^{-2} s^{-1} of white light (a,f); boron (B) and 35 µmol m^{-2} s^{-1} (b,g); 100 µmol $m^{-2}s^{-1}$ (c,h); B and 100 µmol m^{-2} s^{-1} (d,i); or B and 100 µmol $m^{-2}s^{-1}$ with a purple filter (e,j). Column 1: DCF fluorescence, indicative of H_2O_2; columns 2: chlorophyll auto-fluorescence; columns 3: combination of DCF and autofluorescence. Images are representative of at least 30 protoplasts. Bars = 10 µm.

Discussion

Our previous studies indicated that the purple-leafed sweet basil cultivars ('Red Rubin' and 'Dark Opal') were more tolerant of B toxicity than were other green-leafed cultivars, and we postulated that foliar anthocyanins were likely to play a part in the protective mechanism (Landi et al., 2013b). Here, three sets of evidence from both intact plants and isolated protoplasts indicate that anthocyanins serve to mitigate effects of photoinhibitory stress in leaves once photosynthetic machinery is compromised by B toxicity.

First, when B-treated intact plants were given a photoinhibitory light treatment, the purple leaves showed a smaller decline in F_v/F_m, even when supplied with 30% extra light, than did the green leaves (**Table 5.2**). Moreover, when we attempted to simulate the optical effects of a layer of anthocyanic epidermal cells by applying a purple

polycarbonate film over the green leaves, the degree of photoinhibition diminished to a level approaching that of the purple-leafed cultivar (**Table 5.2**). The data are entirely consistent with a light-screening role for anthocyanins, preventing the over-excitation of chloroplasts for which the photosynthetic machinery has already been compromised by B. A photoprotective role for foliar anthocyanins has been reported many times (see reviews by: Chalker-Scott, 1999; Steyn et al., 2002; Gould et al., 2009), but to our knowledge, this is the first demonstration of its use in B-stressed plants. As evidence of its effectiveness, in the presence of the purple filter, the requirement for NPQ in 'Tigullio' leaves apparently diminished (**Fig. 5.1d**). NPQ *via* the xanthophyll cycle is a key mechanism through which leaves dissipate excess excitation energy as heat (Demmig-Adams and Adams 2006); several reports have shown that red leaves have a reduced pool of xanthophyll cycle components, suggesting that anthocyanins may constitute an alternative photoprotective strategy (Manetas et al., 2002; Kytridis et al., 2008; Hughes et al., 2012), although exceptions have been reported (Zeliou et al., 2009). Accordingly, in the absence of anthocyanins green leaves might be expected to have a greater reliance on xanthophylls; maximum NPQ values were 2 to 3 times greater in 'Tigullio' than in 'Red Rubin', irrespective of treatments (**Fig. 5.1b,d**). Thus, the PSII photochemical efficiency under not-saturated light conditions (Φ_{PSII}) might be expected to be comparable in the two cultivars albeit for different reasons: (I) in 'Tigullio' the excitation energy that exceeds photochemistry is channeled through the xanthophylls and dissipated as heat, while (II) in 'Red Rubin', anthocyanins abate quanta that would otherwise be absorbed by chloroplasts.

Second, to disentangle the effects of light-screening by epidermal anthocyanins from possible intrinsic differences between cultivars in light- and/or B-tolerance in the subjacent mesophyll, we measured the photoinhibitory responses of acyanic protoplasts from leaf mesophyll. That the B-treated protoplasts of both cultivars showed a smaller decline in F_v/F_m when shielded from high light by a purple polycarbonate film (**Fig. 5.3**, **Table 5.3**) or by a layer of anthocyanic protoplasts (**Fig. 5.3**), is further evidence of a direct, critical role of anthocyanins in light abatement. The data also confirm that an excess of light does indeed constitute a significant stressor for plant cells already compromised by B toxicity. Moreover, the lower ratio of Chl *a*:*b* in 'Red Rubin' than in

'Tigullio' protoplasts (**Table 5.4**) provides confirmation that the chloroplasts in purple leaves are the more shaded, most likely by the anthocyanic shield. Low Chl *a*:*b* is a characteristic feature of the leaves of shade plants (Lichtenthaler et al., 2000), and has been reported previously for anthocyanic leaf *laminae* (Gould et al., 2002b; Manetas et al., 2003; Kyparissis et al., 2007).

Third, the B-treated leaf tissues produced less H_2O_2 (**Figs.5.2** and **5.6**) and incurred less lipid peroxidation (**Fig. 5.5**) when they were partially shielded from high light by a purple polycarbonate filter, indicating that photoabatement by anthocyanins translates into a measurable benefit. The production of ROS by chloroplasts has long been observed in plants subjected to a variety of abiotic stressors, and this can lead to cell death when the abundance of ROS exceeds the scavenging capacities of the antioxidant pool (Asada, 1999; Mittler et al., 2004). Anthocyanins themselves may directly scavenge a diverse variety of ROS including H_2O_2 (Neill and Gould, 2003). However, a direct antioxidant role is unlikely when anthocyanins are located far from the source of ROS (Kytridis and Manetas, 2006). It is evident from the DCFH-infused protoplast suspensions (**Fig. 5.6**) that chloroplasts in leaf mesophyll are primary sources of H_2O_2 following light and B stress; clearly, the epidermal anthocyanins in 'Red Rubin' leaves (**Fig. 5.1a**) are not optimally located to scavenge those ROS. However, there is another source of H_2O_2 in the midrib and major veins of the leaf lamina (**Fig. 5.2**). It has been shown for other species that the chloroplasts in bundle sheath cells are the primary source of veinal H_2O_2 (Mullineaux et al., 2006). In that case, anthocyanins in the xylary parenchyma (**Fig. 5.1b**) might well contribute directly to the antioxidant pool. Nonetheless, because the effects on F_v/F_m of a layer of anthocyanic protoplasts were similar to those of a purple polycarbonate filter (**Fig. 5.3**), a light-screening role, rather than an antioxidant role of anthocyanins best explains the data in pigmented sweet basil.

Given that the mesophyll of 'Red Rubin' appears to be shade adapted as a result of the overlying anthocyanic cells, once the cells were exposed to high light following protoplast isolation we might have expected them to show more pronounced photoinhibition and greater oxidative damage than the presumably more light-adapted mesophyll protoplasts from 'Tigullio'. However, contrary to our expectations, the data indicate that green protoplasts of 'Red Rubin' continued to exhibit superior

photosynthetic performance when subjected to B and/or light stress, as indicated by the retention of higher F_v/F_m and Φ_{PSII} values (**Table 5.3**). In addition, 'Red Rubin' protoplasts appeared to produce less H_2O_2 (less DCF fluorescence) than did 'Tigullio' protoplasts when subjected to B and/or high light (compare **Fig. 5.6c,d** with **Fig. 5.6h,i**). It is possible that a proportion of the green fluorescence signal was absorbed by the red anthocyanin pigments; however, the ~50% lower MDA levels in 'Red Rubin' than in 'Tigullio' protoplasts subjected to high light plus B (**Fig. 5.5**) suggests that 'Red Rubin' mesophyll cells are intrinsically better fortified against oxidative damage. Thus, we postulate that in addition to the photoprotective role of anthocyanins in 'Red Rubin' leaves, other mechanisms, including a higher antioxidant pool, contribute to its more robust performance under B and light stress. Levels of both ascorbate and glutathione, key antioxidants in plant cells, are 2-fold higher in 'Red Rubin' than in 'Tigullio' (Landi et al., 2013a).

In conclusion, this report represents the first demonstration of a photoprotective role for anthocyanins in mesophyll cells when chloroplast functionality has been compromised by B toxicity. The data do not preclude other possible functions of anthocyanins in B tolerance, such as sequestration of boric acid and/or borate anions in the cell vacuole; these anions are likely able to bind with *cis*-diols as are phenols (Brown et al., 2002) and cyanidin derivates. Our work opens the possibility for future studies on anthocyanin-B interactions.

6. Epidermal acylated anthocyanins protect sweet basil against excess light stress: multiple consequences of light attenuation

Introduction

Many phenylpropanoid compounds are effective attenuators of sunlight, and are therefore considered to serve important functions in protecting photosynthetic organs faced with a superabundance of radiant energy (Agati and Tattini, 2010). Among all the phenylpropanoids, the anthocyanins are unusual as they absorb quanta in the green region of the solar spectrum, possibly protecting chloroplasts from the effects of absorbing supernumerary photons (Kytridis and Manetas, 2006; Lev-Yadun and Gould, 2007; Gould et al., 2010; Hughes, 2011). There is, indeed, good experimental evidence that anthocyanins mitigate photoinhibitory and photo-oxidative damage across a range of species, the pigments acting not only as light attenuators, but also as quenchers of reactive oxygen species (ROS) (Neill and Gould, 2003; Gould, 2004; Kytridis and Manetas, 2006; Hughes, 2011). Nevertheless, the putative involvement of anthocyanins in plants challenged against an excess of light, a condition transiently experienced by leaves on a daily, as well as a seasonal basis (Li et al., 2009), remains contentious (see review by Hughes, 2011).

Nikiforou et al. (2011) argued that foliar anthocyanins might at best serve only a marginal role in photoprotection because these pigments absorb maximally at wavelengths which are poorly used by chlorophyll. Accordingly, red-leafed genotypes of *Cistus creticus* and *Pistacia lentiscus* displayed photosynthetic inferiority as compared with their green counterparts under high light conditions in the winter (Zeliou et al., 2009; Nikiforou and Manetas, 2010; Nikoforou et al., 2010). Similarly, in variegated leaves of *Erytronium dens-canis* L., the red portions incurred greater photoinhibition than did the green portions when shaded plants were transiently exposed to 300 μmol quanta m^{-2} s^{-1} (Esteban et al., 2008). Red leaves often show the 'shade syndrome', having a lower Chl*a* to Chl*b* ratio (and nitrogen content) in comparison with green individuals (Manetas et al., 2003). The red individuals also seem to be less effective to dissipate excess radiant energy through non-photochemical quenching (NPQ) as compared to green leaves (Zeliou et al. 2009); the ratio of xanthophyll cycle

pigments to chlorophyll, as well as the ratio of violaxanthin to its de-epoxidation states increases far less in red than green leaves in response to high sunlight (Liakpoulous et al., 2006; Zeliou et al., 2009). However, such observations should be interpreted with caution. Rather than indicating a reduced capacity to process excess energy, such data might instead indicate that, since epidermal anthocyanins constitute the 'first line of photoprotective defense' (e.g., sustained anthocyanin biosynthesis during early stages of leaf development, Liakopoulos et al., 2006; Hughes et al., 2007, 2012), red leaves need smaller biochemical adjustments to the pool of photosynthetic pigments than do green leaves to cope with an excess of sunlight radiation (Manetas et al., 2002). In other words, fewer photons are incident on chloroplasts in the leaf in red-individuals, consistent with their shade-type leaves.

In our opinion, such contrasting conclusions about the possible role of anthocyanins in photoprotection might well originate from strikingly different experimental set-ups, which include both plant material and growth conditions. For example, attenuation of green light by anthocyanins may be physiologically significant only when plants are exposed to severe high light stress, possibly in combination with low temperatures (Terashima et al., 2009). Hughes et al. (2005) have shown that for overwintering leaves under field conditions the absorption of green wavelengths by anthocyanins protects PSII photochemistry from high light-induced damage. Similarly anthocyanins effectively protected maize leaves from photoinhibitory damage driven by high white-light at low temperature, thus 'attenuating' the requirement of antioxidant enzymes to remove ROS (Pietrini et al., 2002). It is noteworthy that in overwintering leaves, a suite of biochemical traits, which does not exclusively involve flavonoid biosynthesis, undergoes profound modification; these traits may affect the capacity of leaves to quench ROS, not only to avoid their generation by attenuating radiant energy from reaching the chloroplast (Kozlowski and Pallardy, 2002). Thus, anthocyanin biosynthesis is just one of the traits involved in photoprotection *sensu lato*. Similarly, in genotypes that transiently activate anthocyanin biosynthesis during the leaf juvenile phase (Hughes et al., 2007), alterations in the metabolism of photosynthetic pigment concomitantly occur (products of the 2-C-methyl-d-erythritol 4-phosphate, MEP,

pathway strongly compete for the same substrate, Niinemets et al., 2012; Rasulov et al., 2013).

The issue is further complicated because most experiments seeking to understand the significance of anthocyanins in photoprotection have not adequately explored their chemical structures; in most publications, anthocyanins have been quantified using simple spectrophotometric measurements over a narrow range of green-wavelengths. However, anthocyanins when acylated with coumaroyl or sinapoyl moieties (Andersen et al., 2010), are effective attenuators of UV, not only of green solar wavelengths. This is important, as UV-attenuation by phenylpropanoids may have a tremendous impact on leaf/whole-plant architecture, and, in turn, on light-induced adjustments in the physiology and biochemistry of leaves/plants (Tattini et al., 2005; Potters et al., 2007; Pollastri and Tattini, 2011).

Here, we explore the significance of epidermal anthocyanins in photoprotection in sweet basil (*Ocimum basilicum* L.). We grew 'Tigullio' and 'Red Rubin', two cultivars that display green or purple leaves, respectively, independent of light intensity or their developmental stage. Therefore, possible confounding effects driven by environmental changes responsible for anthocyanin biosynthesis (such as cold temperatures and the stage of leaf development) were removed in our study. A number of morph-anatomical, physiological and biochemical traits, including whole-plant and leaf morphology, anatomy and optical properties of leaves, gas exchange and PSII performance, the concentrations of individual photosynthetic pigments and phenylpropanoids, including anthocyanins, were estimated.

Materials and methods

Plant material and growth conditions

Two-week-old potted (1.2 L pots with a sandy soil/sphagnum peat substrate, 60:40, v:v) plants of *O. basilicum*, the green-leafed cultivars 'Tigullio' (country of origin Italy) and purple-leafed cultivars 'Red Rubin' (*O. basilicum* 'Purperescens', country of origin India), were grown outdoors for 10 d under 50% sunlight. Plants were then placed in boxes constructed with black polyethylene nets to receive 30% (shade) or 100% (sun) sunlight. Before the start of the experiment, on July 10th, plants in the full-sunlight

treatment were exposed to increasing sunlight for 6 d (starting from 50% solar radiation, and increasing the irradiance by 20% every 2 d). Light treatments were imposed for an additional 2-wk-period. Plants at the full-sun site received mean daily doses of 10.1 MJ m^{-2}, 0.90 MJ m^{-2} and 17.8 kJ m^{-2} of photosynthetically active radiation (PAR), UV-A and UV-B wavebands, respectively. PAR at midday was 615±53 and 1918±121 µmol photons m^{-2} s^{-1} (mean ± standard deviation, n=14) in the shade and full sun, respectively. UV irradiance (280–400 nm) and PAR inside the greenhouses were measured by a SR9910-PC double-monochromator spectroradiometer (Macam Photometric Ltd., Livingstone, UK), and a calibrated Li-190 quantum sensor (Li-Cor Inc., Lincoln, NE, USA), respectively. Min/Max temperatures were on average 18.5/32.2 °C or 17.5/33.5 °C at the shade or in full sun. All measurements were carried out on expanding leaves, the area of which was approx. 20–25% of the leaf lamina area of fully developed leaves at the beginning of the experiment (i.e. leaves were 25-d-old at the end of the experiment).

Leaf morph-anatomy and optics

Leaf area was measured with a Li-Cor LI-3100 area meter (Li-Cor Inc., Lincoln, NE). Leaf mass per area (LMA, mg dry weight cm^{-2}) was determined as reported previously (Tattini et al., 2000) on six replicate plants. Leaf lamina thickness was measured from 1-µm-thick transverse sections, obtained from material that was fixed, infiltrated and embedded as described by Tattini et al. (2004). Sections were examined in a Leica DM LB2 compound microscope (Leica, Germany), equipped with a high-resolution TK 870E JVC video camera. Hand-cut transverse sections from fresh leaves were examined in a light microscope to visualize anthocyanin location.

Leaf optical properties were determined of adaxial and abaxial surface on mature leaves of six replicate plants by recording reflectance (R) and transmittance (T) spectra in the 380–1100 nm waveband (at 1-nm intervals) using a LI 1800 spectroradiometer equipped with a LI 1800-125 integrating sphere (Li-Cor Inc.). The integrated absorptance (A% = 100 - R - T) over the 400-700 nm and the 520-570 nm wavebands ($A_{400\text{-}700}$, $A_{520\text{-}570}$) and the scattering index [$(R/T)_{850}$] were determined after Lee and Graham (1986). Both the ‘absorptance efficiency’ and the ‘scattering efficiency’ (Knapp

and Carter, 1998) were then normalised for dry weight of 1.65 cm^2 portion of leaf used in the LI 1800. Normalization of optical features on dry mass, rather than area basis, has been successfully used to compare the optical features of leaves differing in their whole-leaf thickness and LMA (Knapp and Carter, 1998), as was also the case in our experiment. Plant growth was estimated in terms of the relative growth rate of the shoot (RGR^{shoot}) of 10 replicate plants as $RGR^{shoot} = \ln (DW_1 - DW_0)/(t_1 - t_0)$. DW is the dry weight of the shoot and $t_1 - t_0$ is the time interval. Shoot dry weight (g) at the beginning of the experiment was measured on a total of 12 plants and was 0.80 ± 0.06 (mean ± standard deviation, *n*=12) in shade or 0.84 ± 0.07 in sun 'Tigullio' plants, and 0.63 ± 0.04 in shade or 0.68 ± 0.05 in sun 'Red Rubin' plants.

Gas exchange and chlorophyll fluorescence imaging

Gas exchange was measured under saturating light, i.e. at PPFD of 800 or 1100 μmol m^{-2} s^{-1} over the photosynthetic active radiation (PAR) waveband, for shade and sun leaves, respectively, of six replicate leaves (leaf temperature of 30 °C). We measured net CO_2 assimilation rate (P_n^{sat}), stomatal conductance (g_s), and intercellular CO_2 concentration (C_i) using a LI-6400 portable photosynthesis system, operating at 380 μL L^{-1} ambient CO_2 concentration. Light response curves for P_n were taken between 0 and 1800 μmol m^{-2} s^{-1}. Diurnal variation in P_n was also recorded *in situ* from 06:00 to 21:00 h on four replicate plants. Daily carbon gain was then calculated by integrating the diurnal curve as described in Tattini et al. (2004). Daily course of net photosynthesis was determined at weekly intervals.

Images of chlorophyll fluorescence were obtained using a MAXI-Imaging-PAM chlorophyll fluorometer (Walz, Effeltrich, Germany). A charge-coupled device (CCD) camera with a resolution of 640×480 pixels collected the fluorescence signal emitted by 40-min dark-adapted leaves. The maximum efficiency of photosystem II (PSII) photochemistry was calculated as $F_v/F_m = (F_m - F_0)/ F_m$, where F_v is the variable fluorescence and F_m is the maximum fluorescence of dark-adapted leaves (leaf T of 28 °C). F_m', i.e. the maximum fluorescence in light conditions, was determined at 800 or 1110 μmol m^{-2} s^{-1} of photons over the PAR waveband, i.e. at light intensities at which saturation of photosynthesis occurred for shade and sun leaves, respectively.

Chlorophyll fluorescence images taken from illuminated leaves were used to calculate the operating photochemical efficiency of PSII ($\Phi_{PSII} = (F_m' - F_s)/F_m'$; Genty et al., 1989). Non-photochemical quenching (NPQ) then calculated as $NPQ = (F_m - F_m')/F_m$ (Bilger and Björkman, 1990). Excess energy to the photosynthetic apparatus (E) was calculated as $E = (1 - q_P) \times (Fv'/Fm') \times 0.5 \times PPFD \times$ absorption coefficient (Kornyeyev et al., 2010), where q_P, the photochemical quenching, was calculated as in Schreiber et al. (1995). The absorption coefficient over the 400-700 nm waveband averaged 0.84 for both sun and shade leaves in 'Tigullio', whereas it was 0.91 or 0.96 for shade or sun leaves, respectively, in 'Red Rubin'.

Analysis of photosynthetic pigments and phenylpropanoids

Individual carotenoids in leaves sampled at predawn and midday were identified and quantified as reported by Beckett et al. (2012), on four replicate plants. Leaves were immediately frozen in liquid nitrogen and kept at -80 °C until analysis. Fresh leaf material (120–150 mg) was extracted with 2 × 4 mL acetone (containing 0.5 g L^{-1} $CaCO_3$) and 15 µL aliquots were injected in a Perkin Elmer Flexar chromatograph equipped with a quaternary 200Q/410 pump and LC 200 diode array detector (all from Perkin Elmer, Bradford, CT, USA). Photosynthetic pigments were separated by a 250 × 4.6 mm Waters Spherisorb ODS1 (5 µm) column operating at 30 °C, eluted with a linear gradient solvent system, at a flow rate of 1.2 mL min^{-1} consisting of CH_3CN/MeOH/H_2O (8.4/0.8/0.7, A) and MeOH/ethyl acetate (6.8/3.2, B) during an 18 min run: 0–12 min from 100 to 0% A;12–18 min at 0% A. Xanthophyll cycle pigments were tentatively identified using visible spectral characteristics and retention times Quantification of violaxanthin (V) and antheraxanthin (A) was done using a calibration curve of an authentic lutein standard (Extrasynthese, Lyon-Nord, Genay, France); that of zeaxanthin (Z) used the calibration curve of an authentic zeaxanthin standard (Extrasynthese). Chlorophylls *a* and *b* were quantified using calibration curves of chlorophylls authentic standards (Sigma-Aldrich, Milan, Italy).

Phenylpropanoids were assayed in leaves of four replicate plants sampled at midday using the following protocol: leaf tissue (50-60 mg) was extracted with 3 mL of $CHCl_3$/CH_3OH/H_2O 12:5:1 (adjusted to pH 2 with HCOOH) under 30 min-sonication in

the dark at 4°C. Then 1.66 mL $CHCl_3$ and 0.77 mL H_2O (pH 2) were added, the mixture stirred for 10 min, and then centrifuged (at 3000 × *g*). The upper phase was collected and 20 µl aliquots injected in the liquid-chromatography system reported above. Cyanidin 3-*O*-rhamnoside and quercetin 3-*O*-galactoside (Extrasynthese) were used as internal standards to estimate the recovery of anthocyanins and phenylpropanoids, respectively. Anthocyanins were separated using a 4.6 × 250 mm Zorbax SB C_{18} column (5 µm), operating at 30 °C, and eluted at the flow rate of 1mL min^{-1} with a linear gradient solvent system consisting of H_2O (plus 5% HCOOH (A), CH_3OH (plus 5% HCOOH) (B), CH_3CN (plus 5% HCOOH (C), during a 47-min run: 0-2 min 80% A, 15% B, 5% C; 2-17 min to 70% A, 20% B, 10% C; 17-32 min to 55% A, 30% B, 15% C; 32-37 min 55% A, 30% B, 15% C; 37-42 min to 20% A, 40% B, 40% C; 42-47 min 20% A, 40% B, 40% C. Individual anthocyanins were tentatively identified using their retention times, UV-spectral characteristics and mass-spectrometric data (details given in Table S3A, in Supplementary Material) Quantification of anthocyanins was performed at 530 nm using calibration curves of cyanidin 3-*O*-glucoside and pelargonidin 3-*O*-glucoside (Extrasynthese). Other phenylpropanoids, namely hydroxycinnamic acid and flavone derivatives were separated using a 4.6 × 250 mm SunFire C_{18} (3.5 µm) column operating at 30 °C and eluted, at the flow rate of 1 mL min^{-1} using a linear gradient solvent consisting of H_2O (plus 10 mM CH_3COONH_4 pH 4.4)/CH_3CN (95:5) (A) and CH_3CN /H_2O (plus 10 mM CH_3COONH_4 pH 4,4) (95:5) (B): 0-10 min 0% B; 10-50 min 85% B; 50-55 min 100% B. Individual phenylpropanoids were identified using UV-spectral characteristics, retention time of authentic standards and by mass spectrometric data (details given in **Table S6.3B** in Supplementary Material). Quantification of chlorogenic and rosmarinic acids was performed at 330 nm using calibration curves of authentic standards (Extrasynthese). Quantification of unknown caffeic acid and flavone derivatives was performed using the calibration curve of caffeic acid and luteolin 4'-*O*-glucoside, respectively.

UV-spectral features of epidermal anthocyanins were measured after the removal of non-anthocyanic metabolites. For this purpose the aqueous phase of leaf extract was partitioned with ethyl acetate (2 mL × 3). Non-anthocyanic compounds removal as well as the recovery of anthocyanins were checked using HPLC-DAD analysis. Then extracts

were diluted (1:100) prior to recording their absorbance spectra on a Perkin Elmer Lambda 25 Spectrophotometer (Perkin-Elmer).

Transmission electron microscopy (TEM)

Light-induced effects on leaf ultrastructure were examined using TEM analysis. Leaf pieces (~ 3 × 3 mm) were fixed for 2 h, at room T in 2.5% glutaraldehyde (in 0.2 M phosphate buffer, pH 7.2). Specimen were then washed twice in phosphate buffer, and post-fixed for 2 h at room T in 2% OsO4 (in phosphate buffer). Specimen were then dehydrated in an ethanol series, infiltrated and embedded in Spurr resin (Sigma-Aldrich; Milan, Italy), and polymerized at 70 C over 24 h, as reported previously (Guidi et al., 2010). Ultrathin transverse section (70-90-nm-thick) were cut with a LKB IV ultramicrotome (LKB Produkter, New York, USA), collected on Formvar coated copper grids (Sigma-Aldrich Italia, Milan), stained with uranyl acetate and lead citrate, and examined in a Philips CM12 transmission electron microscope (Philips, Eindhoven, The Netherlands) operating at 80 kV.

Experimental design and statistics

The experiment was a completely randomized design with 32 plants *per* cultivar. Data were subjected to a two-way analysis of variance (ANOVA), with cultivar and light as fixed factors, with their interaction factor, or a three-way ANOVA (for photosynthetic pigments) with cultivar, light and sampling time as fixed factors with their interaction factors, using the Statistica v. 8.0 software (StatSoft, Inc., 2007, Tulsa, OK, USA). Summary of ANOVA has been reported in Supplementary Material (**Tables S6.1** and **S2**). The extent to which sunlight irradiance affected examined traits, i.e. normalized plasticity index (*sensu* Valladares et al., 2006) was estimated by the normalized index of variation (NIV) which was calculated as NIV = $(X_{sun} - X_{shade})/(X_{sun} + X_{shade})$, where X is the examined trait (Tattini et al., 2006).

Results

Overall, 'Tigullio' was much more plastic than 'Red Rubin' to changes in sunlight irradiance (**Tables 6.1-6.4**). Mean NIV, i.e., calculated for the entire set of 33 traits, was

0.30 in ‘Tigullio’ and 0.15 in ‘Red Rubin’. Interestingly, major differences between the two cultivars were observed for leaf morphometrics and optics (NIV_{TG} = 0.23 *vs* NIV_{RR} = 0.03, **Table 6.1**), and for PSII performance (NIV_{TG} = 0.11 *vs* NIV_{RR} = 0.03, **Table 6.2**). Light-induced changes in biochemical-related traits were also greater in ‘Tigullio’ (NIV = 0.40) than in ‘Red Rubin’ (NIV = 0.23), particularly for photosynthetic pigment concentration and composition (NIV_{TG} = 0.33 *vs* NIV_{RR} = 0.17, **Table 6.3** and **Table 6.4**). Notable exceptions included light-induced variations in net CO_2 assimilation rate at saturating light (P_n^{sat}), daily CO_2 assimilation (CO_2^{daily}) and, consequently, the relative growth rate of the shoot (RGR^{shoot}), which were indeed higher in ‘Red Rubin’ (NIV = 0.31) than in ‘Tigullio’ (NIV = 0.18). Notably, ‘Tigullio’ and ‘Red Rubin’ displayed very different behavior when grown in the shade, not only during the shade-sun transition. These differences in morph-anatomical, physiological and biochemical traits are detailed below.

Table 6.1. Growth, morph-anatomical and optical features of green ('Tigullio') and purple ('Red Rubin') basil at the end of a 2-wk-period of exposure at 30% or 100% solar irradiance. Data are the means ± standard deviation (n=10 for RGR^{shoot}, n=6 for other traits). The normalized index of variation (NIV) estimates the extent to which sunlight irradiance affected examined traits in each cultivar.

Trait	'Tigullio'		'Red Rubin'		$NIV_{TIGULLIO}$	$NIV_{RED\ RUBIN}$
	30%	100%	30%	100%		
RGR^{shoot} ($d^{-1} \times 10^3$)	8.8 ± 0.5	10.7 ± 0.4	5.1 ± 0.3	9.5 ± 0.5	+0.10	+0.30
Leaf size (cm^2)	14.4 ± 1.3	7.6 ± 0.6	5.8 ± 0.7	5.4 ± 0.5	–0.31	–0.04
LMA (mg DW cm^{-2})	5.3 ± 0.2	7.9 ± 0.6	5.9 ± 0.3	6.3 ± 0.4	+0.20	+0.03
Leaf thickness (µm)	213 ± 11	318 ± 19	246 ± 17	254 ± 16	+0.20	+0.02
$A_{400\text{-}700}$ mg^{-1} DW	9.5 ± 0.3	6.1 ± 0.6	9.6 ± 0.4	9.1 ± 0.6	–0.22	–0.03
$A_{520\text{-}570}$ mg^{-1} DW	7.5 ± 0.3	4.4 ± 0.4	9.5 ± 0.3	9.2 ± 0.4	–0.26	–0.02
$(R/T)_{850}$ mg^{-1} DW	0.102 ± 0.010	0.063 ± 0.005	0.093 ± 0.004	0.090 ± 0.006	–0.21	–0.03

Table 6.2. Shoot biomass, gas exchange and PSII performance of green ('Tigullio') and purple ('Red Rubin') basil at the end of a two-week-period of exposure at 30% or 100% solar irradiance. Data are the means ± standard deviation (*n*=6). The normalized index of variation (NIV) estimates the extent to which sunlight irradiance affected examined parameters in each cultivar.

Parameter	'Tigullio'		'Red Rubin'		$NIV_{TIGULLIO}$	$NIV_{RED\ RUBIN}$
	30%	100%	30%	100%		
P_n (µmol m^{-2} s^{-1})	9.9 ± 1.0	15.1 ± 0.8	7.5 ± 0.5	13.6 ± 0.6	+0.21	+0.29
g_s (mmol m^{-2} s^{-1})	265 ± 21	393 ± 34	278 ± 26	406 ± 31	+0.20	+0.18
Φ_{CO2} (µmol mol^{-1} quanta)	66 ± 6	35 ± 4	52 ± 5	45 ± 4	–0.31	–0.07
LCP (µmol quanta m^{-2} s^{-1})	36 ± 4	68 ± 8	47 ± 5	53 ± 4	+0.31	+0.06
C_i (µl L^{-1})	251 ± 11	235 ± 22	249 ± 19	246 ± 13	–0.03	–0.01
CO_2^{daily} (mmol m^{-2} d^{-1})	206 ± 20	337 ± 22	160 ± 12	340 ± 20	+0.24	+0.35
F_v/F_m	0.83 ± 0.01	0.77 ± 0.02	0.82 ± 0.01	0.81 ± 0.01	–0.04	–0.01
Φ_{PSII}	0.57 ± 0.04	0.43 ± 0.03	0.52 ± 0.03	0.50 ± 0.03	–0.14	–0.02
F_v'/F_m'	0.65 ± 0.05	0.54 ± 0.03	0.57 ± 0.03	0.56 ± 0.04	–0.09	–0.00
q_P	0.65 ± 0.03	0.52 ± 0.05	0.70 ± 0.04	0.68 ± 0.04	–0.11	–0.01
NPQ	1.49 ± 0.12	2.22 ± 0.19	1.40 ± 0.11	1.68 ± 0.13	+0.19	+0.09
E (µmol quanta m^{-2} s^{-1})	82 ± 6	146 ± 11	72 ± 6	103 ± 8	+0.28	+0.18

Table 6.3. Changes in the concentration and composition of photosynthetic pigments in leaves of green ('Tigullio') and purple ('Red Rubin') basil, sampled at predawn (*PD*) and midday (*MD*), at the end of a 2-wk-period of exposure at 30% or 100% sunlight irradiance. Data are means ± standard deviation (*n*=4). The normalized index of variation (NIV) estimates the extent to which sunlight irradiance affected examined traits in each cultivar. Chl_{tot}, total chlorophyll, (A+Z)/(V+A+Z) denotes the de-epoxidation state (DES) of violaxanthin-cycle pigments. Carotenoids are expressed on a Chl_{tot} basis (mmol mol^{-1} Chl_{tot}).

Pigment	Time	'Tigullio'		'Red Rubin'		$NIV_{TIGULLIO}$	$NIV_{RED\ RUBIN}$
		30%	100%	30%	100%		
Chl_{tot} (µmol g^{-1} DW)	*PD*	11.0 ± 0.3	7.8 ± 0.4	10.4 ± 0.2	9.7 ± 0.3	–0.17	–0.03
	MD	9.8 ± 0.2	8.0 ± 0.3	9.7 ± 0.3	9.3 ± 0.4	–0.10	–0.02
Chl*a*/Chl*b*	*PD*	1.6 ± 0.2	2.0 ± 0.1	1.4 ± 0.1	1.6 ± 0.1	+0.11	+0.07
	MD	1.7 ± 0.2	2.4 ± 0.2	1.5 ± 0.1	1.6 ± 0.2	+0.17	+0.03
Violaxanthin (V)	*PD*	123 ± 14	210 ± 19	120 ± 14	140 ± 16	+0.26	+0.08
	MD	121 ± 16	133 ± 21	110 ± 9	98 ± 8	+0.04	–0.06
Antheraxanthin (A)	*PD*	8 ± 2	22 ± 4	5 ± 1	10 ± 1	+0.47	+0.33
	MD	19 ± 4	70 ± 7	11 ± 1	20 ± 3	+0.57	+0.29
Zeaxanthin (Z)	*PD*	7 ± 2	26 ± 5	3 ± 1	8 ± 2	+0.58	+0.45
	MD	13 ± 2	165 ± 18	6 ± 1	15 ± 3	+0.85	+0.43
V + A + Z	*PD*	139 ± 8	258 ± 23	128 ± 9	158 ± 17	+0.30	+0.10
	MD	153 ± 11	368 ± 27	127 ± 12	143 ± 15	+0.41	+0.06
(A+Z)/(V+A+Z)	*PD*	0.10 ± 0.02	0.19 ± 0.02	0.06 ± 0.01	0.11 ± 0.02	+0.31	+0.29
	MD	0.18 ± 0.02	0.67 ± 0.03	0.13 ± 0.02	0.26 ± 0.03	+0.58	+0.33

Table 6.4. The concentration of phenylpropanoids (mg g^{-1} DW) and the accumulation of phenylpropanoids normalized to total assimilated CO2 ($Phenyl^{CO2}$, mg phenyl g^{-1} CO_2) in 'Tigullio' and 'Red Rubin' grown at 30% (shade) or 100% (sun) sunlight irradiance over a two-week-period. $Phenyl^{CO2}$ in 'Red Rubin' was calculated including the concentration of anthocyanins. Details on individual phenylpropanoids are given in **Table S3.4.1** snd **Table S3.4.2** in Supplementary Material.

Phenylpropanoids	'Tigullio'		'Red Rubin'		$NIV_{TIGULLIO}$	$NIV_{RED\ RUBIN}$
	Shade	Sun	Shade	Sun		
Rosmarinic acid	5.5 ± 0.8	18.7 ± 1.9	11.8 ± 1.9	26.8 ± 2.6	+0.54	+0.39
Caffeic acid derivatives	1.6 ± 0.2	4.1 ± 0.7	2.6 ± 0.5	6.3 ± 0.3	+0.44	+0.42
Luteolin derivatives	0.8 ± 0.2	2.1 ± 0.2	0.6 ± 0.1	1.2 ± 0.3	+0.45	+0.33
Cyanidin 3-*O*-derivatives	n.d	n.d.	0.7 ± 0.1	1.0 ± 0.3	–	+0.18
Pelargonidin 3-*O*-derivatives	n.d.	n.d.	0.3 ± 0.1	0.4 ± 0.1	–	+0.14
Coumaroyl-cyanidin derivatives	n.d.	n.d.	1.2 ± 0.2	2.1 ± 0.2	–	+0.27
$Phenyl^{CO2}$	2.5 ± 0.4	8.0 ± 1.0	8.7 ± 0.8	10.4 ± 0.6	+0.52	+0.09

Plant growth and morphology, leaf morph-anatomy and optics

'Red Rubin' and 'Tigullio' differed in shoot morphology and leaf anatomy irrespective of the irradiance under which they had been grown (**Fig. 6.1**, **Table 6.1** and **Table S6.1**). 'Tigullio' was taller than 'Red Rubin', more so under 30% sunlight. 'Tigullio' had fewer branches, larger leaf lamina but thinner leaves than 'Red Rubin' under shading. 'Tigullio' showed typical sun-shade dimorphism: sun leaves were smaller and thicker, had a thicker layer of palisade mesophyll, and had more spongy mesophyll layers than did shade leaves. 'Red Rubin' displayed very small differences in whole-plant and leaf morphology, as well as in leaf anatomy in response to the light environment. Shoot biomass increased more under higher light, and the increase in RGR^{shoot} was four-fold greater in 'Red Rubin' (+86%) than in 'Tigullio' (+22%) (**Table 6.1**).

These anatomical changes, as well as the presence of epidermal anthocyanins exclusively in 'Red Rubin' (**Fig. 6.2**), correlated with changes in leaf absorptance efficiency over the 400-700 nm waveband ($A_{400\text{-}700}$), and with the scattering efficiency (R/T_{850}) displayed by 'Tigullio' and 'Red Rubin' (**Table 6.1**). Significant declines in $A_{400\text{-}700}$ (–33%) and R/T_{850} (–38%) were observed in 'Tigullio', but not in 'Red Rubin', when plants were grown in full sunlight. The greatest differences were observed in the absorptance of green-yellow light, e.g., $A_{520\text{-}570}$: in 'Red Rubin' $A_{520\text{-}570}$ was 27% greater in the shade or 109% greater in full sun than in 'Tigullio' (**Table 6.1** and **Table S6.1**). Overall, the transmission, over the whole-leaf thickness, of photosynthetic photons was less, whereas the photon path length was higher in 'Red Rubin' than in 'Tigullio', when grown in full sun (R/T_{850}, **Table 6.1** and **Table S6.1**).

Gas exchange and PSII performance

Quantum yields for CO_2 assimilation (Φ_{CO2}) in the shade were greater for 'Tigullio' than for 'Red Rubin' (**Table 6.2**). However, Φ_{CO2} decreased sharply (–47%) in 'Tigullio' when transferred to full sunlight, whereas for 'Red Rubin' Φ_{CO2} declined by just 15%. Similarly, 'Tigullio' leaves exhibited a lower light compensation point (LCP) in the shade (–22%), but higher in full sun (+31%) as compared with 'Red Rubin'. Net photosynthesis at saturating light was significantly greater (+32%) in 'Tigullio' than in 'Red Rubin' in the shade, but did not differ much (11%) in the sun. The net daily carbon

gain (CO_2^{daily}) did not differ in the sun, whereas CO_2^{daily} was significantly higher in 'Tigullio' than in 'Red Rubin' in the shade (**Table 6.2 and Table S6.1**).

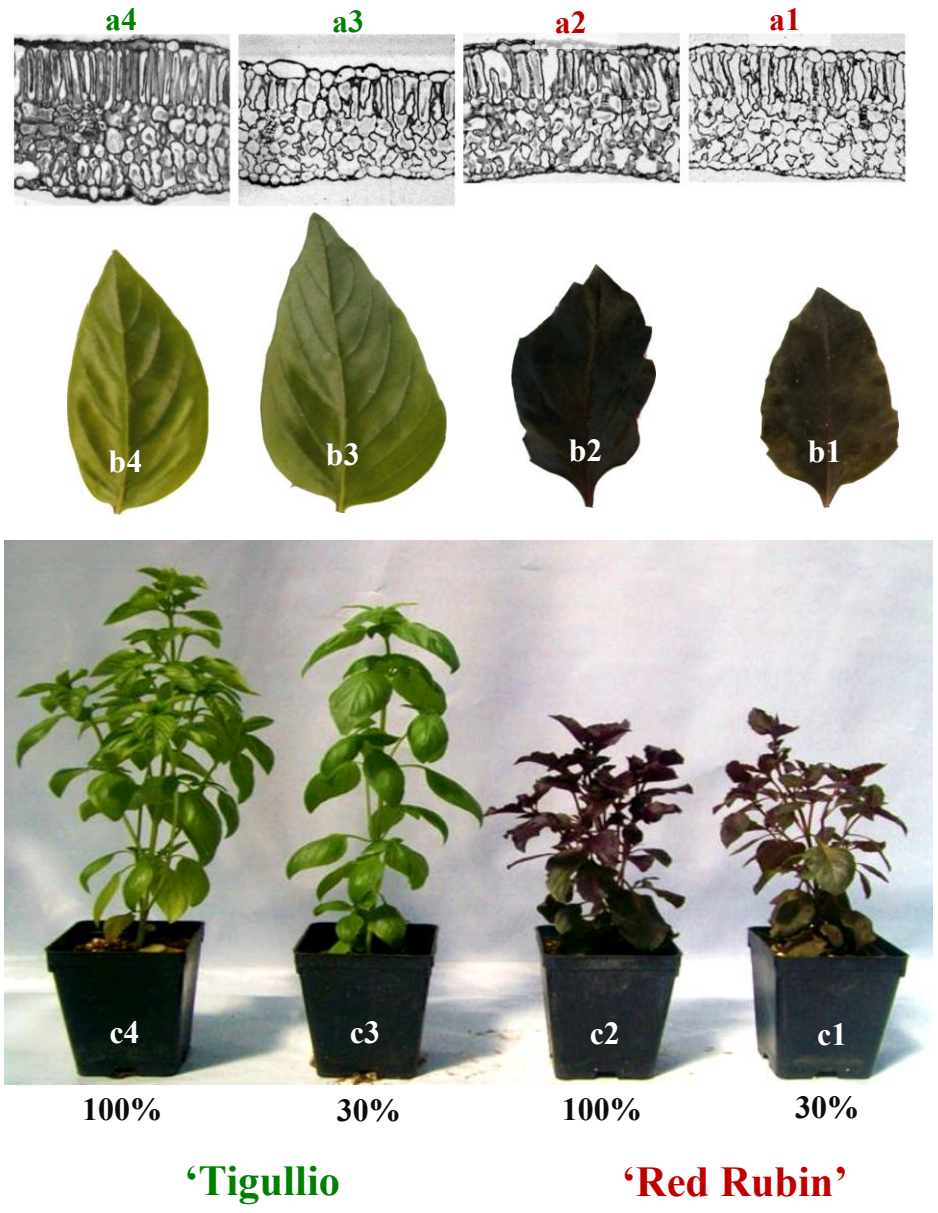

Fig 6.1. Exposure of plants at 30% or 100% sunlight over a 2-wk-period affects the morphology and anatomy of shoots and leaves in green 'Tigullio' but not in purple basil cultivar 'Red Rubin'. Reduction in leaf size (b3-b4), increase in whole-leaf thickness and mesophyll compactness (a3-a4) occur in response to high sunlight only in 'Tigullio' plants. Mesophyll cell shape varies greatly in 'Tigullio' but not in 'Red Rubin' because of high sunlight. Shoots in 'Tigullio' in full sun (c4) have reduced internode length and are more branched as compared with shoots grown at 30% sunlight irradiance (c3). Please note the unusual shoot architecture in 'Red Rubin' in the shade (c1).

'Tigullio' showed a greater depression in net CO_2 assimilation rate (-31%) from 12:00 to 16:00 h, when high solar irradiance coupled with hot air T° (on average ~33 °C over

the whole experimental period), as compared with 'Red Rubin' (-12%), particularly in full sunlight (-37% in 'Tigullio' *vs* -15% in 'Red Rubin', **Table S6.1**).

Cultivar-specific variations in response to high sunlight were also observed for Chl*a* fluorescence-derived parameters (**Table 6.2** and **Table S6.1**). Maximal efficiency of PSII photochemistry (F_v/F_m) did not vary in 'Red Rubin' or significantly declined in 'Tigullio' in response to high sunlight. Photochemical quenching (q_P), as well as PSII quantum yield in the light (Φ_{PSII}) were higher in 'Red Rubin' than in 'Tigullio' leaves exposed to full sunlight. Exposure of plants to full sunlight enhanced non photochemical quenching (NPQ) to a much greater extent in 'Tigullio' (+49%) than in 'Red Rubin' (+20%). Overall, excess energy to PSII, E, was much greater (+42%) in 'Tigullio' than in 'Red Rubin'.

Photosynthetic pigments

'Red Rubin' and 'Tigullio' markedly differed for the concentration and composition of photosynthetic pigments. These differences were particularly evident when comparing 'Red Rubin' and 'Tigullio' sun leaves sampled at midday (**Table 6.3** and **Table S6.2**). In details, Chl_{tot} and the ratio of Chl*a* to Chl*b* did not change much in 'Red Rubin', whereas significantly varied in 'Tigullio' because of sunlight irradiance and sampling time. The concentration of xanthophyll-cycle pigments (VAZ) relative to Chl_{tot} (VAZ/Chl_{tot}) was also much greater (+61%) in 'Tigullio' than in 'Red Rubin', especially in sun leaves (+107%). VAZ/Chl_{tot} increased in 'Tigullio' (in both shade and sun leaves), whereas did not substantially vary in 'Red Rubin' from predawn to midday De-epoxidation state of VAZ (DES) also greatly varied between examined cultivars, as DES in 'Tigullio' exceeded by 47% in the shade or by 132% in the sun that calculated in 'Red Rubin'. As expected, DES steeply increased from predawn to midday (on average +161%), particularly in 'Tigullio' leaves (+193%).

Anthocyanins and phenylpropanoids

Both acylated and non-acylated anthocyanins were located on the adaxial and abaxial epidermises in 'Red Rubin' leaves (**Fig. 6.2**). Acylated anthocyanins were mostly coumaroyl derivatives of cyanidin, whereas non-acylated anthocyanins were glycosides of both cyanidin and pelargonidin (**Table 6.4**, **Table S6.3**). Coumaroyl anthocyanins were more responsive (+75%) to sunlight irradiance than non-acylated anthocyanins (+40%, **Table 6.4**). Sun and shade leaves in 'Red Rubin' mostly differed in their

abilities to absorb UV-B (absorbance over the 300-320 nm waveband was 40% higher in sun leaves than in shade leaves) and not green-yellow solar wavelengths (differences in absorbance between shade and sun leaves were ~12% over the 520-570 nm waveband, **Fig. 6.2**).

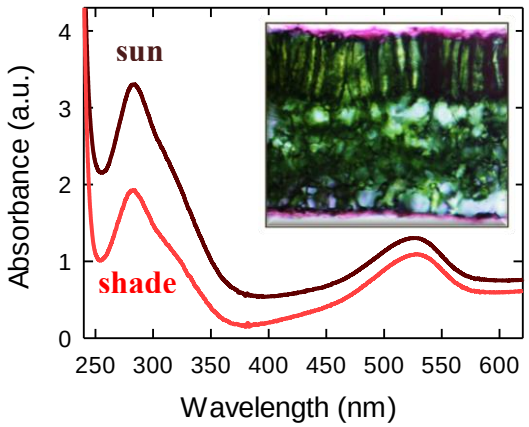

Fig 6.2. Anthocyanins occur in the adaxial and abaxial epidermises in purple basis. Spectral features of leaf extracts in 'Red Rubin' leaves reveal that major anthocyanins are acylated with hydroxycinnamic acid derivatives (please note the shoulder at ~320 nm). Please note that absorbance over the whole UV-B spectral region (280-320 nm) largely exceeds the absorbance over the 490-550 nm spectral region, in both shade and sun leaves.

Phenylpropanoid metabolism (i.e. pooling together anthocyanins, rosmarinic acid, and caffeic acid and luteolin derivatives) was much more active in purple than in green basil in the shade (**Table 6.4**). Light-induced accumulation of phenylpropanoids was much greater in 'Tigullio' than in 'Red Rubin', and, notably, the increase in total phenylpropanoids concentration normalized to net carbon gain ($Phenyl^{CO2}$), increased by 220% in 'Tigullio' but only by 23% in 'Red Rubin' in response to high sunlight.

Leaf ultrastructure

Transmission electron microscopy offers clear evidence of photo-damage in 'Tigullio', but not in 'Red Rubin' leaves exposed to full sunlight (**Fig. 6.3**). The photosynthetic apparatus in palisade cells in 'Tigullio' showed signs of oxidative damage: thylakoids are swollen, display large intra-lammellar spaces (note the ultrastructure of thylakoids in the white circle in **Fig. 6.3b**) and the presence of numerous plastoglobules (see black spots included in dotted circle in **Fig. 6.3b**). Lipid bodies (LB) were also present in these cells. In contrast, both palisade cells in 'Red Rubin' and spongy cells in both cultivars

did not show symptoms of damage; chloroplasts have well-organized thylakoids staked in grana together with well-developed starch grains (SG).

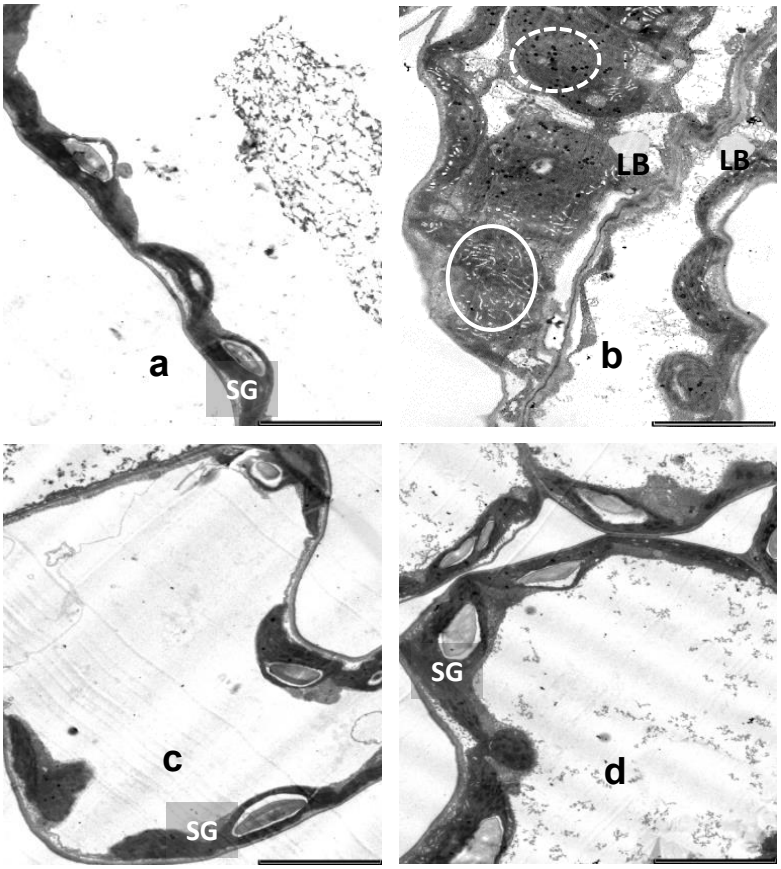

Fig 6.3. Transmission electron microscopy of 'Red Rubin' (a,c) and 'Tigullio' (b,d) leaves exposed for two weeks at full solar irradiance. Views of palisade (a,b) or spongy (c,d) parenchyma cells (bar = 50 nm). Palisade cells in 'Tigullio' have signs of photo-damage in the chloroplast: thylakoids are swalling and display unusual intra-lamellar spaces (note in closed circle in b), and numerous plastoglobules are present (note black spots in dotted circle in b). Lipid bodies are also present in the cell. In contrast, both palisade cells in 'Red Rubin' and spongy cells in 'Red Rubin' and 'Tigullio' do not show symptoms of damage: chloroplasts have well organized thylakoids staked in grana and well developed starch grains (SG).

Discussion

Our data add new insights into the role of anthocyanins in photoprotection, and provide the first comprehensive picture of the multiple effects of these phenylpropanoids on light-induced changes in the suite of morph-anatomical, physiological and biochemical traits in basil. Our study also highlights the particular functions of epidermal coumaroyl anthocyanins in photoprotection, an issue poorly explored in the literature.

First, we show that the 'shade syndrome' usually displayed by red leaves when growing in full sunlight (Manetas et al., 2003) can involve more than simple alterations of chlorophylls *a:b* ratio. Rather, in basil, the red leaf 'syndrome' likely involves a collection of leaf morphological and anatomical features (**Fig. 6.1** and **Table 6.1**, Gould et al., 2002b). Under partial shading, 'Red Rubin' and 'Tigullio' did not display marked differences in leaf anatomy, but 'Red Rubin' had 'shade-type' leaves even when growing in full sun. Most species, including 'Tigullio' in our study, when transferred from the shade to full sun, produce smaller, thicker leaves with higher LMA values and increased mesophyll compactness (Vogelmann, 1993; Niinemets, 2010). This plasticity in functional traits is typically displayed by green leaves, aimed at maximize both an equal distribution of highly collimated light throughout the whole-leaf depth and the CO_2 concentration in the chloroplast, while minimizing heat load as a consequence of excess radiant energy absorption (Vogelmann, 1993; Terashima et al., 2009, 2011). The absence of such light-induced changes in 'Red Rubin' is remarkable; sun leaves were apparently as effective as shade leaves, and much more effective than corresponding 'Tigullio' leaves to use photons to sustain photosynthesis (Φ_{CO2}, **Table 6.1**). In 'Red Rubin' the use of green light for photosynthesis in deep leaf tissues was lower than in 'Tigullio', as revealed by significantly smaller P_n^{sat} in the shade (**Table 6.1**). Nonetheless, leaf functional traits, such as mesophyll density and the shape of mesophyll cells, allowed greater photon path-length in 'Red Rubin' than in 'Tigullio' when grown in full sun (**Table 6.2**, Vogelmann et al., 1996; Terashima et al., 2011). Also anthocyanins located in the abaxial epidermis were likely responsible for marked differences in the shape of spongy mesophyll cells between 'Red Rubin' and 'Tigullio' (shading effects, Hughes et al., 2008). This was of negligible significance in the shade, but conferred to 'Red Rubin' a greater capacity to scatter light than 'Tigullio' when grown at high sunlight (Hughes and Smith, 2007). This may explain the almost identical Pn^{sat} of 'Red Rubin' and 'Tigullio' in full sun. It is noted, that in leaves concomitantly exposed to high T (> 33°C) and high photon flux density (> 1700 µmol m^{-2} s^{-1}), i.e. between 12:00 and 16:00 h in our study, anthocyanins preserved photosynthesis from an excess of sunlight irradiance; P_n decreased more in 'Tigullio' than in 'Red Rubin' over this period (**Fig. S6.1**). As a consequence, the rate of biomass production increased much more in 'Red Rubin' than in 'Tigullio' because of high sunlight.

Notably, shoot morphology was also little affected by sunlight irradiance in 'Red Rubin', whereas shade and sun phenotypes greatly differed in 'Tigullio' (**Fig. 6.1**).

‘Tigullio’ plants in the sun displayed reduced internode lengths and increase axillary branching as compared with their shade counterparts. These morphological adjustments (stress-induced morphogenic responses, *sensu* Potters et al., 2007) are of crucial significance for the acclimation of plants to sunny environments, mitigating photoinhibition at the level of the whole canopy (Pearcy et al., 2005). These morphogenetic responses are typically observed in plants exposed to high UV-B radiation (Jansen, 2002; Frohnmeyer and Staiger, 2003), as downstream responses to the activation of UV-B-specific photoreceptor (Favory et al., 2009; Rizzini et al., 2011). It is possible that the absence of photomorphogenetic responses in ‘Red Rubin’ growing under high UV-B irradiance (17.8 kJ m^{-2} in our study) was due to coumaroyl derivatives of cyanidin 3-*O*-glycosides distributed in adaxial and abaxial epidermises. The concentration of coumaroyl anthocyanins in ‘Red Rubin’ ranged from ~5 mM in shade to ~8 mM in sun leaves, thus constituting an effective shield (Edwards et al., 2008) against the penetration of UV-B wavelengths in the shade, not only in full sun. We hypothesize that this ‘constitutive’, i.e. in leaves growing in the shade irrespective of their developmental stage, anthocyanic filter might have prevented UV-B-induced activation of specific photoreceptors and downstream signaling, when ‘Red Rubin’ plants grew at high sunlight. We cannot exclude that absorption of green light may have exerted a more complex control on leaf and shoot development, by altering interaction between different photoreceptors (Casal, 2000; Heijde and Ulm, 2012), but UV-radiation is likely to have exerted the major role in modulating the light-induced changes in morph-anatomy (Terashima et al., 2005).

‘Red Rubin’ produced less shoot biomass than ‘Tigullio’, irrespective of irradiance, and displayed peculiar shoot architecture in the shade (**Fig. 6.1**). It is known that flavonoid-rich ecotypes display reduced biomass production with respect to their flavonoid-poor relatives (Hofmann et al., 2000; Hofmann and Jahufer, 2011). Anthocyanin-rich mutants of *Arabidopsis* perform more poorly as compared with wild-type controls under optimal growth conditions (Misyura et al., 2013). This conforms to the well-known trade-off between resource allocation to growth or to biosynthesis of carbon-based-secondary-compounds, i.e., to defense compounds *sensu lato* (Dixon and Paiva, 1995). The rate of fresh assimilated carbon invested in phenylpropanoid biosynthesis was indeed 220% higher in ‘Red Rubin’ than in ‘Tigullio’ in the shade. This is remarkable because net daily carbon gain was 25% less in ‘Red Rubin’ than in ‘Tigullio’ in the shade. The biosynthesis of phenylpropanoids is energetically expensive

in ‘Red Rubin’, but the accumulation of these very stable metabolites may be of benefit under a wide range of stress agents, including ‘excess light’ stress (our study, Gould, 2004; Li et al., 2009; Andersen and Jordheim, 2010; Hatier et al., 2013). The presence of axillary branching coupled with small leaves in ‘Red Rubin’ in the shade is also intriguing, as plants inhabiting sunny environments typically display these morphological traits (e.g., ‘Tigullio’ growing in full sun, Jansen, 2002). This may in part result from the unusual – for individuals growing in the shade – high concentrations of phenylpropanoids with a catechol group in the benzene ring detected in ‘Red Rubin’ (Agati et al., 2012, 2013). These dihydroxy benzene-ring-substituted phenylpropanoids, including anthocyanins, are very effective in inhibiting both the movement of auxin (polar auxin transport, PAT, Peer and Murphy, 2007, Kant et al., 2009) and the auxin oxidation driven by IAA-oxidase (Jansen et al., 2001), and hence, in establishing auxin gradients responsible for the development of individual organs and the whole-plant (such as axillary branching, Pollastri and Tattini, 2011).

Therefore, our data suggest that ‘Red Rubin’ will likely perform poorly in environments at limited sunlight availability, as the suite of morph-anatomical and biochemical traits translates into an inherently low ability to maximize light interception and transmission in the leaf (Terashima et al., 2009; Valladares et al., 2012), and possibly in the whole canopy (e.g., axillary branching enhances self-shading, Pearcy et al., 2005).

High sunlight did not significantly alter both the Chl_{tot} concentration and the Chl*a* to Chl*b* ratio, and the carotenoid composition varied little in ‘Red Rubin’ as compared with ‘Tigullio’ (**Table 6.3**). It was hypothesized that an inherently low ability to activate xanthophyll-cycle pigments may relate with the ‘photosynthetic inferiority’ of red-individuals as compared with green-individuals in some instances (Manetas et al., 2003; Nikoforou et al., 2010). This was not the case in our study. Our data of leaf photochemistry clearly evidence that a reduced pool of xanthophyll cycle pigments is unrelated to photoinhibitory damage in basil, as also reported previously in a range of species (Manetas et al., 2002; Hughes et al., 2012). It is conceivable, that NPQ operated less in ‘Red Rubin’ than in ‘Tigullio’, to dissipate excess photons reaching the photosynthetic apparatus, simply because fewer photons reached the chloroplast (Hughes et al., 2012): excess energy to PSII (*E*) was indeed much less in ‘Red Rubin’ than in ‘Tigullio’ in full sunlight (**Table 6.2**). This result is remarkable, since equation we used to calculate *E* has been originally proposed for leaves with the same

absorptance over the PAR waveband (Korneyeyev et al., 2010). It is therefore possible that we have even overestimated *E* in 'Red Rubin' leaves, which displayed indeed higher $A_{400\text{-}700}$ than 'Tigullio' in full sun.

It remains contentious as to whether or not metabolic plasticity – the ability of plants to activate/repress a range of metabolic pathways in response to changes in environmental conditions – confers 'stress-tolerance' (Valladares et al., 2000; van Kleunen and Fischer, 2004; Tardieu and Tuberosa, 2010). It has been shown that light-induced biochemical adjustments, particularly those involving secondary metabolism (e.g., isoprenoids and phenylpropanoids in our study; **Table 6.3** and **Table 6.4**), follow a species-specific suite of primary defenses, such as specialized surface organs, cuticle and whole-leaf thickness (Tattini et al., 2005, 2006). Here we have shown that epidermal coumaroyl anthocyanins constitute a shield against an excess of solar energy reaching the leaf. Their ability to absorb effectively in the UV-region of the solar spectrum assigns to this class of anthocyanins a key role in the adaptive mechanisms to high sunlight, not dissimilar to that previously attributed to secretory/non-secretory trichomes distributed on the adaxial and abaxial leaf surfaces in a range of species (Manetas 2003; Tattini et al., 2000, 2005). Therefore, our study suggests that the 'shade syndrome' typically displayed by red-leafed species, and previously hypothesized to be responsible for the lower adaptive potential to high sunlight of red-individuals as compared with green individuals, may have adaptive value in sunny environments.

As already mentioned metabolic plasticity (as well as morph-anatomical plasticity, Tattini et al., 2005, 2006) does not relate with photo-tolerance, rather it likely confers species-specific capacity to inhabit environments at different sunlight availability (Miner et al., 2005; de V Barros et al., 2012). The whole-set of data of our study allow conclude that 'Red Rubin' is more tolerant to high sunlight than 'Tigullio'. Nonetheless, the light-induced activation of phenylpropanoid biosynthesis was much greater in 'Tigullio' than in 'Red Rubin'. As for the mechanisms responsible for this strikingly different behavior of 'Red Rubin' and 'Tigullio', we offer several explanations. First, UV-B-induced up-regulation of phenylpropanoid biosynthesis through the activation of UV-B responsive proteins might have been prevented in 'Red Rubin' by an effective shield constituted by coumaroyl anthocyanins located on both the adaxial and abaxial epidermis (Favory et al., 2009). This is interesting, as low UV-B doses are required to activate the phenylpropanoid pathway (Jenkins, 2009). Second, PAR-induced activation

of phenylpropanoid pathway (Agati et al., 2009, 2011) was additionally 'attenuated' by epidermal anthocyanins in 'Red Rubin', which are also effective in absorbing green-yellow wavelengths. Third, light-induced alteration in redox homeostasis, which activates MYB transcription factors (Heine et al., 2004; Taylor and Grotewold, 2005), and, in turn the biosynthesis of phenylpropanoids, should have been likely greater in 'Tigullio' than in 'Red Rubin'. Signs of photo-damage were indeed evident only in palisade cells in 'Tigullio' leaves in full sun, which supports the idea that light-induced ROS generation was greater in 'Tigullio' than in 'Red Rubin'. This is consistent with previous suggestions that the accumulation of phenylpropanoids in the leaf follows both a massive generation of ROS, particularly H_2O_2, when excess light stress becomes severe (Vanderauwera et al., 2005; Hatier and Gould, 2008) and the species-specific ability to effectively absorb solar wavelengths (Agati et al., 2013). Under severe excess light stress, depression of primary defenses, such as the activity of enzymes aimed at H_2O_2 removal, has been recently observed to be paralleled by increased concentrations of antioxidant flavonoids and peroxidase activity (Fini et al., 2011, 2012). Possibly, this is again consistent with permanent photo-oxidative injury observed in 'Tigullio' leaves in full sun.

Conclusions

Epidermal coumaroyl anthocyanins have a tremendous impact on the response mechanisms to high light stress in sweet basil. Overall, 'Red Rubin' is much less plastic than 'Tigullio' to changes in sunlight irradiance. A greater plasticity in morph-anatomical traits makes 'Tigullio' more performing in the shade and capable to acclimate to contrasting sunlight environments. Morph-anatomical plasticity is crucial for the acclimation of green leaves to high sunlight, but is a costly process (Valladares et al., 2012). In contrast, anthocyanins conferred greater photosynthetic plasticity, thus making 'Red Rubin' highly specialized for high light environments (Valladares et al., 2003; Snell-Rood and Papaj, 2009). Purple basil indeed seems to display a sort of "conservative resource use strategy" (*sensu* Valladares et al., 2000) as usually observed in high-tolerant species, but with limited distribution along environmental gradients. Based on Tardieu and Tuberosa (2010), 'Red Rubin' is more tolerant than 'Tigullio' at high light, as metabolic cost of photo-protective mechanisms is low and the increase in biomass production is high passing from shade to full sun. Epidermal coumaroyl anthocyanins are unusual in being effective in absorbing mostly UV-B than green-

yellow solar wavelengths. The specific absorbing features of anthocyanins in sweet basil have been likely responsible for the lack of light-induced plasticity in the suite of morph-anatomical and biochemical traits observed in ‘Red Rubin’. Therefore, our findings have some limitations in explaining the response mechanisms of a wider range of anthocyanin-synthesizing species to high sunlight irradiance. On the other side, our study opens to future experiments, in which the identification of individual anthocyanins, in addition to their location, becomes an objective of primary significance. This may also help understand the extent to which anthocyanins affect light-induced activation of specific photoreceptors and downstream photomorphogenic response.

Supplementary material

Table S6.1.. Summary of two-way analysis of variance (ANOVA) for the effects of cultivar (Cv) and sunlight irradiance(light), with their interaction factor (Cv × light) , on morph-anatomical, physiological and biochemical traits in sweet basil (total degrees of freedom df = 39 for RGR^{shoot}, df = 23 for other traits).

Trait	Cultivar	Light	Cv × light
	p	*p*	*p*
RGR^{shoot}	0.0000	0.0000	0.1948
Leaf size	0.0000	0.0000	0.0000
LMA	0.0346	0.0000	0.0000
Leaf thickness	0.0184	0.0000	0.0000
$A_{400\text{-}700}$	0.0000	0.0000	0.0003
$(R/T)_{850}$	0.0016	0.0000	0.0000
P_n^{sat}	0.0001	0.0000	0.4100
CO_2^{daily}	0.0041	0.0000	0.0172
g_s	0.5034	0.0000	0.8432
C_i	0.3789	0.5613	0.8817
Φ_{CO2}	0.3641	0.0000	0.0000
LCP	0.4328	0.0000	0.0000
F_v/F_m	0.0197	0.0000	0.0005
Φ_{PSII}	0.4947	0.0000	0.0004
F_v'/F_m'	0.0597	0.0013	0.0085
q_P	0.0000	0.0009	0.0090
NPQ	0.0000	0.0000	0.0001
E	0.0004	0.0000	0.0156
$Phenyl^{CO2}$	0.0000	0.0000	0.0004
Rosmarinic acid	0.0001	0.0000	0.3594
Caffeic derivatives	0.0008	0.0000	0.1786
Luteolin derivative	0.0026	0.0000	0.0394

Table S6.2. Summary of three-way analysis of variance (ANOVA) for the effects of cultivar (Cv), sunlight irradiance (light) and sampling time (time), with their interaction factors, on the concentration of photosynthetic pigments in sweet basil (total degrees of freedom df = 31).

	cultivar	light	time	Cv × light	Cv × time	light × time	Cv × light × time
	p	*p*	*p*	*p*	*p*	*p*	*p*
Chl_{tot}	0.0007	0.0000	0.0025	0.0000	0.8201	0.0076	0.1584
Chl*a*/Chl*b*	0.0000	0.0000	0.0051	0.0009	0.3254	0.2790	0.3176
Violaxanthin	0.0000	0.0001	0.0000	0.0005	0.2250	0.0001	0.0649
Antheraxanthin	0.0000	0.0000	0.0000	0.0000	0.0000	0.0000	0.0000
Zeaxanthin	0.0000	0.0000	0.0000	0.0000	0.0000	0.0000	0.0000
V+ A + Z	0.0000	0.0000	0.0000	0.0000	0.0000	0.0014	0.0000
(A+Z)/(V+A+Z)	0.0000	0.0000	0.0000	0.0000	0.0000	0.0000	0.0000

Table S6.3. (A). Retention time, UV and mass spectrometric data features of epidermal anthocyanins in purple basis ('Red Rubin'). HPLC-MS analysis was performed with an Agilent 6410 triple quadrupole MS detector equipped with an ESI source (all from Agilent Technologies, Santa Clara, CA). The mobile phase flow was split before the MS to achieve a flow rate of 0.5 mL min^{-1}. Nitrogen was the nebulizer at a pressure of 65 psi and a flow rate of 11 L/min. The capillary T and voltage were 350°C and 4 kV, respectively. Mass spectra were acquired in positive ion mode in the range *m*/*z* 50- 1000.

Metabolite	RT (min)	Molecular ion M^+ (m/z)	Fragment ion M (m/z)	λ_{max} (nm)
cyanidin 3,5-diglucoside	7.78	611	287	285, 523
cyanidin 3-sophoroside	11.60	611	287	284, 523
cyanidin 3-glucoside	14.63	449	287	288, 523
cyanidin 3-(3''-malonylglucoside)	21.91	535	287	285, 530
cyanidin 3-(6''-malonyl)glucoside	30.53	535	287	285, 530
pelargonidin-3-glucoside	26.39	433	271	285, 527
pelargonidin-3,5-glucoside	28.42	595	271	287, 527
pelargonidin-3-(2''glucosil rutinoside)	29.91	741	271	285, 527
cyanidin 3-(*p*-coumarylglucoside) derivative*	22.84	595	287,449	284, 320 sh, 530
cyanidin 3-(*p*-coumarylglucoside) derivative	24.94	757	595,611,287	286, 328 sh, 530
cyanidin 3-(*p*-coumarylglucoside) derivative	27.69	>1000	595	285, 328 sh, 530

**p*-coumaroyl derivatives of cyanidin have likely both *p*-coumaric moiety and dihydroxy hydroxycinnamic moiety (λ_{max} of these compounds indeed is in the 320-328 nm range). Metabolite identification was based on reference to published data and searching for mono-isotopic mass ions on the flavonoid database at http://metabolomics.jp/wiki/index:FL.

Table S6.4. (B). Retention time, UV and mass spectrometric data features of phenylpropanoids in purple and green basil. HPLC-MS analysis was performed as reported in Table S1 A, except for the mass spectra that were acquired in negative ion mode (in the range m/z 50-1000) at a voltage of 5-20 kV.

Metabolite	RT (min)	[M – H] m/z	MS2 [M – H] m/z	λ_{max} (nm)
Caffeic acid derivative	3.63	311	149	302, 326 sh
Chlorogenic acid	5.28	353	191, 179	300, 330 sh
Caffeic acid derivative	9.10	473	293, 149	292, 318 sh
Rosmarinic acid	19.67	359	161	295, 329 sh
Chrysoeriol-gly deriv	25.03	409	313, 161	310, 339 sh

Metabolite identification was based on reference to published data and searching for mono-isotopic mass ions on the flavonoid database at http://metabolomics.jp/wiki/index:FL.

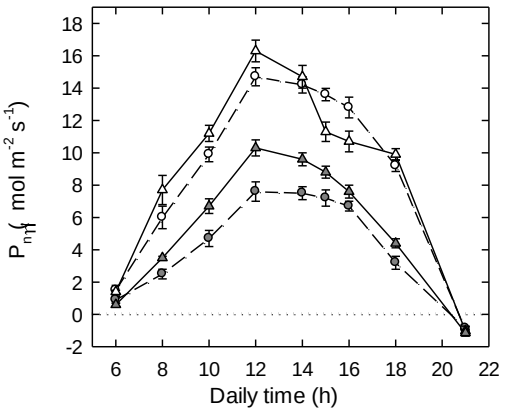

Fig. S6.1. Daily variation in CO2 assimilation rate (Pn) in 'Tigullio' (circles and dotted lines) and Red Rubin (triangles and solid lines) grown at 30% (grey symbols) or 100% (open symbols sunlight irradiance. Measurements were conducted on four replicate plants after one and two weeks of light treatment. Data are means ± SD (n = 8)

7. Conclusions

The initial hypothesis to test green *vs* purple genotypes under B toxicity originated from the well-documented observation that usually anthocyanin-enriched morphs better tolerate a wide range of environmental stressors. To the best of our knowledge, anthocyanin-leafed genotypes have never been compared to anthocyanin-less morphs in relation to their relative tolerance to B excess. Sweet basil has been chosen as model species because it is characterized by a high inter-specific variability, and either green or purple cultivars belong to that species. In addition, it is a widely cultivated Mediterranean species, with a relatively short life cycle.

The first series of experiments were carried out to evaluate the tolerance of excess B in a large number of sweet basil genotypes (the same utilized in the third experiment, see **chapter 4**) with either purple or green leaves and grown hydroponically. Under high B supply both the purple cultivars, 'Red Rubin' and 'Dark Opal', had less necrotic areas over the leaves compared to all the other green genotypes. The cultivar 'Tigullio' was the most sensitive while 'Red Rubin' the most tolerant; therefore these genotypes were utilized for the following experiment.

In the second experiment (**chapter 3**) 'Red Rubin' plants exhibited reduced oxidative stress and better photosynthetic performances as compared to the green 'Tigullio'. However, this study did not clarify the possible protective role of anthocyanins against B toxicity. Indeed, lower B accumulated as well as 2-fold higher level of ascorbate and glutathione was found in leaves of 'Red Rubin' than those found in 'Tigullio'. Those molecules are well-knownpowerful antioxidant that may potentially represent a benefitagainst the B-triggered oxidative stress.

A further experiment was addressed to verify wheather the tolerance of 'Red Rubin' was associated with a reduced accumulation or B in leaves (**chapter 4**). In view of above, we investigated photosynthesis, B accumulation and oxidative stress in all the ten cultivars tested in the first experiments only for foliar damages. We observed a wide range of B accumulation within leaves among all the ten cultivars and a close correlation between leaf B content and the severity of lef burn and oxidative stress (assessed by MDA assay). 'Red Rubin' and 'Dark Opal' were the two genotypes that accumulate less

B and for which the MDA by-products accumulation was the lowest as compared to the others green. However, when we compared the photosynthetic performances of areas close to necrotic spots, genotypes which accumulated an amount of B reasonably comparable to that accumulated by the two purple morphs (Greco a Palla, Limone, Liquirizia and Sweet Thai) exhibited a steeper decline in the efficiency of PSII as well as in the ability to sustain the electron transport rate. In addition, despite a general reduction of stomatal conductance found in all the ten cultivars, the eight green genotypes showed also a reduced CO_2 utilization (higher Ci levels) within mesophyll, suggesting that in the latters the photosynthetic process is affected not only by stomatal limitation, but by mesophyll limitations, too. That the less accumulation of B within leaves of purple basil did not completely explain the higher tolerance of the purple morphs represented the main result of that series of experiments.

After those studies, the hypothesis of a role for anthocyanins in B tolerance became stronger and due to the preferential epidermis localization of anthocyanin in basil we started to hypothesize a photoprotective role for those pigments. We considered the presence of anthocyanins not far from having a constitutive layer of sunblock over the leaves which confers an advantage to purple-leafed cultivars. This may represent a great benefit especially if we consider that B, once in excess, might potentially bind to $NADP^+$, NADPH, ADP and ATP lead to a disruption of those molecules that are no longer available for the photosynthetic process. This phenomenon increases the accumulation of undissipated energy due to a down-stream of the photochemical process. As a consequence, the abatement of a proportion of light burden to chloroplast may translate into a diminished ROS production.

Thus, the purpose of the fourth trial (**chapter 5**) was the evaluations of the anthocyanin contribute in the mitigation of photo-oxidative insult in B-stressed plants in which the efficiency of photosystems is reduced than those of healthy plants. In that experiment we use two different scales of investigation: intact plants and protoplasts. In both cases we imposed a strong photoinhibitory treatment to B-treated plants and protoplasts to confirm or disentangle a positive effect sorted by anthocyanins on photosynthetic performances preservation and oxidative load reduction. The contribution of anthocyanins was evident either by a direct comparison of ‘Red Rubin’ *vs* ‘Tigullio’ photosynthetic performances or by the use of a purple polycarbonate filter

over the acyanic leaves of ‘Tigullio’ with the aim to simulate the presence of anthocyanins. The same anthocyanin-simulating filter was applied over the acyanic mesophyll protoplasts of both the cultivars. In addition, some anthocyanin-rich protoplasts isolated from epidermis of ‘Red Rubin’ were stratified over the green to disentangle an antioxidant activity of anthocyanins. All the dataset provided clear evidences that photosynthetic tissues, protected by anthocyanins from photoinhibition (either when present or simulated), performe better than the unscreened counterpart subjected to B toxicity. Consequently, the oxidative stress was attenuated in protoplasts as well as in leaves preserving them from oxidative damages. In addition, NPQ reached values 2-fold higher in ‘Tigullio’ than ‘Red Rubin’ leaves at high irradiances after the photoinhibitory treatment, suggesting that anthocyanins represent a valid alternative to xanthophyll in the dissipation of light excess. Surprisingly, mesophyll protoplasts of ‘Red Rubin’ showed lesser photoinhibition and oxidative damage than did ‘Tigullio’ protoplasts, even without the photoprotection provided by the overlying anthocyanic layer. If one suppose that the mesophyll of ‘Red Rubin’ appears to be shade-adapted as a consequence of the overlying anthocyanic cells, once the cells were exposed to high light following protoplast isolation we might have expected them to show more pronounced photoinhibition and greater oxidative damage than the presumably more light-adapted mesophyll protoplasts isolated from ‘Tigullio’. We observed exactly the opposite situation. From these results we infer that, in addition to the photoprotection provided by anthocyanins, other mechanisms, including a higher antioxidant pool, contribute to the more robust performance of ‘Red Rubin’ mesophyll cells under B and light stress. Levels of both ascorbate and glutathione were indeed 2-fold higher in ‘Red Rubin’ than in ‘Tigullio’ (**chapter 3**).

Since the benefit to be anthocyanin-equipped resulted a great advantage when light is in excess for the requirements of photosystems, in that last experiment we pushed aside the use of B in the attempt to focus our attention on the behavior of ‘Red Rubin’ and ‘Tigullio’ plants grown under full sun or partially shade conditions (-70% PAR) during a typical hot Mediterranean summer (**chapter 6**). In **Fig 7.1** is outlined the benefit of anthocyanins in diminishing the light absorbed by mesophyll and consequently reducing the level of ROS production within leaves.

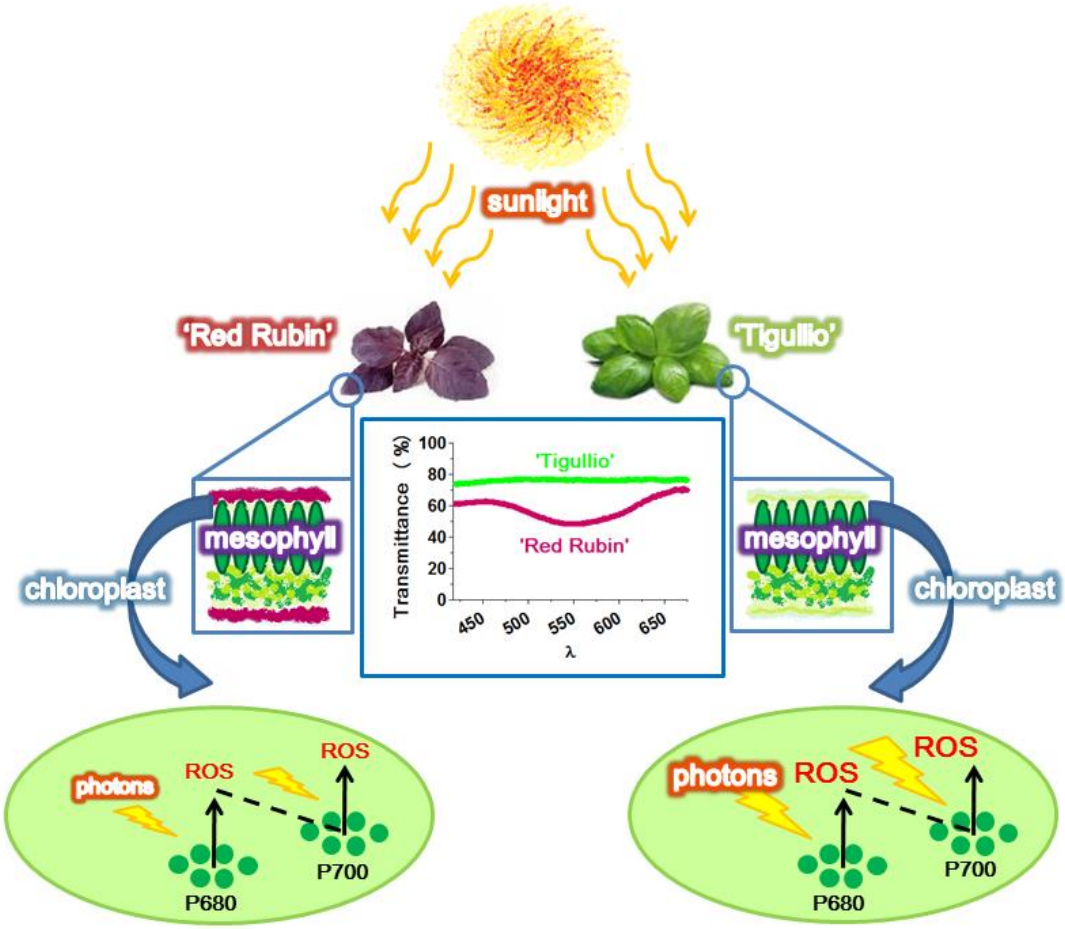

Fig. 7.1. Photoprotective mechanism proposed for anthocyanins in pigmented leaves of sweet basil. The abatement of a proportion of light burden to chloroplast might reduce the amount of ROS within the electron transport chain, especially with a reduced availability of $NADP^+$ and NADPH due to B-binding.

That experiment added new insight into the role of anthocyanins in photoprotection, and provide the first comprehensive picture of the multiple effects of these phenylpropanoids on light-induced changes in the suite of morph-anatomical, physiological and biochemical traits in sweet basil. That study also highlights the particular functions that epidermal coumaroyl anthocyanins might have in 'Red Rubin' leaves. Acylated anthocyanins are not commonly found in leaves and less commonly on leaf epidermises. Thus their presence in 'Red Rubin' may constitute a shield not only against the visible spectrum waveband due to the optical properties of cyanindine derivate, but also against UV radiation (**Fig. 7.2**).

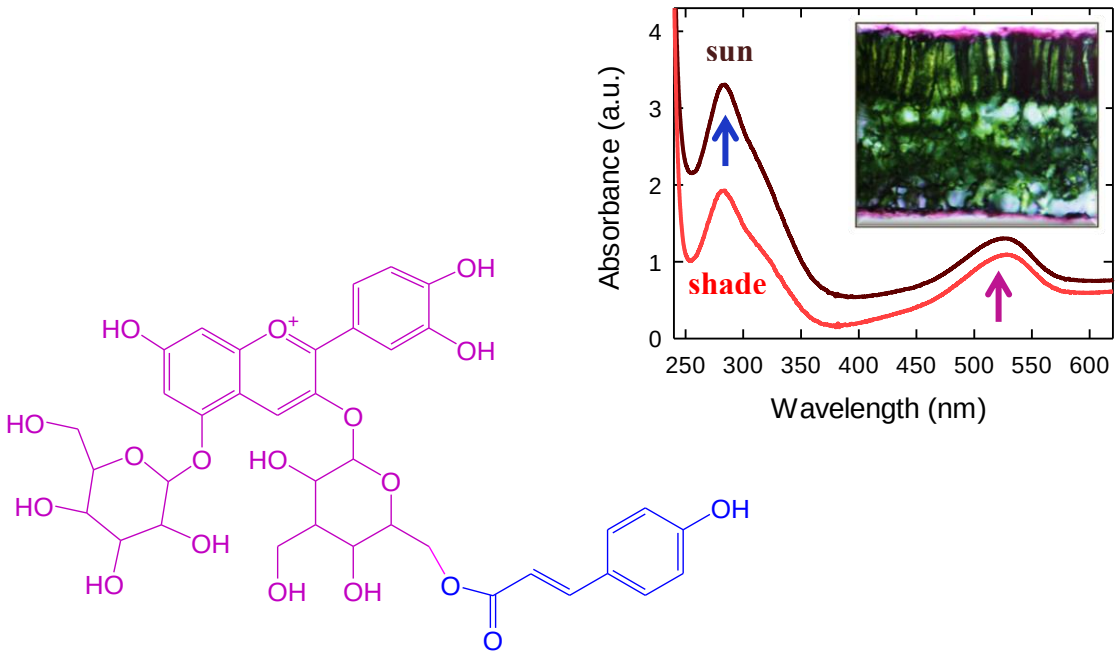

Cyanidin-3-*O*-(6-*O*-*p*-coumaroyl)glucoside-5-*O*-glucoside

Fig. 7.2. Cyanidin-3-*O*-(6-*O*-*p*-coumaroyl)glucoside-5-*O*-glucoside, one of the most abundant acylated anthocyanins in 'Red Rubin' leaves. Spectral features of leaf extracts of 'Red Rubin' leaves reveal that major anthocyanins are acylated. The absorbance over the whole UV-B spectral region due to the presence of *p*-coumaric acid (280-320 nm; blue arrow) largely exceeds that over the 490-550 nm waveband (purple arrow). Plants grown under sun exhibited higher anthocyanins in leaves and consequently higher light absorbance than leaves of plants grown partially shaded.

Purple basil displays a sort of conservative resource use strategy (driven by anthocyanins), a behavior typically observed in high stress-tolerant species, but with limited distribution along environmental gradients. This makes 'Red Rubin' less plastic than 'Tigullio' to changes in sunlight irradiance, in terms of morph-anatomical and biochemical-related traits. The main conclusion of this work was that, the 'shade syndrome' typically displayed by red-leafed species may be of adaptive value in sunny environments.

Concluding, due to the sunscreen effect of anthocyanins, and probably for the high amount of antioxidants, 'Red Rubin' plants appear naturally equipped to tolerate excess B especially under high irradiances as typically occurs in many Mediterranean areas.

References

Abdel-Aal ESM, Huel PA (1999) Rapid method for quantifying total anthocyanins in blue aleurone and purple pericarp wheat. Cereal Chemistry 76: 350-354.

Agati G, Azzarello E, Pollastri S, Tattini M (2012) Flavonoids as antioxidants in plants: location and functional significance. Plant Science 196: 67-76.

Agati G, Biricolti S, Guidi L, Ferrini F, Fini A, Tattini M (2011) The biosynthesis of flavonoids is enhanced similarly by UV radiation and root zone salinity in *L. vulgare* leaves. Journal of Plant Physiology 168: 204-212.

Agati G, Brunetti C, Di Ferdinando M, Ferrini F, Pollastri S, Tattini M (2013) Functional roles of flavonoids in photoprotection: new evidence, lessons from the past. Plant Physiology and Biochemistry 72: 35-45.

Agati G, Matteini P, Goti A, Tattini M (2007) Chloroplast-located flavonoids can scavenge singlet oxygen. New Phytologist 174: 77-89.

Agati G, Stefano G, Biricolti S, Tattini M (2009) Mesophyll distribution of antioxidant flavonoids in *Ligustrum vulgare* leaves under contrasting sunlight irradiance. Annals of Botany 104: 853-861.

Agati G, Tattini M (2010) Multiple functional roles of flavonoids in photoprotection. New Phytologist 186: 786-793.

Alpaslan M, Gunes A (2001) Interactive effects of boron and salinity stress on the growth, membrane permeability and mineral composition of tomato and cucumber plants. Plant and Soil 136: 128-133.

Alscher RG, Donahue JL, Cramer CL (1997) Reactive oxygen species and antioxidants: relationships in green cells. Physiologia Plantarum 100: 224-233.

Andersen MØ, Jordheim M, Byamukama R, Mbabazi A, Skaar I, Kiremire B (2010) Anthocyanins with unusual furanose sugar (apiose) from leaves of *Synadeniumgrantii* (Euphorbiaceae). Phytochemistry 71: 1558-1563.

Andersen MØ, Jordheim M. 2006. Anthocyanins. In Anderson OM, Markham KR (Eds) Flavonoids, chemistry biochemistry and application, CRC Press, Boca Raton, FL 471-530.

Angers P, Morales MR, Simon JE (1996) Fatty acid variation in seed oil among *Ocimum* species. Journal of American Oil Chemistry Society 73: 393-395.

Ardic M, Sekmen AH, Tokur S, Ozdemir F, Turkan I (2009) Antioxidant response of chickpea plants subjected to boron toxicity. Plant Biology 11: 328-338.

Asada K (1999) The water-water cycle in chloroplasts: scavenging of active oxygens and dissipation of excess photons. Annual Review Plant Physiology and Plant Molecular Biology 50: 601-639.

Bahler, BD, Steffen KL, Orzolek MD (1991) Morphological and biochemical comparison of a purple-leafed and a green-leafed pepper cultivar. HortScience 26: 736.

Beckett M, Loreto F, Velikova V, Brunetti C, Di Ferdinando M, Tattini M, Calfapietra C, Farrant JM (2012) Photosynthetic limitations and volatile and non-volatile isoprenoids in the poikilochlorophyllous resurrection plant *Xerophyta humilis* during dehydration and rehydration. Plant Cell and Environment 35: 2061-2074.

Ben-Gal A, Shani U (2002) Yield, transpiration and growth of tomatoes under combined excess boron and salinity stress. Plant and Soil 247: 211-221.

Beyer WF, Fridovich I (1987) Assaying for superoxide dismutase activity: some large consequences of minor changes in conditions. Analytical Biochemistry 161: 559-566.

Bi Y, Chen W, Zhang W, Zhou Q, Yun L, Xing D (2009) Production of reactive oxygen species, impairment of photosynthetic function and dynamic changes in mitochondria are early events in cadmium-induced cell death in *Arabidopsis thaliana*. Biology of the Cell 101: 629-643.

Bilger W, Björkman O (1990) Role of the xanthophyll cycle in photoprotection elucidated by measurements of light-induced absorbance changes, fluorescence and photosynthesis in leaves of *Hedera canariensis*. Photosynthesis Research 25: 173-185.

Björkman O, Demmig-Adams B (1994) Regulation of photosynthetic light energy capture, conversion, and dissipation in leaves of higher plants. In: Schulze ED, Caldwell MM (Eds.), Eco-physiology of photosynthesis. Springer, Berlin, 17-47.

Boeseken J (1949) The use of boric acid for the determination of the configuration of carbohydrates. In: Pigman WW, Wolfrom ML (Ed), Advances in carbohydrate chemistry. Academic Press, New York, NY, 189-210.

Bolaños L, Lukaszewski K, Bonilla I, Blevins D (2004) Why boron? Plant Physiology and Biochemistry 42: 907-912.

Bolhar-Nordenkampf HR, Long SP, Baker NR, Oquist G, Schreiber U, Lechner EG (1989) Chlorophyll fluorescence as a probe of the photosynthetic competence of leaves in the field: a review of current instrumentation. Functional Ecology 3: 497-514.

Bradford MM (1976) A rapid and sensitive method for the quantitation of microgram quantities of protein utilizing the principle of protein-dye binding. Analitical Biochemistry 72: 248-254.

Brown PH, Bellalou N, Hu H, Dandekar A (1999) Transgenically enhanced sorbitol synthesis facilitates phloem boron transport and increases tolerance of tobacco to boron deficiency. Plant Physiology 119: 17-20.

Brown PH, Bellaloui N, Wimmer MA, Bassil ES, Ruiz J, Hu H, Pfeffer H, Dannel F, Römheld V (2002) Boron in plant biology. Plant Biology 4: 205-223.

Brown PH, Hu H (1996) Phloem mobility of boron is species dependent: evidence for phloem mobility in sorbitol-rich species. Annals of Botany 77: 497-505.

Brown PH, Shelp BJ (1997) Boron mobility in plants. Plant and Soil 193: 83-101

Buchweitz M, Gudi G, Carle R, Kammerer DR, Schulz H (2012) Systematic investigation of anthocyanin-metal interactions by Raman spectroscopy. Journal of Raman Spectroscopy 43: 2001-2007.

Buhkov NG, Sabat SC, Mohanty P (1990) Analysis of chlorophyll fluorescence changes in weak light in heat treated *Amaranthus* chloroplasts. Photosynthesis Research 23: 81-87.

Burger J, Edwards G (1996) Photosynthetic efficiency, and photodamage by UV and visible radiation, in red versus green leaf *Coleus* varieties. Plant and Cell Physiology 37: 395-399.

Butterwick L, De Oude N, Raymond K (1989) Safety assessment of boron in aquatic and terrestrial environments. Ecotoxicology and Environmental Safe 17: 339-371.

Cakmak I, Marschner H (1992) Magnesium-deficiency and high light-intensity enhance activities of superoxide-dismutase, ascorbate peroxidase, and glutathione-reductase in bean-leaves. Plant Physiology 98: 1222-1227

Camacho-Cristóbal JJ, Rexach J, González-Fontes A (2008) Boron in plants: deficiency and toxicity. International Journal of Plant Biology 50: 1247-1255.

Camacho-Cristóbal JJ, Anzellotti D, Gonzàlez-Fontez A. (2002) Changes in phenolic metabolism of tobacco plants during short-term boron deficiency. Plant Physiology and Biochemistry 40, 997-1002.

Casal JJ (2000) Phytochromes, cryptochromes, phototropin: Photoreceptors interactions in plants. Photochemistry and Photobiology 71: 1-11.

Cervilla LM, Blasco B, Rios JJ, Romero L, Ruiz JM (2007) Oxidative stress and antioxidants in tomato (*Solanum lycopersicum*) plant subjected to boron toxicity. Annals of Botany 100: 747-756

Chalker-Scott L (1999) Environmental significance of anthocyanins in plants stress response. Photochemistry and Photobiology 70: 1-9.

Chalker-Scott L (2002) Do anthocyanins function as osmoregulators in leaf tissues? Advances in Botanical Research 37: 103-106.

Choinski JS, Johnson JM (1993) Changes in photosynthesis and water status of developing leaves of *Brachystegia spiciformis* Benth. Tree Physiology 13: 17-27.

Close DC, Beadle CL (2003) The ecophysiology of foliar anthocyanin. Botanical Review 69: 149-161.

Crozier A, Yokota T, Jaganath IB, Marks SC, Saltmarsh M, Clifford MN (2006) Secondary metabolites in fruits, vegetables, beverages and other plant based dietary components, In: Crozier A, Clifford MN, Ashihara H (Eds.), Plant secondary metabolites: occurrence, structure and role in the human diet. Blackwell, Oxford, 208-302.

D'Onofrio C, Morini S, Vitigliano C (1999) Isolation of protoplasts from *in vitro*-grown quince BA29 leaves. In Vitro Cellular & Developmental Biology 35: 421-423.

Dannel F, Pfeffer H, Romheld V (1998) Compartmentation of boron in roots and leaves of sunflower as affected by boron supply. Journal of Plant Physiology 153: 615-622.

Dannel F, Pfeffer H, Romheld V (2000) Characterization of root boron pools, boron uptake and boron translocation in sunflower using the stable isotopes ^{10}B and ^{11}B. Australian Journal of Plant Physiology 27: 397-405.

Darrah H (1974) Investigations of the cultivars of basils (*Ocimum*). Economic Botany 28: 63-67.

de V Barros F, Goulart MF, Sá Telles SB, Lovato MB, Valladares F, de Lemos-Filho JP (2012) Phenotypic plasticity to light of two congeneric trees from contrasting habitats: Brazilian Atlantic Forest *versus* cerrado (savanna). Plant Biology 14: 208-215

Degl'Innocenti E, Guidi L, Pardossi A, Tognoni F (2005) Biochemical study of leaf browning in minimally processed leaves of lettuce. Journal of Agriculture and Food Chemistry 53: 9980-9984.

Demmig-Adams B, Adams III WW (2006) Photoprotection in an ecological context: the remarkable complexity of thermal energy dissipation. New Phytologist 172: 11-21.

Dewanto V, Adom KK, Liu RH (2002) Thermal processing enhances the nutritional value of tomatoes by increasing total antioxidant activity. Journal of Agriculture and Food Chemistry 50: 3010-3014.

Di Cagno R, Guidi L, De Gara L, Soldatini GF (2001) Combined cadmium and ozone treatments affect photosynthesis and ascorbate-dependent defences in sunflower. New Phytologist 151: 627-636.

Dixon RA, Paiva NL (1995) Stress-induced phenylpropanoid metabolism. The Plant Cell 7, 1085-1097.

Dordas C, Brown PH (2000) Permeability of boric acid across lipid bilayers and factors affecting it. The Journal of Membrane Biology 175: 95-105.

Dordas C, Chrispeels MS, Brown PH (2000) Permeability and channel-mediated transport of boric acid across membrane vesicles isolated from squash roots. Plant Physiology 124: 1349-1362.

Edwards WR, Hall JA, Rowlan AR, Schneider-Barfield T, Sun TJ, Patil MA, Pierce ML, Fulcher RG, Bell AA, Essenberg M. 2008. Light filtering by epidermal flavonoids during the resistant response of cotton to *Xanthomonas* protects leaf tissue from light-dependent phytoalexin toxicity. Phytochemistry 69: 2320-2328.

Elhabiri M, Figueiredo P, Toki K, Saito N, Brouillard R (1997) Anthocyanin-aluminium and -gallium complexes in aqueous solution. Journal of Chemical Society Perkin Transaction 2: 355-362.

Eraslan F, Inal A, Gunes A, Alpaslan M (2007a) Impact of exogenous salicylic acid on the growth, antioxidant activity and physiology of carrot plants subjected to combined salinity and boron toxicity. Scientia Horticolturae 113: 120-128

Eraslan F, Inal A, Savasturk O, Gunes A (2007b) Changes in antioxidative system and membrane damage of lettuce in response to salinity and boron toxicity. Sci Hortic 114: 5–10

Eryılmaz F (2006) The relationships between salt stress and anthocyanin content in higher plants. Biotechnology and Biotechnological Equipment 20: 47-52.

Esteban R, Fernández-Marín B, Becerril JM, García-Plazaola JI (2008) Photoprotective implications of leaf variegation in *E. dens-canis* L. and *P. officinalis* L. Journal of Plant Physiology 165: 1255-1263.

Favory JJ, Stec A, Gruber H (2009) Interaction of COP1 and UVR8 regulates UV-B-induced photomorphogenesis and stress acclimation in *Arabidopsis*. The EMBO Journal 28: 591-601.

Feild TS, Lee DW, Holbrook NM (2001) Why leaves turn red in Autumn. The role of anthocyanins in senescing leaves of red-osier dogwood. Plant Physiology 127: 566-574.

Fini A, Brunetti C, Di Ferdinando M, Ferrini F, Tattini M (2011) Stress-induced flavonoid biosynthesis and the antioxidant machinery of plants. Plant Signaling and Behavior 6: 709-711.

Fini A, Guidi L, Ferrini F, Brunetti C, Di Ferdinando M, Biricolti S, Pollastri S, Calamai L, Tattini M (2012) Drought stress has contrasting effects on antioxidant enzymes activity and phenylpropanoid biosynthesis in *Fraxinus ornus* leaves: an excess light stress affair? Journal of Plant Physiology 169: 929-939.

Foyer CH, Lelandais M, Kunert KJ (1994) Photooxidative stress in plants. Physiologia Plantarum 92: 696-717.

Foyer CH, Noctor G. (2005) Oxidant and antioxidant signaling in plants: a re-evaluation of the concept of oxidative stress in a physiological context. Plant, Cell & Environment 28: 1056-1071.

Frohnmeyer H, Staiger D (2003) Ultraviolet-B radiation-mediated responses in plants. Balancing damage and protection. Plant Physiology 133: 1420-1428.

Genty B, Briantais JM, Baker NR (1989) The relationship between the quantum yield of photosynthetic electron transport and quenching of chlorophyll fluorescence. Biochimica et Biophysica Acta 990: 87-92.

Gitelson AA, Merzylak MN, Chivkunova OB (2001) Optical properties and nondestructive estimation of anthocyanin content in plant leaves. Photochemistry and Photobiology 74: 38-45.

Goldbach HE, Wimmer MA (2007) Boron in plants and animals: is there a role beyond cell-wall structure? Journal of Plant Nutrition and Soil Science 170: 39-48.

Goldbach HE, Yu Q, Wingender R, Schulz M, Wimmer M, Findeklee P, Baluska F. (2001) Rapid response reactions of roots to boron deprivation. Journal of Plant Nutrition and Soil Science 164: 173-181.

Gould KS (2004) Nature's Swiss army knife: the diverse protective roles of anthocyanins in leaves. Journal of Biomedicine and Biotechnology 5: 314-320.

Gould KS, Davies K, Winefield C (2009) Anthocyanins: biosynthesis, functions and applications. Springer-Verlag New York, Dordrecht.

Gould KS, Dudle DA, Neufeld HS (2010) Why some stems are red: cauline anthocyanins shield photosystem II against high light stress. Journal of Experimental Botany 61: 2707-2717.

Gould KS, McKelvie J, Markham KR (2002a) Do anthocyanins function as antioxidants in leaves? Imaging of H_2O_2 in red and green leaves after mechanical injury. Plant, Cell & Environment 25: 1261-1269.

Gould KS, Vogelmann TC, Han T, Clearwater MJ (2002b) Profiles of photosynthesis within red and green leaves of *Quintinia serrata* A. Cunn. Physiologia Plantarum 116: 127-133.

Gould, KS, Markham KR, Smith RH, Goris, JJ (2000) Functional role of anthocyanins in the leaves of *Quintinia serrata* A. Cunn. Journal of Experimental Botany 51: 1107-1115.

Grayer RJ, Bryan SE, Veitch NC, Goldstone FJ, Paton A, Wollenweber E (1996) External flavones in sweet basil, *Ocimum basilicum*, and related taxa. Phytochemistry 43: 1041-1047.

Guidi L, Degl'Innocenti E, Carmassi G, Massa D, Pardossi A (2011) Effects of boron on leaf chlorophyll fluorescence of greenhouse tomato grown with saline water. Environmental and Experimental Botany 73: 57-63.

Guidi L, Degl'Innocenti E, Giordano C, Biricolti S, Tattini M (2010) Ozone tolerance in *Phaseolus vulgaris* depends on more than one mechanism. Environmental Pollution 158: 3164-3171.

Guidi L, Mori S, Degl'Innocenti E, Pecchia S (2007) Effects of ozone exposure or fungal pathogen on white lupin leaves as determined by imaging of chlorophyll *a* fluorescence. Plant Physiology and Biochemistry 45: 851-857.

Gunes A, Alpaslan M, Cikili Y, Ozcan H (1999) Effect of zinc on the alleviation of boron toxicity in tomato. Journal of Plant Nutrition 22: 1061-1068.

Gunes A, Inal A, Bagci EG, Coban S, Pilbeam DJ (2007) Silicon mediates changes to some physiological and enzymatic parameters symptomatic for oxidative stress in spinach (*Spinacia oleracea* L.) grown under B toxicity. Scientia Horticolturae 113: 113-119.

Gunes A, Soylemezoglu G, Inal A., Bagci EG, Coban S, Sahin O (2006) Antioxidant and stomatal responses of grapevine (*Vitis vinifera* L.) to boron toxicity. Scientia Horticolturae 110: 279-284.

Gupta UC, Jame YW, Campbell CA, Leyshon AJ, Nicholaichuck W (1985) Boron toxicity and deficiency: a review. Canadian Journal of Soil Science 65: 381-409.

Hale KL, McGrath S, Lombi E, Stack S, Terry N, Pickering IJ, George GN, Pilon-Smits EAH (2001) Molybdenum sequestration in *Brassica*: a role for anthocyanins? Plant Physiology 126: 1391-1402.

Hale KL, Tufan HA, Pickering IJ, George GN, Terry N, Pilon M, Pilon-Smits EAH (2002). Anthocyanins facilitate tungsten accumulation in *Brassica*. Physiologia Plantarum 116: 351-358.

Han S, Tang N, Jiang H-X, Yang LT, Lee Y, Chen LS (2009) CO_2 assimilation, photosystem II photochemistry, carbohydrate metabolism and antioxidant system of citrus leaves in response to boron stress. Plant Science 176: 143-153

Harley MM, Paton A, Harley RM, Cade PG (1992) Pollen morphological studies in the tribe Ocimeae (Nepetoideae: Labiatae): *Ocimum* L. Grana 31: 161-176.

Hatier JHB, Clearwater MJ, Gould KS (2013) The functional significance of black-pigmented leaves: photosynthesis, photoprotection and productivity in *Ophiopogon planiscapus* 'Nigrescens'. PLoS ONE 8: 1-5.

Hatier JHB, Gould KS (2008) Foliar anthocyanins as modulators of stress signals. Journal of Theoretical Biology 253: 625-627.

Heijde M, Ulm R (2012) UV-B photoreceptor-mediated signalling in plants. Trends in Plant Science 17: 230-237.

Heine GF, Hernandez JM, Grotewold E (2004) Two cysteines in plant R2R3 MYB domains participate REDOX-dependent DNA binding. Journal of Biological Chemistry 279: 37878-37885.

Herms DA, Mattson WJ (1992) The dilemma of plants: to grow or defend. Quartarterly Review of Biology 67: 283-335.

Hodges DM, DeLong JM, Forney CF, Prange RK (1999) Improving the thiobarbituric acid reactive substances assay for estimating lipid peroxidation in plant tissues containing anthocyanin and other interfering compounds. Planta 207: 604-611.

Hofmann RW, Jahufer MZZ (2011) Tradeoff between biomass and flavonoid accumulation in white clover reflects contrasting plant strategies. PLoS ONE 6, e18949.

Hofmann RW, Swinny EE, Bloor SJ, Markham KR, Ryan KG, Campbell BD, Jordan BR, Fountain DW (2000) Responses of nine *Trifolium repens* L. populations to ultraviolet-B radiation: differential flavonol glycoside accumulation and biomass production. Annals of Botany 86: 527-537.

Holton TA, Cornish EC (1995) Genetics and biochemistry of anthocyanin biosynthesis. The Plant Cell 7: 1071-1083.

HSDB (2003) Boron. Division of Specialized Information Services, National Library of Medicine.

Hu H, Brown PH (1997) Absorption of boron by plant roots. Plant and Soil 193: 49-58.

Hughes NM, Burkey KO, Cavender-Bares J, Smith WK (2012) Xanthophyll cycle pigment and antioxidant profiles of winter-red (anthocyanic) and winter-green (acyanic) angiosperm evergreen species. Journal of Experimental Botany 63: 1895-1905.

Hughes NM, Burkey KO, Neufeld HS (2005) Functional role of anthocyanins in high-light winter leaves of the evergreen herb, *Galax urceolata*. New Phytologist 168: 575-587.

Hughes NM, Morley CB, Smith WK (2007) Coordination of anthocyanin decline and photosynthetic maturation in juvenile leaves of three deciduous tree species. New Phytologist 175: 675-685.

Hughes NM, Vogelmann TC, Smith WK (2008) Optical effects of abaxial anthocyanins on absorption of red wavelengths by understory species: revisiting the back-scatter hypothesis. Journal of Experimental Botany 59: 3435-3442.

Hughes NM (2011) Winter leaf reddening in 'evergreen' species. New Phytologist 190: 573-581.

Jansen MAK, van der Noort RA, Tan A, Prinsen E, Lagrimini ML, Thorneley RNF (2001) Phenol-oxidizing peroxidases contribute to the protection of plants from ultraviolet radiation stress. Plant Physiology 126: 1012-1023.

Jansen MAK (2002) Ultraviolet-B radiation effects on plants: induction of morphogenic responses. Physiologia Plantarum 116: 423-429.

Javanmardi J, Khalighi A, Kashi A, Bais HP, Vivanio JM (2002) Chemical characterization of basil (*Ocimum basilicum* L.) found in local accessions and

used in traditional medicines in Iran. Journal of Agriculture and Food Chemistry 50: 5878-5883.

Jenkins GI (2009) Signal transduction in response to UV-B radiation. Annual Review of Plant Biology 60: 407-431.

Jingxian Z, Kirkham MB (1996) Antioxidant response to drought in sunflower and sorghum seedlings. New Phytologist 132: 361-373.

Kampfenkel K, Van Montagu M, Inze D (1995) Extraction and determination of ascorbate and dehydroascorbate from plant tissue. Analytical Biochemistry 225: 165-167.

Kant S, Bi YM, Zhu T, Rothstein SJ (2009) *SAUR3*9, a small auxin-up RNA gene, acts as a negative regulator of auxin synthesis and transport in rice. Plant Physiology 151: 691-701.

Karageorgou P, Manetas Y (2006) The importance of being red when young: anthocyanins and the protection of young leaves of *Quercus coccifera* from insect herbivory and excess light. Tree Physiology 26: 613-621.

Kaur S, Nicolas ME, Ford R, Norton R, Paul WJT (2006) Selection of *Brassica rapa* genotypes for tolerance to boron toxicity. Plant and Soil 285: 115-123

Kaya C, Levent Tuna, A, Dikilitas M, Ashraf M, Koskeroglu S, Guneri M (2009) Supplementary phosphorus can alleviate boron toxicity in tomato. Scientia Horticolturae 121: 284-288.

Keren R, Bingham FT (1985) Boron in water, soils, and plants. Advances in Soil Science 1: 230-276.

Kiferle C, Lucchesini M, Mensuali-Sodi A, Maggini R, Raffaelli A, Pardossi A (2011) Rosmarinic acid content in basil plants grown *in vitro* and in hydroponics. Central European Journal of Biology 6: 946-957.

Kim HY, Chen F, Wang Z, Rajapakse N (2005) Effect of chitosan on the biological properties of sweet basil. Journal of Agriculture and Food Chemistry 53: 3696-3701.

Klughammer C, Schreiber U (2008) Saturation pulse method for assessment of energy conversion in PS I. PAM Application Notes 1: 11-14.

Knapp AK, Carter GA (1998) Variability in leaf optical properties among 26 species from a broad range of habitats. American Journal of Botany 85: 940-946.

Kobayashi M, Matoh T, Azuma JI (1996) Two chains of rhamnogalacturonan II are cross-linked by borate-diol ester bonds in higher plant cell walls. Plant Physiology 110: 1017-1020.

Kohl HC, Oertli JJ (1961) Distribution of boron in leaves. Plant Physiology 36: 420-424.

Kornyeyev D, Logan BA, Holaday AS (2010) Excitation pressure as a measure of the sensitivity of photosystem II to photoinactivation. Functional Plant Biology 37: 943-951.

Kozlowski TT, Pallardy SG (2002) Acclimation and adaptive responses of woody plants to environmental stresses. Botanical Review 68: 270-334.

Krall JP, Edwards GE (1982) Relationship between photosystem II activity and CO_2 fixation. Physiologia Plantarum 86: 180-187.

Kyparissis A, Grammatikopoulos G, Manetas Y (2007) Leaf morphological and physiological adjustments to the spectrally selective shade imposed by anthocyanins in *Prunus cerasifera*. Tree Physiology 27: 849-857.

Kytridis VP, Karageorgou P, Levizou E, Manetas Y (2008) Intra-species variation in transient accumulation of leaf anthocyanins in *Cistus creticus* during winter: evidence that anthocyanins may compensate for an inherent photosynthetic and photoprotective inferiority of the red-leaf phenotype. Journal of Plant Physiology 165: 952-959.

Kytridis VP, Manetas Y (2006) Mesophyll versus epidermal anthocyanins as potential in vivo antioxidants: evidence linking the putative antioxidant role to the proximity of oxy-radical source. Journal of Experimental Botany 57: 2203-2210.

Lan, JX, Li AL, Chen CX (2011) Effect of transient accumulation of anthocyanin on leaf development and photoprotection of *Fagopyrum dibotrys* mutant. Biologia Plantarum 55: 766-770.

Landi M, Pardossi A, Remorini D, Guidi L (2013a) Antioxidant and photosynthetic response of a purple-leafes and a green-leafed cultivar of sweet basil (*Ocimum basilicum*) to boron excess. Environmetal and Experimental Botany 85: 64-75.

Landi M, Remorini D, Pardossi A, Guidi L (2013b) Purple *versus* green-leafed genotypes of sweet basil (*Ocimum basilicum*): which differences occur in photosynthesis under boron toxicity. Journal of Plant Nutrition and Soil Science 176: 942-951.

Landi M, Remorini D, Pardossi A, Guidi L (2013c) Boron excess affects photosynthesis and antioxidant apparatus of greenhouse *Cucurbita pepo* and *Cucumis sativus*. Journal of Plant Research 126: 775-786.

Lee KDW, Graham R (1986) Leaf optical properties of rainforest sun and extreme shade plants. American Journal of Botany 73: 1100-1108.

Lee J, Scagel CF (2009) Chicoric acid found in basil (*Ocimum basilicum* L.) leaves. Food Chemistry 115: 650-656.

Lev-Yadun S, Gould KS (2007) What do red and yellow autumn leaves signal? Botanical Review 73: 279-289.

Li Z, Wakao S, Fischer BB, Niyogi KK (2009) Sensing and responding to excess light. Annual Review of Plant Biology 60: 239-260.

Liakopoulos G, Nikolopoulos, Klouvatou A, Vekkos KA, Manetas Y, Karabourniotis G (2006) The photoprotective role of epidermal anthocyanins and surface pubescence in young leaves of grapevine (*Vitis vinifera*). Annals of Botany 98: 257-265.

Lichtenthaler HK (1987) Chlorophylls and carotenoids: pigments of photosynthetic biomembranes. Methods in Enzymology 148: 350-382

Lichtenthaler HK, Babani F, Langdorf G, Buschmann C (2000) Measurement of differences in red chlorophyll fluorescence and photosynthetic activity between sun and shade leaves by fluorescence imaging. Photosynthetica 38: 521-529.

Lovatt CJ, Bates LM (1984) Early effects of excess boron on photosynthesis and growth of *Cucurbita pepo.* Journal of Experimental Botany 35: 297-305.

Makri O, Kintzios S (2007) *Ocimum* spp. (basil): botany, cultivation, pharmaceutical properties and biotechonology. Journal of Herbs Spices & Medicinal Plants 13: 123-150.

Manetas Y (2003) The advantage of being hairy: The adverse effects of hairy removal on stem photosynthesis of *Verbascum speciosum* are due to solar UV-B radiation. New Phytologist 158: 503-508.

Manetas Y (2006) Why some leaves are anthocyanic, and why most anthocyanic leaves are red. Flora 201: 163-177.

Manetas Y, Drinia A, Petropoulou Y (2002) High contents of anthocyanins in young leaves are correlated with low pools of xanthophyll cycle components and low risk of photoinhibition. Photosynthetica 40: 349-354.

Manetas Y, Petropoulou Y, Psaras GK, Drinia A (2003) Exposed red (anthocyaninc) leaves of *Quercus coccifera* display shade characteristics. Functional Plant Biology 30: 265-270.

Matoh T, Takasaki M, Kobayashi M, Takabe K (2000) Boron nutrition of cultured tobacco BY-2 cells. III. Characterization of the boron-rhamnogalacturonan II complex in cells acclimated to low levels of boron. Plant and Cell Physiology 41: 363-366.

Maxwell K, Johnson GN (2000) Chloropyll fluorescence: a pratical guide. Journal of Experimental Botany 51: 659-668.

Melgar, JC, Guidi L, Remorini D, Agati G, Degl'innocenti E, Castelli S, Baratto MC, Faraloni, C, Tattini M (2009) Antioxidant defenses and oxidative damage in salt-treated olive plants under contrasting sunlight irradiance. Tree Physiology 29: 1187-1198.

Merzlyak, MN, Melo TB, Naqvi KR (2008) Effect of anthocyanin, carotenoids and flavonoids on chlorophyll fluorescence excitation spectra in apple fruit: signature analysis, assessment, modelling and relevance to photoprotection. Journal of Experimental Botany 59: 349-359.

Miner BG, Sultan SE, Morgan SG, Padilla DK, Relyea RA (2005) Ecological consequences of phenotypic plasticity. Trends in Ecology and Evolution 20: 685-692.

Mittler R (2002) Oxidative stress, antioxidants and stress tolerance. Trends in Plant Science 7: 405-410.

Mittler R, Vanderauwera S, Gollery M, Breusegem FV (2004) Reactive oxygen gene network of plants. Trends in Plant Science 9: 490-498.

Miwa K, Takano J, Omori H, Seki M, Shinozaki K, Fujiwara T (2007) Plants tolerant of high boron levels. Science 318: 1417.

Molassiotis A, Sotiropoulos T, Tanou G, Diamantidis G, Therios I (2006) Boron induced oxidative damage and antioxidant and nucleolytic responses in shoot tips culture of the apple rootstock EM9 (*Malus x domestica* Borkh). Environmental and Experimental Botany 56: 54-62.

Moore JW (1991) Inorganic contaminants of surface water: research and monitoring priorities. Springer-Verlag, Berlin.

Morales MR, Simon JE (1996) New basil selections with compact inflorescence for the ornamental market. In: Janick J (Ed), Progress in new crops. ASHS Press, Alexandria, VA 543-546.

Mullen W, Marks SC, Crozier A (2007) Evaluation of phenolic compounds in commercial fruit juices and fruit drinks. Journal of Agriculture and Food Chemistry 55: 3148-3157.

Mullineaux PM, Karpinski S, Backer NR (2006) Spatial dependence for hydrogen peroxide-directed signalling in light-stressed plants. Plant Physiology 141: 346-350.

Mysiura M, Colasanti J, Rothstein SJ (2013) Physiological and genetic analysis of Arabidopsis thaliana anthocyanin biosynthesis mutants under chronic adverse environmental conditions. Journal of Experimental Botany 64: 229-240.

Nable RO (1988) Resistance to boron toxicity amongst several barley and wheat cultivars: A preliminary examination of the resistance mechanism. Plant and Soil 112: 45-57.

Nable RO, Banuelos GS, Paull JG (1997) Boron toxicity. Plant and Soil 198: 181-198.

Nable RO, Lance RCM, Cartwright B (1990) Uptake of boron and silicon by barley genotypes with differing susceptibilities to boron toxicity. Annals of Botany 66: 83-90.

Nakagawa Y, Hanaoka H, Kobayashi M, Miyoshi K, Miwa K, Fujiwara T (2007) Cell-type specificity of the expression of OsBOR1, a rice efflux boron transporter gene, is regulated in response to boron availability for efficient boron uptake and xylem loading. The Plant Cell 19: 2624-2635.

Nakano Y, Asada K (1981) Hydrogen peroxide is scavenged by ascorbate-specific peroxidase in spinach chloroplasts. Plant and Cell Physiology 22: 867-880.

Neill SO, Gould KS (2003) Anthocyanins in leaves: light attenuators or antioxidants? Functional Plant Biology 30: 865-873.

Niinemets U (2010) A review on light interception in plant stands from leaf to canopy in different plant functional types and in species with varying shade tolerance. Ecological Research 25: 693-714.

Niinemets U, García-Plazaola JI, Tosens T (2012) Photosynthesis during leaf development and ageing. In: Flexas J, Loreto F, Medrano H (Eds) Terrestrial photosynthesis in a changing environment. A molecular, physiological and ecological approach. Cambridge University Press, Cambridge, UK 353-372.

Nikoforou C, Manetas Y (2010) Strength of winter leaf redness as an indicator of stress vulnerable individuals in *Pistacia lentiscus*. Flora 205: 424-427.

Nikoforou C, Nikolopoulos D, Manetas Y (2011) The winter-red-leaf syndrome in Pistacia lentiscus: Evidence that the anthocyanic phenotype suffers from nitrogen deficiency, low carboxylation efficiency and high risk of photoinhibition. Journal of Plant Physiology 168, 2814-2817.

Nikoforou C, Zeliou K, Kytridis V-P, Kyzeridou A, Manetas Y (2010) Are red leaf phenotypes more or less fit? The case of winter leaf reddening in *Cistus creticus*. Environmental and Experimental Botany 67: 509-514.

Nishio JN (2000) Why are higher plants green? Evolution of the higher plant photosynthetic pigment complement. Plant, Cell & Environment 23: 539-548.

Niyogi KK (2000) Safety valves for photosynthesis. Current Opinion in Plant Biology 3: 455-460.

Niyogi KK, Li XP, Rosenberg V, Jung HS (2005) Is PsbS the site of non-photochemical quenching in photosynthesis? Journal of Experimental Botany 56: 375-382.

Noguchi K, Ishii T, Matsunaga T, Kakegawa K, Hayashi H, Fujiwara T (2003) Biochemical properties of the cell wall in the Arabidopsis mutant bor1-1 in relation to boron nutrition. Journal of Plant Nutrition and Soil Science 166: 175-178.

O'Neill MA, Ishii T, Albersheim P, Darvill AG (2004) Rhamnogalacturonan II: structure and function of a borate cross-linked cell wall pectic polysaccharide. Annual Review of Plant Biology 55: 109-139.

O'Neill MA, Warrenfeltz KK, Pellerin P, Doco T, Darvill AG, Albersheim P (1996) Rhamnogalacturonan-II: a pectic polysaccharide in the walls of growing plant cell, form a dimer that is covalently cross-linked by a borate ester: in vitro conditions for the formation and hydrolysis of the dimer. Journal of Biological Chemistry 271: 22923-22930.

Oxborough K (2004) Imaging of chlorophyll a fluorescence: theoretical and practical aspects of an emerging technique for the monitoring of photosynthetic performance. Journal of Experimental Botany 55: 1195-1205.

Papadakis IE, Dimassi KN, Bosabalidis AM, Theorios IN, Patakas A, Giannakoula A (2004a) Effects of B excess on some physiological and anatomical parameters of 'Navelina' orange plants grafted on two rootstocks. Environmental and Experimental Botany 51: 247-257.

Papadakis IE Dimassi KN, Bosabalidis AM, Theorios IN, Patakas A, Giannakoula A (2004b) Boron toxicity in 'Clementine' mandarin plants grafted on two rootstocks. Plant Science 166: 539-547.

Paton A (1992) A synopsis of Ocimum L. (Labiatae) in Africa. Kew Bullettin 47: 403-435.

Paton A, Putievsky E (1996) Taxonomic problems and cytotaxonomic relationships between varieties of *Ocimum basilicum* and related species (Labiatae). Kew Bullettin 5: 1-16.

Pearcy RW, Muraoka H, Valladares F (2005) Crown architecture in shade and sun environments: assessing function and trade-offs with a three-dimensional simulation model. New Phytologist 166: 791-800.

Peer WA, Murphy AS (2007) Flavonoids and auxin transport: modulators or regulators? Trends in Plant Science 12: 556-563.

Pennisi M, Gonfiantini R, Grassi S, Squarci P (2006) The utilization of boron and strontium isotopes for the assessment of boron contamination of the Cecina River

alluvial aquifer (central-western Tuscany, Italy). Applied Geochemistry 21: 643-655.

Phippen WB, Simon JE (1998) Anthocyanins in basil. Journal of Agriculture and Food Chemistry 46: 1734-1738.

Phippen WB, Simon JE (2000) Anthocyanin inheritance and instability in purple basil (*Ocimum basilicum* L.). Journal of Heredity 91: 289-296.

Pietrini F, Iannelli MA, Massacci A (2002) Anthocyanin accumulation in the illuminated surface of maize leaves enhances protection from photo-inhibitory risks at low temperature, without further limitation to photosynthesis. Plant, Cell & Environment 25: 1251-1259.

Pollastri S, Tattini M (2011) Flavonols: old compounds for old roles. Annals of Botany 108: 1225-1233.

Polle A (2001) Dissecting the superoxide dismutase-ascorbate peroxidase-glutathione pathway in chloroplasts by metabolic modelling. Computer simulations as a step towards flux analysis. Plant Physiology 126: 445-462.

Potters G, Pasternak TP, Guisez Y, Palme KJ, Jansen MAK (2007) Stress-induced morphogenic responses: growing out of trouble? Trends in Plant Science 12: 98-105.

Poustka F, Irani NG, Feller A, Lu Y, Pourcel L, Frame K, Grotewold E (2007) Trafficking pathway for anthocyanins overlaps with the endoplasmic reticulum-to-vacuole protein-sorting route in Arabidopsis and contributes to the formation of vacuolar inclusions. Plant Physiology 145: 1323-1335.

Ralston NVC, Hunt CD (2001) Diadenosine phosphates and S-adenosylmethionine: novel boron binding biomolecules detected by capillary electrophoresis. Biochimica et Biophysica Acta 1527: 20-30.

Rasulov B, Bichele I, Laisk A, Niinemets U (2013) Competition between isoprene emission and pigment synthesis during leaf development in aspen. Plant Cell and Environment 37: 724-741.

Reid RJ (2007) Identification of boron transporter genes likely to be responsible for tolerance to boron toxicity in wheat and barley. Plant and Cell Physiology 48: 1673-1678.

Reid RJ, Hayes JE, Post A, Stangoulis JCR, Graham RD (2004) A critical analysis of the causes of boron toxicity in plants. Plant, Cell & Environment 27: 1405-1414.

Rice-Evans CA, Miller N, Paganga G (1997) Antioxidant properties phenolic compounds. Trends in Plant Science 2: 152-159.

Rizzini L, Favory JJ, Cloix C (2011) Perception of UV-B by the Arabidopsis UVR8 protein. Science 332: 103-106.

Rozema J, Van de Staaij J, Bjorn LO, Caldwell M (1997) UV-B as an environmental factor in plant life: stress and regulation. Trends in Ecology & Evolution 12: 22-28.

Ruiz JM, Rivero RM, Romero L (2003) Preliminary studies on the involvement of biosynthesis of cysteine and glutathione in the resistance to boron toxicity in sunflower plants. Plant Science 165: 811-817.

Ruuhola T, Keinanen M, Keski-Saari S, Lehto T (2011) Boron nutrition affects the carbon metabolism of silver birch seedlings. Tree Physiology 31: 1251-1261.

Ryang SZ, Woo SY, Know SY, Kim SH, Lee SH, Kim KN, Lee KD (2009) Changes of net photosynthesis, antioxidant enzyme activities, and antioxidant contents of *Liriodendron tulipifera* under elevated ozone. Photosynthetica 47: 19-25.

Schreiber U, Bilger W, Neubaer C (1995) Chlorophyll fluorescence as a non-intruder indicator of rapid assessment of in vivo photosynthesis. In: Schulze ED, Caldwell MM (Eds) Ecophysiology of photosynthesis. Springer Verlag, Berlin, 49-70.

Schreiber U, Schliva U, Bilger B (1986) Continuous recording of photochemical and non-photochemical chlorophyll fluorescence quenching with a new type of modulation fluorometer. Photosynthesis Research 10: 51-62.

Shan B, Cai YZ, Sun M, Corke H (2005) Antioxidant capacity of 26 spice extracts and characterization of their phenolic constituents. Journal of Agriculture and Food Chemistry 53: 7749-7759.

Shelp BJ (1988) Boron mobility and nutrition in broccoli (*Brassica oleracea* var. Italica). Annals of Botany 61: 83-91.

Sherwin HW, Farrant JM (1998) Protection mechanisms against excess light in the resurrection plants *Craterostigma wilmsii* and *Xerophyta viscosa*. Plant Growth and Regulation 24: 203-210.

Simon JE, Morales MR, Phippen WB, Vieira RF, Hao Z (1999). A source of aroma compounds and a popular culinary and ornamental herb. In Janick J (Ed), Perspectives on new crops and new uses. ASHS Press, Alexandria, VA 499-505.

Simon JE, Quinn J, Murray RG (1990) Basil: a source of essential oils. In: Janick J, Simon JE (Eds), Advances in new crops. Timber Press, Portland, OR 484-489.

Singh DP, Belay J, Mclnerney JK, Day L (2012) Impact of boron, calcium and genetic factors on vitamin C, carotenoids, phenolic acids, anthocyanins and antioxidant capacity of carrots (*Daucus carota*). Food Chemistry 132: 1161-1170.

Snell-Rood EC, Papaj DR (2009) Patterns of phenotypic plasticity in common and rare environments: A study of host use and color learning in the cabbage white butterfly *Pieris rapae*. American Naturalist 173: 615-631.

Somaatmadja D, Powers JJ, Hamdy MH (2006) Anthocyanins. VI. Chelation studies on anthocyanins and other related compounds. Journal of Food Science 29:655-660.

Sotiropoulos TE, Molassiotis A, Almaliotis D, Mouhtaridou G, Dimassi K, Therios I, Diamantidis G (2006) Growth, nutritional status, chlorophyll content, and antioxidant responses of the apple rootstock MM 111 shoots cultured under high boron concentrations in vitro. Journal of Plant Nutrition 29: 575-583.

Sotiropoulos TE, Therios NI, Dimassi NK, Bosbalidis A, Kofilids G (2002) Nutritional status, growth, CO2 assimilation and leaf anatomical responses in two kiwi fruit species under boron toxicity. Journal of Plant Nutrition 25: 1249-1261.

Soylemezoglu G, Demir K, Inal A, Gunes A (2009) Effect of silicon on antioxidant and stomatal response of two grapevine (Vitis vinifera L.) rootstocks grown in boron toxic saline and boron toxic-saline soil. Scientia Horticulturae 123: 240-246.

Stangoulis JCR, Brown PH, Bellaloui N, Reid RJ, Graham RD (2001) The efficiency of boron utilization in canola. Australian Journal of Plant Physiology 28: 1109-1114.

Steyn WJ, Wand SJE, Holcroft DM, Jacobs G (2002) Anthocyanins in vegetative tissues: a proposed unified function in photoprotection. New Phytologist 155: 349-361.

Surveswaran S, Cai YZ, Corke H, Sun M (2007) Systematic evaluation of natural phenolic antioxidants from 133 Indian medicinal plants. Food Chemistry 102: 938-953.

Sutton T, Baumann U, Hayes J, Collins NC, Shi BJ, Schnurbusch T, Hay A, Mayo G, Pallotta M, Tester M, Langridge P (2007) Boron-toxicity tolerance in barley arising from efflux transporter amplification. Science 318: 1446-1449.

Takahashi A, Takeda K, Ohnishi T (1991) Light-induced anthocyanin reduces the extent of damge to DNA in UV-irradiated Centaurea cyanus cells in culture. Plant and Cell Physiology 32: 541-547.

Takahashi S, Badger MR (2011) Photoprotection in plants: a new light on photosystem II damage. Trends in Plant Science 16: 53-60.

Takano J, Miwa K, Yuan LX, von Wiren N, Fujiwara T (2005) Endocytosis and degradation of BOR1, a boron transporter of *Arabidopsis thaliana*, regulated by boron availability. Procedings of the National Academic Science 102: 12276-12281.

Takano J, Noguchi K, Yasumori M, Kobayashi M, Gajdos Z, Miwa K, Hayashi H, Yoneyama T, Fujiwara T (2002) Arabidopsis boron transporter for xylem loading. Nature 420: 337-340.

Takano J, Wada M, Ludewig U, Schaaf G, von Wiren N, Fujiwara T (2006) The Arabidopsis major intrinsic protein NIP5 is essential for efficient boron uptake and plant development under boron limitation. The Plant Cell 18: 1498-1509.

Tanaka M, Fujiwara T (2008) Physiological roles and transport mechanisms of boron: perspectives from plants. Pflugers Archives European Journal of Physiology 456: 671-677.

Tardieu F, Tuberosa R (2010) Dissection and modelling of abiotic stress tolerance in plants. Current Opinion in Plant Biology 13: 206-212.

Tattini M, Galardi C, Pinelli P, Massai R, Remorini D, Agati G (2004) Differential accumulation of flavonoids and hydroxycinnamates in leaves of *Ligustrum vulgare* under excess light and drought stress. New Phytologist 163: 547-561.

Tattini M, Gravano E, Pinelli P, Mulinacci N, Romani A (2000) Flavonoids accumulate in leaves and glandular trichomes of *Phillyrea latifolia* exposed to excess solar radiation. New Phytologist 148: 69-77.

Tattini M, Guidi L, Morassi-Bonzi L, Pinelli P, Remorini D, Degl'Innocenti E, Giordano C, Massai R, Agati G (2005) On the role of flavonoids in the integrated mechanisms of response of *Ligustrum vulgare* and *Phillyrea latifolia* to high solar radiation. New Phytologist 167: 457-470.

Tattini M, Remorini D, Pinelli P, Agati G, Saracini E, Traversi ML, Massai R (2006) Morph-anatomical, physiological and biochemical adjustments in response to root zone salinity stress and high solar radiation in two Mediterranean evergreen shrubs, *Myrtus communis* and *Pistacia lentiscus*. New Phytologist 170: 779-794.

Taylor LP, Grotewold E (2005) Flavonoids as developmental regulators. Current Opinion in Plant Biology 8: 317-323.

Terashima I, Araya T, Miyazawa SI, Sone K, Yano S (2005) Construction and maintenance of the optimal photosynthetic systems of the leaf, herbaceous plant and tree: an eco-developmental treatise. Annals of Botany 95: 507-519.

Terashima I, Fujita T, Inoue T, Chow WS, Oguchi R (2009) Green light drives leaf photosynthesis more efficiently than red light in strong white light: revisiting the enigmatic question of why leaves are green. Plant and Cell Physiology 39: 1020-1026.

Terashima I, Hanba YT, Tholen D, Niinemets U (2011) Leaf functional anatomy in relation to photosynthesis. Plant Physiology 155: 108-116.

Tsuda T, Shiga K, Ohshima K, Kawakishi S, Osawa T (1996) Inhibition of lipid peroxidation and the active oxygen radical scavenging effect of anthocyanin pigments isolated from *Phaseolus vulgaris* L. Biochemical Pharmacology 52: 1033-1039.

Valladares F, Hernández LG, Dobarro I, García-Pérez C, Sanz R, Pugnaire FI (2003) The ratio of leaf to total area influences shade survival and plastic response to light of green-stemmed leguminous shrub seedlings. Annals of Botany 91: 577-584.

Valladares F, Martinez-Ferri E, Balaguer L, Perez-Corona E, Manrique E (2000) Low-leaf-level response to light and nutrients in the Mediterranean evergreen oaks: a conservative resource-use strategy? New Phytologist 148: 79-91.

Valladares F, Saldaña A, Gianoli E (2012) Costs versus risks: Architectural changes with changing light quantity and quality in saplings of temperate rainforest trees of different shade tolerance. Australian Ecology 37: 35-43.

Valladares F, Sanchez-Gomez D, Zavala MA (2006) Quantitative estimation of phenotypic plasticity: bridging the gap between the evolutionary concept and its ecological implications. Journal of Ecology 14: 1103-1116.

van Kleunen M, Fischer M (2004) Constraints on the evolution of adaptive phenotypic plasticity in plants. New Phytologist 166: 49-60.

Vanderauwera S, Zimmermann P, Rombauts S, Vandenabeele S, Langebartels C, Gruissem W, Inzé D, van Breusegem F (2005) Genome-wide analysis of hydrogen peroxide-regulated gene expression in Arabidopsis reveals a high light-induced transcriptional cluster involved in anthocyanin biosynthesis. Plant Physiology 139: 806-821.

Vogelman TC (1993) Plant tissue optics. Annual Review of Plant Physiology and Plant Molecular Biology 44: 231-251.

Vogelmann TC, Nishio JN, Smith WK (1996) Leaves and light capture: Light propagation and gradients of carbon fixation within leaves. Trends in Plant Science 1: 65-70.

Wang JZ, Tao ST, Qi KJ, Wu J, Wu HQ, Zhang SL (2011) Changes in photosynthetic and antioxidative system of pear leaves to boron toxicity. African Journal of Biotechnology 10: 19693-19700.

Warington K (1923) The effect of boric acid and borax on the broad been and certain other plants. Annals of Botany 37: 629-672.

WHO (1998) Environmental Health Criteria. World Health Organization, Geneva, Switzerland.

Winthrop BP, James ES (1998) Anthocyanins in basil (*Ocimum basilicum* L.). Journal of Agriculture and. Food Chemistrey 46: 5165-5170.

Wolf B (1974) Improvement in the Azomethine-H method for determination of boron. Communication in Soil Science and Plant Analyses 5: 39-44.

Woods GW (1996) Review of possible boron speciation relating to its essentiality. The Journal of Trace Element in Experimental Medicine 9: 153-163.

Yermiyahu U, Ben-Gal A, Keren R, Reid RJ (2008) Combined effect of salinity and boron on plant growth and yield. Plant and Soil 304: 73-87.

You CF, Spivack AJ, Gieskes JM, Rosenbauer R, Bischoff JL (1995) Experimental study of boron geochemistry: implications for fluid processes in subduction zones. Geochimica et Cosmochimica Acta 59: 2435-2442.

Zeggwagh NA, Sulpice T, Eddouks M (2007) Antihyperglycaemic and hypolipidemic effects of *Ocimum basilicum* aqueous extract in diabetic rats. American Journal of Pharmacology and Toxicology 2: 123-129.

Zeliou K, Manetas Y, Petropoulou Y (2009) Transient winter leaf reddening in *Cistus creticus* characterizes weal (stress-sensitive) individuals, yet anthocyanins cannot alleviate the adverse effects on photosynthesis. Journal of Experimental Botany 60: 3031-3042.

Zheng W, Wang SY (2001) Antioxidant activity and phenolic compounds in selected herbs. Journal of Agriculture and Food Chemistry 49: 5165-5170.

Life on Earth appears dominated by a great number of paradigms.

Aerobic organisms need oxygen to survive; but oxygen can originate free radicals.

Plants need light to survive; but light can originate free radicals.

We are quite far from understanding the intimal mechanisms driving

our Planet.

We can only describe what we experience every day wishing that the little grain we add

on knowledge might increase our comprehension of life

on Earth.

This spirit have motivated *my* work